DEVELOPMENT OF FUNCTIONAL ELECTRICAL STIMULATION SYSTEM USING MECHANOMYOGRAPHY AS MUSCLE STATE FEEDBACK FOR PARAPLEGICS

JANNATUL NAEEM

FACULTY OF ENGINEERING
UNIVERSITY OF MALAYA
KUALA LUMPUR

2021

DEVELOPMENT OF FUNCTIONAL ELECTRICAL STIMULATION SYSTEM USING MECHANOMYOGRAPHY AS MUSCLE STATE FEEDBACK FOR PARAPLEGICS

JANNATUL NAEEM

THESIS SUBMITTED IN FULFILMENT OF THE REQUIREMENTS FOR THE DEGREE OF DOCTOR OF PHILOSOPHY

FACULTY OF ENGINEERING
UNIVERSITY OF MALAYA
KUALA LUMPUR

2021

UNIVERSITY OF MALAYA

ORIGINAL LITERARY WORK DECLARATION

Name of Candidate: Jannatul Naeem

Matric No: 17057517/1 | KHA150067

Name of Degree: Doctor of Philosophy

Title of Thesis ("this Work"): Development of Functional Electrical Stimulation System Using Mechanomyography as Muscle State Feedback for Paraplegics

Field of Study: Biomedical Engineering (Engineering & Engineering Trades)

I do solemnly and sincerely declare that:

(1) I am the sole author/writer of this Work;
(2) This Work is original;
(3) Any use of any work in which copyright exists was done by way of fair dealing and for permitted purposes and any excerpt or extract from, or reference to or reproduction of any copyright work has been disclosed expressly and sufficiently and the title of the Work and its authorship have been acknowledged in this Work;
(4) I do not have any actual knowledge nor do I ought reasonably to know that the making of this work constitutes an infringement of any copyright work;
(5) I hereby assign all and every rights in the copyright to this Work to the University of Malaya ("UM"), who henceforth shall be owner of the copyright in this Work and that any reproduction or use in any form or by any means whatsoever is prohibited without the written consent of UM having been first had and obtained;
(6) I am fully aware that if in the course of making this Work I have infringed any copyright whether intentionally or otherwise, I may be subject to legal action or any other action as may be determined by UM.

Candidate's Signature Date: 25/10/2021

Subscribed and solemnly declared before,

Witness's Signature Date: 28/10/2021

Name:

Designation:

DEVELOPMENT OF FUNCTIONAL ELECTRICAL STIMULATION SYSTEM USING MECHANOMYOGRAPHY AS MUSCLE STATE FEEDBACK FOR PARAPLEGICS

ABSTRACT

Functional electrical stimulation (FES) supported exercises aid purposeful muscle contractions to restore the lost motor functions with associated health benefits in individuals with spinal cord injury (SCI). The use of this device globally is majorly still restricted to the laboratory, especially in developing countries such as countries in Asia. This challenge is principally due to the high cost of the device for home care use and even for clinical deployment and the complexity of the commercially available options. One limitation of the available options is the inefficient muscle stimulation outcome due to the early onset of muscle fatigue. The reversal of motor unit recruitment in FES-evoked muscle contractions is one of the reasons for quicker muscle fatigue than the natural muscle contractions that occur from the central nervous system in a healthy person. The FES systems with sensor feedback are used to lessen this limitation with improved functional outcomes. The use of muscle contraction signals such as electromyography marred with stimulation artefacts, and the removal of these artefacts often presents another challenge. The studies reported in this thesis proposed and developed an FES system to monitor muscle condition using mechanomyography (MMG) without the limitation of stimulation artefacts. Before the implementation, a unique Mel-frequency cepstral coefficient (MFCC) feature of the MMG signal was introduced to classify the fresh muscle and muscle fatigue contractions in cycling exercise. Using this MFCC feature of MMG, 90.7% average classification accuracy was achieved, while the root mean square (RMS) feature of MMG had an accuracy of 74.5%. However, the computational cost needed for this research is supported using the RMS amplitude feature of MMG. This is also based on the literature that the MMG-RMS has a positive and primarily linear relationship with torque generated from FES-evoked muscle actions. The developed FES system created sufficient stimulation power to support standing exercise and monitor muscle condition using MMG signal related to knee-buckling, which indicates muscle fatigue.

Furthermore, the developed FES system was applied to detect muscle fatigue in real-time using the MMG-RMS feature during isometric knee extension. The torque generated when tested on the isometric dynamometer was related to 70% drop in MMG-RMS threshold as actual muscle fatigue. Finally, an investigation of different modes of user control strategies of FES standing was simulated as the increase of amplitude by button pressing to sustain standing and detect muscle fatigue using the MMG-RMS feature. The outcome of this investigation showed that the single press 10 s mode provides optimal standing duration compared to other modes. Overall, this research shows the development of real-time muscle monitoring and prevention FES system with MMG sensor.

Keywords: Functional Electrical Stimulation, Mechanomyography, Spinal Cord Injury

PEMBANGUNAN SISTEM RANGSANGAN ELEKTRIK BERFUNGSI MENGGUNAKAN MEKANOMIOGRAFI SEBAGAI MAKLUMBALAS KEADAAN OTOT UNTUK PARAPLEGIK

ABSTRACT

Bantuan senaman yang disokong oleh Rangsangan Elektrik Berfungsi (*FES*) untuk kontraksi otot bertujuan untuk membantu pemulihan kemahiran motor dan kesihatan individu dengan kecederaan saraf tunjang (SCI). Penggunaan peranti FES ini masih terhad kepada kegunaan makmal terutamanya dalam keadaan ekonomi negara-negara membangun seperti negara-negara di Asia. Kegunaan peranti untuk kegunaan di rumah mahupun penggunaan klinikal melibatkan kos yang tinggi dan merupakan cabaran asas bagi pengguna. Kerumitan peranti *FES* sedia ada secara komersial juga adalah satu lagi cabaran yang perlu dihadapi oleh pihak pengguna. Limitasi pilihan peranti *FES* sedia ada ialah rangsangan otot yang tidak cekap. Ini berkaitan dengan kelesuan otot lumpuh yang dirangsang oleh *FES* berlaku lebih awal daripada kontraksi otot sihat yang dirangsang melalui fisiologi normal. Hal ini disebabkan oleh kontraksi unit motor secara terbalik oleh *FES* apabila dibandingkan dengan kontraksi otot secara semula jadi yang dikawal oleh sistem saraf pusat yang utuh dalam individu sihat. Sistem *FES* yang dilengkapi dengan sistem maklumbalas keadaan otot telah dipromosikan untuk mengurangkan limitasi ini dengan hasil fungsi otot yang lebih baik. Penggunaan isyarat kontraksi otot seperti elektromiografi boleh dicemari oleh artifak dari rangsangan *FES* dan usaha untuk menyingkirkan artifak ini telah menimbulkan cabaran-cabaran lain. Kajian yang dilaporkan di dalam tesis ini mencadangkan dan membangunkan satu sistem *FES* yang dilengkapi sistem maklumbalas yang menggunakan isyarat kontraksi otot berdasarkan mekanomiografi (MMG) yang tidak dibatasi oleh artifak rangsangan *FES*. Perlaksanaan ciri pekali cepstral kekerapan-Mel (MFCC) yang unik dalam isyarat MMG telah diperkenalkan untuk mengkelaskan otot segar dan otot lesu sepanjang senaman berbasikal

yang dirangsang oleh *FES*. Dengan menggunakan ciri MFCC MMG, purata ketepatan pengelasan sebanyak 90.7% telah diperoleh manakala ciri *'root mean square'* (RMS) MMG mempunyai ketepatan sebanyak 74.5%. Ini sangat berguna dalam profil kontraksi otot yang dinamik seperti berbasikal. Namun begitu, kos pengiraan MFCC yang tinggi sebaliknya menyokong penggunaan ciri amplitud MMG-RMS dalam aktiviti yang melibatkan pergerakan stabil seperti berdiri dengan *FES*. Ini adalah berdasarkan tinjauan literatur yang melaporkan hubungan positif dan linear antara MMG-RMS dan tork yang dihasilkan oleh aktiviti otot yang dirangsang oleh *FES*. Pembangunan sistem *FES* beserta maklumbalas status otot telah dapat menghasilkan kuasa rangsangan yang cukup untuk menyokong senaman unjuran kaki secara isometrik dan semasa berdiri. Tork yang dijana secara rangsangan elektrik melalui *FES* pada dinamometer isometrik adalah berkaitan dan boleh dipantau melalui amplitud MMG-RMS. Tork otot yang dibangkitkan semasa aktiviti berdiri dengan *FES* juga boleh dipantau secara tidak langsung menerusi MMG-RMS lebih awal daripada kejatuhan sudut lutut disebabkan oleh keletihan otot. Penemuan ini mencadangkan bahawa MMG-RMS boleh digunakan untuk memantau kelesuan otot dan menggalakkan aktiviti yang dirangsang oleh *FES* bertahan lebih lama menerusi maklumbalas keadaan otot dan penggunaan parameter rangsangan *FES* yang optimal. Akhirnya, untuk membuktikan kemampuan sistem *FES* yang dilengkapi maklumbalas status otot ini dalam memanjangkan tempoh berdiri dengan *FES*, satu kajian simulasi telah dijalankan untuk menunjukkan kesan pelbagai mod berdiri dengan menggunakan MMG-RMS sebagai isyarat maklum balas terhadap pelbagai mod berdiri termasuk secara lingkaran terbuka, iaitu tanpa sebarang maklumbalas berkenaan status otot yang dirangsang oleh *FES*. Kajian ini mencadangkan penggunaan amplitud rangsangan yang dioptimumkan menggunakan MMG-RMS sebagai maklum balas untuk kegunaan masa nyata untuk aktiviti berdiri dengan *FES* yang lebih efektif dan berguna dari segi klinikal. Pada masa hadapan, sistem *FES* yang dikawal oleh MMG dapat dibangunkan untuk menyokong senaman tangan pula seperti melunjurkan dan melenturkan pergelangan tangan untuk meningkatkan aktiviti kehidupan harian.

Kata kunci: Rangsangan Elektrik Berfungsi (FES), mekanomiografi, kecederaan saraf tunjang

ACKNOWLEDGEMENTS

First and foremost, I glory to Almighty Allah for keeping me healthy and being patient during my thesis journey. First of all, I would like to express my thankfulness and gratefulness to my main supervisor and co-supervisors, Associate Professor Dr. Nur Azah Hamzaid, Associate Professor Dr. Amelia Wong Azman, and Associate Professor Dr. Manfred Bijak, respectively. They gave me good guidance, support, and motivation throughout the completion of this study. Without their inspiration, enthusiasm, and positive critics, this thesis will not even be possible.

Also, special words of thanks to Professor Dr. Nazirah Hasnan for monitoring spinal cord injury individual's health to conduct clinical trials and data collection successfully with safety. all my laboratory colleagues, Muhammad Afiq Dzulkifli, Dhamayanthi Nair, and Mohd Faiz Azmi for helping to prepare experiment setup, and most importantly special thanks to the participants who volunteer.

Finally, mention should be made to the forbearance and patience of my beloved father, mother, and wife in who they are my main source of purpose and inspiration, during the period of this research and also throughout whole my life. Last but not least, an expression and gratitude to all individuals who are involved either directly or indirectly in making this project. Many thanks to University Malaya Research Grant (UMRG) RP-035 15HTM for financially support the research activities and scholarship.

TABLE OF CONTENTS

Abstract iii

Abstract v

Acknowledgements viii

Table of Contents ix

List of Figures xiii

List of Tables xvi

List of Symbols and Abbreviations xvii

List of Appendices xix

CHAPTER 1: INTRODUCTION 1

1.1 Background 1

1.2 Statement of problem and research scope 5

1.3 Research objectives 6

1.4 Significance of the research 7

1.5 Scope of research 8

1.6 Thesis organization 8

CHAPTER 2: LITERATURE REVIEW 11

2.1 Introduction 11

2.2 MMG feature extraction methods 13

2.3 Muscle action classification using MMG signals 18

2.4 The principle of FES system 24

2.4.1 Overview of closed-loop FES system 27

2.4.1.1 FES closed-loop system with non-muscle response feedback .. 27

2.4.1.2 FES closed-loop system with muscle response feedback 35

2.5 Procedure for FES parameter optimisation to support standing 39

CHAPTER 3: MECHANOMYOGRAPHY-BASED MUSCLE FATIGUE DETECTION DURING ELECTRICALLY-ELICITED CYCLING IN PATIENTS WITH SPINAL CORD INJURY 44

3.1 Introduction... 44

3.2 Methods 48

3.2.1 Participants 48

3.2.2 FES experimental protocol 49

3.2.3 MMG signal acquisition 51

3.2.4 Signal processing.. 51

3.3 MMG Classification 52

3.3.1 MFCC Feature 52

3.3.2 Support vector machine (SVM) 56

3.3.3 Muscle fatigue prediction among subjects 58

3.4 Result and analysis 58

3.4.1 MFCC and RMS features predicted contractions and accuracy 58

3.4.2 Muscle fatigue prediction accuracy among subjects 61

3.4.3 Cross-validation of the combined results of three sensors (RF, VL, and VM) 62

3.5 Discussion.. 65

3.6 Conclusions 69

CHAPTER 4: DEVELOPMENT OF FES SYSTEM WITH MECHANOMYOGRAPHY FEEDBACK FOR COMPLETE SPINAL CORD INJURY STANDING 71

4.1 Introduction... 71

4.2 Design of proposed FES system 72

4.2.1 Block diagram of the proposed closed-loop system 73

4.2.2 Stimulator 73

4.2.3 MMG Sensor 77

4.3 FES experiment during standing 77

4.3.1 Subject 77

4.3.2 Apparatus 78

4.3.3 Protocol 79

4.4 Result and discussion 80

4.5 Conclusion 82

CHAPTER 5: ELECTRICAL STIMULATOR WITH MECHANOMYOGRAPHY-BASED REAL-TIME MONITORING, MUSCLE FATIGUE DETECTION, AND SAFETY SHUT-OFF: A PILOT STUDY 84

5.1 Introduction 84

5.2 Experiment Protocol 87

5.2.1 Participants: 87

5.2.2 Experiment setup 87

5.2.3 Instrumentation 89

5.2.3.1 MMG measurement 89

5.3 Results and analysis 91

5.4 Discussion 93

5.5 Conclusion 96

CHAPTER 6: SIMULATION OF DIFFERENT MODES OF USER CONTROL STRATEGY TO SUSTAIN STANDING DURATION WITH SCI TO PREVENT MUSCLE FATIGUE WITH MMG FEEDBACK 97

6.1 Introduction 97

6.2 Methodology 99

6.2.1 Study population 100

6.2.2 FES set up and MMG signal acquisition 100

6.2.3 FES five modes of simulation 101

6.3 Result 103

6.4 Discussion 107

6.5 Conclusion 109

CHAPTER 7: CONCLUSION AND RECOMMENDATION 110

7.1 Conclusion 110

7.2 Study contributions 112

7.3 Study limitation 113

7.4 Future work and recommendations 113

List of Publications and Papers Presented 141

Appendix 145

CO-AUTHORS CONSENT 175

LIST OF FIGURES

Figure 1.1: Functional electrical stimulation muscle activation after spinal cord injury. Reused with permission from the publisher (Popovic et al., 2012) 1

Figure 2.1: Functional electrical stimulation parameter (biphasic square wave)............ 11

Figure 2.2: A scheme of a closed-loop FES system modified from (Lynch & Popovic, 2008) 27

Figure 2.3: The block diagram of a neuro-PID control system. Reproduced with permission from the publisher (Gwo-Ching et al., 1997) 29

Figure 2.4: Nested-loop control structure. Reproduced with permission from the publisher (Hunt et al., 2001) 30

Figure 2.5: The control systems evaluated in (Ferrarin et al., 2001)'s study. (a) Open-loop controller. (b) Closed-loop PID controller (c) Combination feed-forward feedback controller. (d) Adaptive controller 31

Figure 2.6: FES sliding mode controller. Reproduced with permission from the publisher (Gwo-Ching et al., 1997) 32

Figure 2.7: Schematic of the experimental setup. Reused with permission from the publisher (Previdi et al., 2005)... 33

Figure 2.8: The structure of the stimulated muscle model for model identification. Note that the muscle contraction dynamics model relates sEMG to torque and the excitation dynamics model relates stimulation to sEMG. Reproduced with permission from the publisher (Zhang et al., 2013) 35

Figure 2.9: Example of stimulation electrodes and voltage measuring electrode placements. Reproduced with permission from the publisher (Yusoff & Hamzaid, 2014) 36

Figure 2.10: Process of predictive model control of FES-muscle activation. Reproduced with permission from the publisher (Li et al., 2015)... 37

Figure 3.1: Schematic diagram of pulse train synchronized with ergometer pedal angle position in early non-fatigued condition, at 40 rpm.. 50

Figure 3.2: (a) Experimental setup, and (b) MMG sensor placement over the muscles (RF: rectus femoris, VL: vastus lateralis, VM: vastus medialis) represented by the solid black circles 51

Figure 3.3: Block diagram of the MFCC algorithm.. 53

Figure 3.4: Typical normalized (to gmax) MMG signals during one revolution of cycling: (a) non-fatigued and (b) fatigue muscle contractions from sensors placed at RF (top), VL (mid), and VM (bottom).. 54

Figure 3.5: Time series of MFCC Cepstrum index plot in frame index of 0.25s MMG signal 54

Figure 3.6: Block diagram of MMG signal training and recognition method 55

Figure 3.7: Selection of contractions used for training and testing from a cycling session 56

Figure 3.8: SVM hyper plane separated by Support Vectors (Hashem & Mabrouk, 2014) 57

Figure 4.1: Block diagram of the proposed closed-loop system.................................... 73

Figure 4.2: Voltage step-up circuit... 74

Figure 4.3: Circuit diagram of the output stage 75

Figure 4.4: Stimulation pattern generation table.. 75

Figure 4.5: Biphasic square wave output across 1K Ohm resistor 76

Figure 4.6: Graphical User interface to send control signal and to process MMG signal 76

Figure 4.7: MMG sensor setup 77

Figure 4.8: FES supported standing... 79

Figure 4.9: (A) MMG signal in fixed-parameter (B) MMG signal in parameter optimization 81

Figure 4.10: A shows the subject started to stand by FES, B shows the knee angle started to drop, and C clearly shows that the knee angle drops to 30° 81

Figure 5.1: Experimental setup for the proposed real-time monitoring FES system...... 88

Figure 5.2: Flow chart of the FES system with MMG-based real-time fatigue monitoring and safety shut off. 90

Figure 6.1: The experimental setup for FES supported standing, one MMG sensor showing at the lateral side only 101

Figure 6.2: Five settings for simulation environment adopted in this study................ 102

Figure 6.3: Simulated MMG-RMS output of 20 Hz for five settings of subject 2 as a representative case 104

LIST OF TABLES

Table 2.1: Summary of the common MMG signal features extraction methods 16

Table 2.2: Literature review summary of FES systems and their control parameters 41

Table 3.1: Participant demography 49

Table 3.2: Number of Expected and Predicted Contractions sample in confusion matrix and accuracy using MFCC feature. Each subject's first and second row shows expected (first row: expected True, second row: expected False) and predicted number (first row: predict) 59

Table 3.3: Number of Expected and Predicted Contractions sample in confusion matrix and accuracy using RMS feature. Each subject's first and second row shows expected and predicted number of contractions (first row: expected and predicted True, second row: expect) 60

Table 3.4: Predicted inter-subject accuracy using MFCC feature 61

Table 3.5: Predicted inter-subject accuracy using RMS feature 62

Table 3.6: Accuracy results for MFCC features with four repetitions........................... 63

Table 3.7: Accuracy results for RMS features 64

Table 3.8: Accuracy for combined MFCC and RMS features....................................... 64

Table 3.9: Individual three muscles performance accuracy of RF, VL, and VM. 66

Table 5.1: Stimulation end time (s) at different RMS threshold drop 93

Table 6.1: Average simulation time of sensors combinations in 20 and 35 Hz frequency in five subjects.. 105

Table 6.2: Average simulation time of three sensor combinations for the different five setting modes... 106

LIST OF SYMBOLS AND ABBREVIATIONS

AB	:	Able Bodied
CF	:	Center Frequency
CWT	:	Continuous Wavelet Transform
EMG	:	Electromyography
FES	:	Functional Electrical Stimulation
FFT	:	Fast Fourier Transform
MDF	:	Medial Frequency
MFCC	:	Mel-Frequency Cepstral Coefficients
MMG	:	Mechanomyography
MPF	:	Mean Power Frequency
RF	:	Rectus Femoris
RMS	:	Root Mean Square
SCI	:	Spinal Cord Injured
STFT	:	Short Time Fourier Transform
SVM	:	Support Vector Machine
VL	:	Vastus Lateralis
VM	:	Vastus Medialis
WPT	:	Wavelet Packet Transform
b	:	Bias
m_j	:	log filter bank amplitudes
w	:	Weight Vector
x	:	Input Vector From Input Space
x_i	:	Support Vectors
y_i	:	Vector of MMG Signal

α_i	:	Weight of the Vectors
γ	:	Kernel Width
$\|\|.\|\|$	:	Euclidean Norm
μs	:	Micro Second

LIST OF APPENDICES

Appendix A: Consent Form (Malay)…………………………………………...... 145

Appendix B: Consent Form (English).…………………………………………... 146

Appendix C: Ethics approval of the study……………………………………….. 147

Appendix D: Labview Code (Auto stimulation termination)…………………… 148

Appendix E: Python Coding (Open-Loop simulation)…………………………... 149

Appendix F: Python Coding (Closed-loop simulation double press)……………. 150

Appendix G: Patent File…………………………………………………………. 153

Appendix H: Matlab Code (Muscle fatigue classification)……………………… 156

Appendix I: Stimulator circuit (Controller)……………………………………… 159

Appendix J: Stimulator circuit (Output Stage)………………………………….. 160

Appendix K: Arduino Code (Stimulator Control……………………………….. 161

Appendix L: Permission from Publisher………………………………………… 165

CHAPTER 1: INTRODUCTION

1.1 Background

Spinal cord injury (SCI) leads to partial or complete paralysis in the affected individuals depending on the level of injury. The secondary complications of this injury may include pressure sores (Liu, Moody, Traynor, Dyson, & Gall, 2014), muscle spasticity (Elbasiouny, Moroz, Bakr, & Mushahwar, 2010), loss of muscle strength, impaired muscle functions (Galea, 2012; Jayaraman et al., 2006), cardiovascular disease (Furlan & Fehlings, 2008) and osteoporosis (Tan, Battaglino, & Morse, 2013). One significant consequence of impaired muscle function is the loss of motor function responsible for executing physical tasks. The functional electrical stimulation (FES) technique has been used widely for restoring lost motor function through muscle strengthening related exercise in spinal cord injured persons (Gorgey, Dolbow, Dolbow, Khalil, & Gater, 2015; Hamid & Hayek, 2008). Technically, FES applies a series of modulated electrical pulses to the skin surface or percutaneously using a pair of electrodes to affect muscle contractions, as shown in Figure 1.1 (Popovic, Masani, & Micera, 2012).

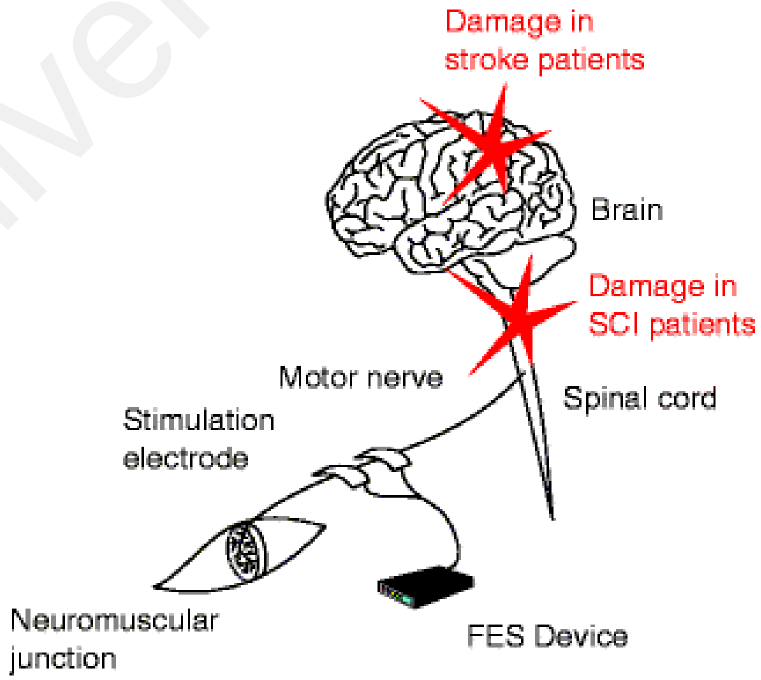

Figure 1.1: Functional electrical stimulation muscle activation after spinal cord injury. Reused with permission from the publisher (Popovic et al., 2012)

However, muscle fatigue is one of the limitations in the application of FES to evoke muscle contractions. Muscle fatigue is defined as the decline in muscle response during continuous and steady muscle contractions (Ibitoye, Hamzaid, Hasnan, Wahab, & Davis, 2016a). Muscle fatigue during electrically-evoked functional muscle response is complicated (Thrasher, Graham, & Popovic, 2005) as the muscle contraction pattern is nonlinear (Dorgan & O'Malley, 1997). Therefore, optimising the performance of FES-evoked contractions and subduing the early onset of muscle fatigue (Cogan, Ludwig, Welle, & Takmakov, 2016) is of research interest. One method is the promotion of continuous FES-evoked exercises for a longer duration. Several methods measure muscle fatigue as FES-induced torque, angle, and speed (Spendiff, Longford, & Winter, 2002). However, these techniques suffer some limitations in the clinical or home use applications due to the bulkiness of their sensors and the complication of associated signal processing methods.

While surface electromyography (sEMG) has gained prominence in studying the muscle response during voluntary muscle contractions, applications of this signal to study muscle performance, i.e., force/torque generation, during FES-evoked muscle activities is debatable (Ibitoye, Estigoni, Hamzaid, Wahab, & Davis, 2014a; Popović, 2014) due to the intensity of stimulation artefacts with the EMG signals (Merletti, Knaflitz, & DeLuca, 1992).

Due to this limitation of EMG signal, application of Mechanomyography (MMG) signal for muscle performance assessment during FES-evoked contractions is recommended (Ibitoye et al., 2016b; Yamamoto & Takano, 1994; Yoshitake & Moritani, 1999). MMG signals measure muscle contractions in mechanical muscle response, i.e., vibration generated by electrical stimulation, representing muscle activities. Hence this signal modality is free from stimulation artefacts due to its mechanism.

The selection of appropriate MMG features is an important step to detect muscle fatigue. Furthermore, it also depends on the experimental settings and the type of FES-evoked contraction used (i.e., isometric contraction, isokinetic contraction, etc.), and the nature of physical exercise adopted, such as FES cycling. To interpret the muscle responses, MMG features in time (Ibitoye et al., 2016b), frequency (Ryan, Cramer, Egan, Hartman, & Herda, 2008b), and joint time-frequency (TF) (Al-Mulla & Sepulveda, 2014) domain are necessary to analyse FES-evoked muscle contractions. However, MMG responses in the time and frequency domain of dynamic evoked-muscle contractions such as hand grasp have been reported to be nonlinear (Hong-Bo, Yong-Ping, & Jing-Yi, 2009). Also, the signal nature is considered non-stationary during functional muscle activities such as FES cycling exercise (Bonato, Roy, Knaflitz, & Luca, 2001). This nonlinearity may be due to several factors, including changes in the muscle fiber length, the number of active firing rate of the motor units, and tissue thickness between muscle fibers (Bonato et al., 2001; Cramer et al., 2005).

In order to analyse the non-stationary MMG signals, wavelet transform (WT), short-time Fourier transform (STFT), and Wigner-Ville transform as joint TF signal processing technique has been proposed (Akataki, Mita, & Watakabe, 2004; Barry & Cole, 1990; Hong-Bo et al., 2009). Beck et al. (2009) also proposed a new wavelet analysis method to analyse MMG signals where eleven nonlinearly scaled wavelet filter banks. The authors proposed that the intensity of the MMG signals can be useful for statistical pattern identification of dynamic muscle contractions. Furthermore, Ryan et al. (2008b) compared the short-time Fourier transform (STFT) feature with the continuous wavelet transform (CWT) feature for MMG signal analysis during voluntary isometric contraction and showed that the two methods had similar performance in the time-frequency domain. Another study by Silva, Heim, and Chau (2004) acquired MMG signals from a microphone-accelerometer-based MMG sensor pair to classify two activities of the prosthesis to control wrist extension and wrist flexion using root mean square (RMS) feature and compared with EMG. The author applied RMS feature to classify muscle contractions, and reported approximately 70% accuracy for both subjects. This result could be adjudged satisfactory when compared to EMG based estimation system.

Another potentially viable MMG feature extraction method is MFCC. The MFCC feature is most commonly used in automatic speech recognition because in speech recognition, speech is dynamic (McQueen, Norris, & Cutler, 2006) due to different uttered speech frequency changes with sound generated by the vocal cord; hence speech feature is extracted using MFCC to detect different frequency ranges of sound. During contractions, muscles generate low-frequency vibration (5-50 Hz) (Silva, Heim, & Chau, 2005), similar to the generated changes in frequency in uttered human speech. Similarly, the nature of muscle contraction, which also generates low-frequency vibration, hypothesized that MMG signal classification using the MFCC feature could be applied to detect muscle fatigue contractions in FES cycling exercise. The support vector machine (SVM) classifier will classify the non-fatigue and fatigue contractions during cycling exercises. For the implementation of a cycling setup, functional electrical stimulation will be run by three fixed parameters, including pulse amplitude (mA), pulse frequency (Hz), and pulse width (Doucet, Lam, & Griffin, 2012; Naeem, Amelia, Sheroz, & Yasir, 2013). The experiment will be such that the pre-set stimulation parameter will remain unchanged throughout the training session (Newham & Donaldson, 2007) to ensure muscle fatigue occurs during the cycling session.

In the available FES systems, the onset and parameters of FES are controlled by a pre-set time scheme or by user input. Currently, most of the clinically available FES systems operate in an open-loop mode. In these types of FES systems, users have the additional responsibility of predefining the stimulation parameter (e.g., pulse amplitude) or change parameters manually during stimulation to achieve the desired task without sensory feedback information used to monitor the muscle condition (Li et al., 2016) to optimise FES system performance.

Conversely, to overcome the limitation of the open-loop FES systems, a closed-loop FES system has been introduced (Braz, Russold, & Davis, 2009; Ibitoye, Hamzaid, Hayashibe, Hasnan, & Davis, 2019). A closed-loop FES system employs feedback signals to maintain desired muscle contraction output by controlling joint angle control, while stimulation parameters will be adjusted automatically with this control system (Lynch & Popovic, 2005). In a closed-loop FES system, various types of sensors are used as control signal inputs, including electromyographic (EMG) signals (Yochum, Binczak, Bakir, Jacquir, & Lepers, 2010), movement detected with kinematic sensors with generated signals (Veltink et al., 1998), and gait control using position sensors and signals (Chen, Li, Kuo, & Lai, 2001). Although there are many ongoing research studies on closed-loop FES systems, this effort has not been extensively applied in clinical settings. This thesis aims to explore implementing the MFCC feature to classify muscle fatigue in cycling and develop a real-time MMG sensor-based FES system muscle monitoring system to detect and prevent muscle fatigue during FES-isometric and standing exercises in SCI individuals.

1.2 Statement of problem and research scope

Muscle fatigue is one of the critical limitations of FES-evoked muscle contractions, especially for dynamic exercise training such as FES cycling (Leung et al., 2017; Thrasher et al., 2005). Detection of muscle fatigue before the critical stage is an important research question. One crucial way to achieve this is by selecting appropriate MMG features to detect various muscle states or conditions.

Dynamic muscle contraction responses are mainly analysed using time-frequency domain analysis methods for MMG features extraction such as wavelet transform, short-time Fourier transform, short wavelet transform, wavelet packet transform (Qian & Chen, 1999), and others. One other method for MMG signal feature extraction is Mel Frequency Cepstral Coefficient, widely used in automatic speech recognition to detect human voices because the human voice is also very sensitive to changes of uttered speech, similar to muscle contractions generated by low-frequency vibrations, i.e., MMG signals.

Detection of muscle fatigue by this method will aid the implementation of an FES system for worthwhile clinical exercise with safety in persons with SCI. For this implementation, the stimulation parameters will be fix before the cycling exercise begins. Most MMG-based FES system research focuses on offline analysis (Dzulkifli et al., 2018; Ibitoye et al., 2020b). Thus, it is essential to develop MMG based real-time FES system to monitor muscle fatigue and prevent over-stimulation, which may cause tissue damage. To prevent muscle fatigue and extend the exercise session, such as FES supported standing and isometric knee extension, the muscle will be monitored using an MMG sensor in real-time using the developed FES system and stimulation will be stopped before the critical muscle fatigue stage.

1.3 Research objectives

This research aims to design and develop a real-time FES system using MMG signal as a feedback signal to monitor muscle conditions. Specifically, the following objectives are going to address the general aim. These specific objectives are:

1. To implement MFCC feature extraction method to detect muscle fatigue using MMG sensor during FES cycling with SCI individuals.
2. To develop MMG-based FES system to monitor muscle condition in real-time.
3. To apply the developed FES system to detect and prevent muscle fatigue in real-time during isometric knee extension using MMG signal.

4. To investigate the simulation effect of different stimulation modes on standing duration in individuals with SCI to prevent muscle fatigue with MMG feedback.

1.4 Significance of the research

The application of FES to rehabilitate motor and sensory functions in individuals with SCI improves their quality of life as this technology provides physical, psychological, and functional benefits. Typically, efficient selection of stimulator parameters is key to effectively controlling these benefits. However, due to the unnatural activation of muscle by FES, rapid muscle fatigue onset precludes efficient muscle response to the FES-evoked muscle contraction and joint actions for task execution. Therefore, efficient control of muscle response following FES-supported movements is a significant limitation for using FES in clinical rehabilitation. One crucial clinical rehabilitation exercise is FES-supported cycling. During FES cycling, muscle contraction signal behavior is dynamic and nonlinear, making muscle analysis complex during this exercise.

To monitor muscle responses using MMG as a physical sensor for the muscle response is well established to study muscle behavior and performance. Considering the non-stationarity of the MMG signals during FES-supported cycling, information on muscle responses are sparse in the literature. Therefore, in this present research study, the MFCC method and its features are introduced to study MMG response during FES-supported cycling task, and the MFCC features used to classify MMG signals into muscle fatigue and non-fatigue contraction states with the support vector machine (SVM) classifier. Secondly, for muscle fatigue monitoring system using MMG sensor, a custom FES system was developed to enable users to have easy access to control the FES seamlessly and improve its performance outcome in clinical rehabilitation. This semi-automated custom-made FES device was developed by incorporating MMG sensors to use MMG signals as feedback to control muscle contractions and monitor muscle condition. This device was tested in real-time for critical muscle fatigue management during FES-supported isometric muscle contraction exercise using the MMG-amplitude feature. Finally, different stimulation modes are simulated (user button press modes) to prolong standing exercise in individuals with SCI using MMG feedback in the presence of unavoidable muscle fatigue. Clinical clearance is approved by the University Malaya medical center ethical committee to implement the developed FES system in the SCI individuals.

1.5 Scope of research

This thesis comprises developing and testing a functional electrical stimulation system using mechanomyography as the muscle state feedback signal in real-time. The developed semi-automated system was tested during stand and isometric knee extension. Different user control strategies were investigated for standing exercises with SCI to test their effectiveness in delaying muscle fatigue with MMG feedback. The device's performance for delaying muscle fatigue during other clinically useful exercise regimens such as gait could be a promising research study for future studies, which is beyond the scope of this thesis. The clinical subjects recruited in this study were those with motor and sensory incompleteness due to SCI. Other clinical populations, especially those with stroke, were not considered in this research.

1.6 Thesis organization

This thesis consists of seven Chapters. This thesis is based on article thesis format and, therefore, apart from Chapters One, Two, and Seven, which are Introduction, Literature Review, and Conclusion, respectively, each of the other Chapters uniquely presents each thesis objective as a standalone article.

Chapter One presents the general background to the thesis objectives and introduces the problem of the FES applications to solve in this thesis. The Chapter also provides an overview of the thesis aim and describes the challenges of FES application for clinical rehabilitation of persons with SCI. This chapter also presents the thesis scope, objectives, and significance.

Chapter Two covers the literature review, which is the previously reported studies related to this current work. Furthermore, this Chapter presents relevant information to understand better the problem identified in the literature and the systematic solution offered to solve the problem by this thesis.

Chapter Three presents the MFCC feature and SVM application to classify muscle contractions into fresh contraction and fatiguing and contractions during FES-assisted cycling exercise using MMG signals collected from SCI individuals. The Chapter essentially contains the author's manuscript texts that have been published and presented with permission from the publisher.

Chapter Four describes developing a semi-automated and custom-made FES system that uses MMG signals as feedback to monitor muscle conditions and control stimulation parameters for FES optimisation in clinical rehabilitation.

Chapter Five discusses the muscle fatigue detection and safety shut-off procedure in real-time FES during isometric knee extension exercise in SCI individuals using MMG signal as feedback. The Chapter essentially contains the author's manuscript texts that have been published and are now representing with permission from the publisher.

Chapter Six reports the five modes of FES standing stimulation implementation in simulation from experimental data using MMG feedback to prolong FES-aided standing in individuals with SCI. Finally, Chapter Seven summarises the implications of the results obtained in the previous Chapters. The Chapter briefly presents the thesis limitations and provides valuable recommendations for researchers in the related field of study.

CHAPTER 2: LITERATURE REVIEW

2.1 Introduction

Functional Electrical Stimulation (FES) has been widely used to evoke muscle contraction for muscle strengthening and lost motor function restoring in spinal cord injured persons (Hamid & Hayek, 2008). The FES uses short-duration electrical pulses (Figure 2.1) on the skin surface to elicit muscle contractions by activating nerve cells.

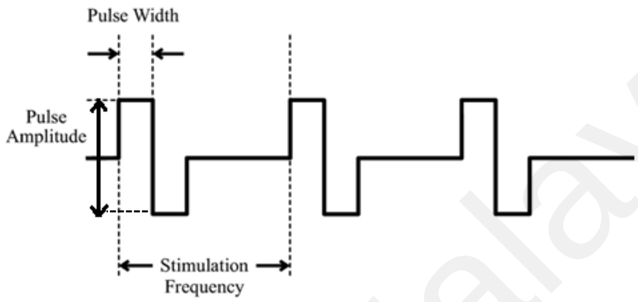

Figure 2.1: Functional electrical stimulation parameter (biphasic square wave)

For reaching to ambulation, FES-assisted leg exercise needs to be promoted. One common leg exercise is FES-supported cycling for lower limb muscle training to regain muscle functionality (Donaldson, Perkins, Fitzwater, Wood, & Middleton, 2000). However, muscle fatigue limits FES-evoked contractions and cycling exercises (Kesar, Chou, & Binder-Macleod, 2008). There is no specific reason that tells the exact reason of muscle fatigue which occurs early due to unnatural stimulation, has not been clearly defined, perhaps due to its nonlinear nature (Giat, Mizrahi, & Levy, 1993).

Although there are several methods to track the onset of muscle fatigue, including muscle force/joint torque measurement, joint angle measurement, and speed of muscle contraction (Spendiff et al., 2002), these methods are not perfect. Surface Electromyography (sEMG) has been commonly used to quantify muscle condition by directly measuring electrical activities of muscle contractions (Rainoldi, Melchiorri, & Caruso, 2004). The sEMG signal remains a good alternative for voluntary force/torque estimation following voluntary muscle contractions (Ibitoye et al., 2014a). In contrast, the sensitivity of the EMG signals is limited due to skin impedance changes due to perspiration when in use (Yamamoto & Takano, 1994), external electromagnetic interference. The stimulation artefacts merged with EMG signal especially during NMES-evoked contractions (Frigo, Ferrarin, Frasson, Pavan, & Thorsen, 2000; Orizio, 1993). Furthermore, the reliability of sEMG estimation of muscle force production during NMES-evoked muscle contractions is questionable due to the magnitude of stimulation artefacts current (Merletti et al., 1992; Popović, 2014).

Thus, quantification of NMES-evoked force production by sEMG alone during muscle contraction may be adjudged deficient (Levin, Mizrahi, & Isakov, 2000). Because of these limitations of sEMG signals, the current research by Yamamoto and Takano (1994) recommended to apply Mechanomyography (MMG) signals to assess muscle performance. When muscle contracts, it produces low-frequency muscle vibration or sound. The MMG sensor reads the movement or vibration of muscle during muscle activities. The three most common types of MMG sensors used to read muscle contractions are acousticmyography (AMG), vibromyography (VMG), and phonomyography (PMG). The AMG sensor reads generated sound during muscle contraction, in which sound becomes stronger when muscle contraction force increases. The PMG sensor's functionality is similar to the AMG sensor, which records the low-frequency sounds using a microphone generated during muscle contraction. However, these two methods of mechanomyography sensor require more processing, such as noise removal from actual signal and need to be carefully placed on the skin for better contact to reduce sensor tissue signal loss. On the other hand, the VMG sensor reads muscle vibration when muscle contracts and is most common in the muscle monitoring system. Therefore, this research uses an accelerometer as VMG type sensor.

To accurately capture specific muscle action using the MMG signals, several feature extraction and classification methods have been proposed and applied (Beck et al., 2009;

Beck et al., 2007; Beck et al., 2005b; Ibitoye, Hamzaid, Zuniga, Hasnan, & Wahab, 2014b). Sub-sessions 2.2 and 2.3 discuss the literature elaborately on MMG signal features, extraction methods, classification, section 2.4 includes a discussion of closed-loop systems with non-muscle and muscle feedback, and section 2.5 discusses FES parameter optimisation methods in standing support.

2.2 MMG feature extraction methods

The application of MMG signal features for the assessment of muscle is gaining wider prominence in rehabilitation engineering and related fields. Time-domain and frequency domains (Beck et al., 2005a; Ibitoye et al., 2014b; Orizio, 1993) analyses of MMG signals have been mostly applied. However, due to some helpful information that may not be ordinarily evident in the time or frequency domain, the joint time-frequency (TF) domain (Beck et al., 2009; Ibitoye et al., 2014b) has been suggested for the joint time-frequency domain representations of MMG signal features. Time-domain and frequency-domain analyses have been applied to study isometric and dynamic muscle actions. The joint TF method has been proposed due to the non-stationary behavior of MMG signals that is useful for some applications relating to the study of motor unit activation strategies (Akataki, Mita, Watakabe, & Itoh, 2001). Therefore, the selection of MMG features and methods are application-dependent during FES-evoked muscle contractions. During muscle contractions, either isometric or dynamic, muscle typically undergoes dimensional changes. For example, dynamic muscle contractions entail several changes, including muscle length, tissue thickness between muscles, and the number of motor units activated for task execution (Frangioni, Kwan-Gett, Dobrunz, & McMahon, 1987;

Jaskólska et al., 2004). Due to these changes, the application of the classical time series analysis methods may have limited application.

The prominent time-domain features of MMG signals include root mean square (RMS) amplitude, peak to peak (PTP) amplitude, and mean average value (MAV) (Ibitoye et al., 2016c). The standard frequency-domain features of MMG signals include mean power frequency (MPF) (Perry et al., 2001), median frequency (MDF), center frequency (CF), and frequency variance (Malek & Coburn, 2012). The various algorithms are suggested for the joint time-frequency domain representations of the MMG signal include short-time Fourier transform (STFT), wavelet transform (WT), and the recently suggested time scale representations (Beck et al., 2008; Ibitoye et al., 2014b). These modalities have been widely used to estimate the muscle contractile information embedded in the MMG signals. However, to reliably and accurately capture and utilise the information contained in MMG signals, it is essential to observe some signal conditioning rules, including MMG signal acquisition using appropriate sensors, signal amplification if necessary, signal filtering, parameter extraction followed by classification and pattern recognition. These processes are required to identify the MMG signals that contain the muscle contraction information needed to access muscle performance and for related applications in clinical rehabilitation, sports medicine, and related fields.

Specifically, the sequel to the observance of the highlighted procedures, the MMG signal features can be used for different applications, including muscle function monitoring such as muscle force assessment (Sarlabous, Torres, Fiz, Morera, & Jané, 2013) and applications in neuroprosthesis. The MMG signal could also be used to describe motor unit activation strategies (Beck et al., 2007) to understand motor unit recruitment and firing rate. In addition, the MMG signals could also be applied to discriminate muscle fiber types in different muscle types, whether in healthy or diseased conditions (Herda et al., 2010). This signal could also be helpful for clinical examination of neuromuscular disorders and aid the rehabilitation physician or other allied professionals in making informed decisions on the appropriate disease management plan. During FES-evoked muscle contractions, MMG signals have been recommended to control muscle activation patterns (Barry, Leonard, Gitter, & Ball, 1986; Gobbo, Cè, Diemont, Esposito, & Orizio, 2006). Table 2.1 summarises the common MMG signal features, their domains, and areas of application.

Table 2.1: Summary of the common MMG signal features extraction methods

Method		Strength	Weakness	Area of Application	References
Type	Domain				
Wigner Ville transform (WVT)	Time-frequency	The Power spectrum displays good localisation properties. Energy conservation (energy of the signal can be easily obtained)	It generates interference terms (i.e., noise that overlaps the signal terms and disallows the high TF resolution). Not suitable to analyse multi-component signals.	During muscle contractions, monitoring of the muscle resonance	(Barry & Cole, 1990;)
Mean power frequency (MPF)	Frequency domain	Polynomial regression analyses show MMG amplitude linearly increases to output power	There are no changes in MPF with the cycling power output	Relations of MMG mean power frequency (MPF) and power output during cycling ergometry	(Perry et al., 2001)
Short-time Fourier transform (STFT), continuous wavelet transform (CWT)	Time-frequency	Similarities between the CWT and STFT in responses of MMG and EMG signal	MMG response may be influenced by the selection of window for analysis of signal	Time and frequency domain responses of the VL and RF muscles during isometric ramp contraction	(Ryan et al., 2008b)
Wavelet packet transform (WPT), singular value decomposition (SVD),	Time frequency	Combined feature extraction method by implemented by WPT then use of SVD and distance evaluation technique to get an optimal feature	It requires an optimal amount of force to increase classification accuracy	Hand motion classification	Xie et al., 2009)
Wavelet analysis	Time-frequency	Frequency space by multiplying each of the wavelets with the Fourier transform. The real and imaginary wavelet transformed signals were converted into the time domain.	No equal responses among three muscles due to differences in architecture, muscle stiffness, and intramuscular pressure	To examine MMG responses of the VL, RF, and VM muscles	(Beck et al., 2009)

Table 2.1: Continue

Method		Strength	Weakness	Area of Application	References
Type	Domain				
Time-domain (TD), frequency-domain (FD) and time-frequency (TF)	Combination of Time, Frequency and time-frequency domain	Multiple 60 sets of feature types, including TD, FD, and TF	The higher number of feature sets needs to be optimised with a better feature selection method for higher accuracy	Multisite MMG signals exhibit distinctive patterns of forearm muscle activity	(Natasha Alves & Tom Chau, 2010)
MMG-RMS	Time Domain	Positive correlation with MMG-RMS and muscle response	Diaphragmatic MMG signal is affected by impulsive movement noise	Muscle force assessment based on the Lempel–Ziv algorithm: the Multistate Lempel–Ziv (MLZ) index	Sarlabous, Torres, Fiz, Morera, & Jané, 2013
MMG-root mean square (RMS) and peak to peak (PTP)	Time Domain	The high coefficient correlation is found between MMG feature and torque	Data set of RMS and PTP feature contraction used for training was a small number for actual prediction	Knee torque estimation from mechanomyography signal	Ibitoye et al., 2016c

2.3 Muscle action classification using MMG signals

There are several feature extraction methods from which muscle contractions could be classified during FES-related activities, hence could be used to detect muscle fatigue. Fresh muscle contraction activities are typically preceded by fatiguing muscle contraction during FES stimulation, which indicates exhaustion. Accurate and reliable muscle fatigue is of research and clinical interest depending on the muscle state and health condition. Several previous studies on MMG signals analysis have been on muscle fatigue identification because the study of muscle fatigue onset and progression would provide helpful information about the recruitment strategies of motor units and firing frequency during fatiguing contraction being within the continuum of purposeful muscle contractions.

Many studies have documented the MMG signal response to muscle contraction, mostly involuntary muscle contractions, rarely in FES-induced muscle contractions. For example, the muscle fatigue contraction study by Enoka and Stuart (1992) showed that a reduction of motor unit firing rate led to a lesser vibration or pressure and was reflected as a reduction in MMG signal amplitude. In terms of the pattern of MMG signal response and muscle contractions, Søgaard, Orizio, and Sjøgaard (2006) showed a linear relationship between the MMG signal amplitude and the muscle force generated from the biceps brachii at different contraction levels up to about 70% maximum voluntary contraction (MVC). Using MMG amplitude characteristics, the authors also reported that the inability of the MMG amplitude to increase with the intramuscular pressure beyond approximately 70% MVC could describe by the “fusion-like” motor unit contractions due to high motor unit firing frequency (Søgaard et al., 2006).

In the time domain, the muscle activity performance used to estimate muscle torque may be assessed by the MMG signal amplitude parameters RMS and peak-to-peak (PTP) features (Lei, Tsai, Lin, & Lee, 2011). Basmajian and De Luca (1985) had recommended that RMS is the most crucial parameter of muscle electromyographic signal in time-domain analysis. This amplitude parameter of muscle MMG signals which is the mechanical counterpart of EMG" (Beck et al., 2005a), has demonstrated various patterns depending on the nature of muscle action.

Perry-Rana et al. (2002) reported that the relationship between MMG signal amplitude and the workload was quadratic during incremental isokinetic muscle contractions of vastus medialis muscles. Akataki et al. (2004) investigated the relationship between MMG signals (i.e., amplitude and frequency responses) and voluntary force production to understand the motor unit activation strategy underlying the incremental and voluntary muscle force generation. The authors identified that MMG amplitude could be used to explain the motor units' recruitments responsible for muscle contractions, while the MMG frequency may explain the motor unit rate coding or firing rates (Akataki et al., 2004). This observation is important in understanding the recruitment strategy of slow and fast-twitch muscle fibers that work during muscle contraction. MMG signals are consistently applied to study fresh muscle and muscle fatigue contractions, mostly during voluntary muscle contractions and paralysed muscle contraction in healthy or SCI volunteers.

MMG peak-to-peak (PTP) amplitude, is defined by the "distance between the signal peak (highest amplitude value), and the trough (lowest amplitude value)" (Ibitoye et al., 2014b) has also been used to assess muscle performance. However, the application of this parameter is still rudimentary in studying muscle performance, especially in muscle fatigue contraction. The MMG PTP amplitude feature was previously studied in muscle fatigue, involuntary muscle contractions (Orizio et al., 1999), and electrically-evoked muscle contractions to monitor muscle property changes. The consistent reduction (i.e., suggestive of lack of motor unit recovery) in the MMG PTP amplitude showed the reduction of muscle force production during the period of muscle stretching (Esposito, Limonta, & Cè, 2011), sustained muscle contractions, or muscle fatigue (Gobbo et al., 2006; Orizio et al., 1999).

The non-stationarity nature of the MMG signals explain the changes in the muscle fiber length during muscle contractions, the number of active motor units recruitment for a particular muscle action (Alves & Chau, 2008; Alves & Chau, 2010a) and motor units firing rates during different types of muscle actions (Cramer et al., 2005). These variables were identified to vary with the thickness of the tissue between the muscle of interest and the MMG sensor used for MMG signal acquisition (Cramer et al., 2005). The analysed non-stationarity nature of the MMG signal time-frequency domain analysis could also be used. This procedure has enabled the MMG signals to reflect rapid muscle changes underlying various muscle movements during different task execution.

The wavelet transform (WT), short-time Fourier transform (STFT), Wigner-Ville transform were the common joint TF signal processing techniques that have been proposed and applied in MMG signal analyses (Akataki et al., 2004; Barry & Cole, 1990; Beck et al., 2005a). For example, wavelet transform was used to analyse the MMG signals to classify fresh and fatigue muscle contraction in healthy individuals (Al-Mulla & Sepulveda, 2014; Beck et al., 2005b) for prosthesis control amputees during voluntary muscle contractions. For the wavelet transform analysis, the inverse Fourier transform converted the time domain signals into real and imaginary wavelet transformed MMG signals (Beck et al., 2009; Ibitoye et al., 2014b). This study also showed that wavelet bands were different for different muscles, and this was specific to a different ratio of maximum voluntary contraction in isometric muscle contractions over the total MMG signal amplitude (Beck et al., 2009).

Beck et al. (2009) proposed a new wavelet analysis technique where eleven "nonlinearly scaled wavelet filter banks" were used for MMG signal analysis. MMG signal analysis using wavelet transform could analyse dynamic muscle contractions as the MMG signals used for this analysis are non-stationary (Beck et al., 2009).

In pursuit of excellent analysis methods for MMG signal, Ryan et al. (2008b) compared short-time fourier transform (STFT) and continuous wavelet transform (CWT) using MMG center frequency after the signal was transformed. This study showed similarities in the pattern of responses of these analysis methods (Ryan et al., 2008b). One possible explanation could be the study was conducted on isometric muscle contractions, which may be considered stationary.

Armstrong (2011) investigated the MMG intensity as a stochastic signal and a function of time and frequency by applying a filter bank of eleven morlet wavelets and showed an effectual output on the muscle fatigue analysis and postural control. Tarata (2011) investigated the dynamic muscle contractions using CWT combined with the "Mexican Hat" wavelet on fatiguing MMG signals. The authors showed that the MMG signals could show small changes in the muscle contractions, especially during muscle fatigue contractions.

To date, research studies on muscle fatigue classification are sparse; the majority of the available evidence are on prosthetic control using MMG signal and some types of classifiers. Specifically, Xie, Zheng, and Guo (2009) used a "linear discriminant analysis (LDA) classifier" to classify the decomposed MMG signals using "wavelet packet transform," "singular value decomposition," and a distance evaluation criteria's feature selection and achieved 89.7% accuracy between two classes of data (i.e., wrist flexion and extension) which showed a better accuracy compared to using short-time fourier transformation (STFT), stationary wavelet transforms (SWT), and S-transform combined with singular value decomposition (SVD) for MMG signals' feature extraction and decomposition. This study focused on upper limb muscles only and assumed that the

MMG signal was stationary. There is a possibility that dynamic muscle contractions may change the accuracy reported.

Alves and Chau (2010b) recorded MMG signals from the flexor carpi radialis and extensor carpi radialis muscles in 12 able-bodied using two accelerometers to classify three muscle activities of these muscles using pattern classifier. The data obtained were segmented into 256 ms for MMG feature extraction. The accuracy achieved was 89% over five sessions. Furthermore, their study showed that accuracy did not reduce for short-time signals. This classification study was also conducted on upper limbs (i.e., forearm muscle activity). Silva et al. (2005) used MMG signal collected from below elbow during wrist flexion and extension tasks to classify between the two classes of muscle activities to control prosthesis hand to open and closed based on intention infusion with EMG emulation board. Their study sought to classify MMG signals using the RMS amplitude feature for prosthetic control. The classification accuracy of 88% and 71% was subsequently reported in this study for subjects 1 and 2. This research study was conducted only on two individuals, which might be responsible for the low accuracy reported.

Alves, Sejdić, Sahota, and Chau (2010) studied the effect of the location of the MMG sensor (i.e., accelerometer) to classify MMG signal obtained from a single-site forearm in twelve able-bodied individuals. A set of features such as time, frequency, and time-frequency domain features in a total of 70 features were extracted from the MMG signals using a Genetic Algorithm (Gang, Zhiguo, Xiao, Hongbo, & Zhizhong, 2006) with the application of linear discriminant analysis (LDA) classifier to find the accuracy of sensor placement at a different location. This research study reported accuracy of up to 73% and found that the sensor placement affected the performance of the classifiers.

Amaral, Dias, Wolczowski, and Fernão Pires (2012) applied a linear neural network to classify surface EMG and MMG signals for prosthetic control. The classification error reported was 28.4% and 11.1% for MMG and EMG, respectively. This research study was conducted on one participant only, and the experimental setting was not standardised to prevent the activation of extrinsic muscles, which might have contaminate the signal obtained.

Furthermore, apart from LDA, other notable classifiers have been used for MMG signals classifier following the appropriate signal feature extractions. For example, thirteen healthy volunteers had MMG signals acquired from bicep muscle to classify fresh muscle and fatigue muscle contractions during dynamic fatiguing biceps muscle contractions in healthy individuals. The authors used a genetic algorithm to develop a novel pseudo-wavelet function to classify the MMG signals. An accuracy of 80.63% was obtained, which improved the classification accuracy obtained when compared to the results obtained from the standard wavelet functions. Kurzynski, Krysmann, Trajdos, and Wolczowski (2016) proposed a new method for prosthetic control using multi-classifiers. The experiment was conducted on healthy persons using both EMG and MMG signals with a microphone sensor. The results obtained showed that the combined MMG and EMG signals' accuracy for the multi classifier was up to 94%.

These studies suggested that the MMG signals can be applied to complement the performance of surface EMG signals for classification purposes in prosthetic control. The research outcome showed why many classification methods which were already established for sEMG classification were introduced and applied to classify MMG signals for prosthetic control. For example, genetic programming/genetic algorithm was used for sEMG signal feature extraction, and classifications (Al-Mulla, Sepulveda, & Colley, 2011; Kattan, Al-Mulla, Sepulveda, & Poli, 2009). Mel Frequency Cepstral Coefficients (MFCC) has also been applied for sEMG signal classification by Szu-Chen, Maier-Hein, Schultz, and Waibel (2006).

MFCC is the most common and widely used feature extraction method in automatic speech recognition (ASR), and its effectiveness for MMG signal feature extraction for classification was not investigated previously. The literature showed that research studies had not been carried out on applying the MFCC feature for MMG signal feature extractions for clinical applicability. Apart from the dearth of studies on MFCC for MMG feature extractions, the studies discussed so far are limited only to voluntary muscle contractions. The application of FES-evoked muscle contractions (i.e., involving isometric and/or dynamic) may pose different challenges and may be attractive to clinicians managing people with SCI. One of such common clinically relevant activities is FES-supported cycling. Therefore, a new MMG signal feature extraction method using MFCC has been proposed in the current research. The extracted MMG signal features will classify the muscle state into fresh and fatigue contraction during FES cycling. A support vector machine (SVM) classifier will be used for training non-fatigued and fatigue contraction and muscle fatigue pattern recognition during cycling exercises. The principle of FES stimulation is discussed next for involuntary muscle contraction and cycling exercise in persons with SCI.

2.4 The principle of FES system

The electrical stimulation of muscle is the process of artificial elicitation of muscle contractions using electrical signals at tolerable and acceptable thresholds (Enoka, Amiridis, & Duchateau, 2019). For many reasons, this technology is gaining tremendous research and clinical attention. For example, electrical stimulation or neuromuscular stimulation can be used to train strength in abled volunteers, especially athletes. The technology has also been widely used and continues to be re-assessed as a rehabilitative tool to promote functional restoration following a partial or complete motor or sensory loss in persons with paralysis due to SCI, stroke, or other neuromuscular related diseases (Carson & Buick, 2019; Maffiuletti, Minetto, Farina, & Bottinelli, 2011). Essentially, the electrical impulses are delivered by a network of stimulating electrodes to artificially replicate the action potential sent by the central nervous system to activate muscle contractions (Martin, Sadowsky, Obst, Meyer, & McDonald, 2012; Rattay, 1999). The muscle contraction is controlled by providing electrical impulses at predetermined amplitude/voltage, frequency, and pulse width to the specified specialised electrodes placed on the target muscle for contraction.

Typically, an FES system comprises of (a) a controller, (b) a stimulator, and (c) electrodes. The main focus of this research in on the controlling methods being the thesis focus. The literature review discussion mainly covers the FES control system and the feature extraction methods for the feedback signal to control the FES system. The FES controller controls the stimulation parameters amplitude, pulse width, and frequency generated by electrical circuits and also be able to monitor muscle using sensor feedback. The stimulator circuit produces either voltage or current controlled monophasic or biphasic electrical pulses, while electrodes deliver the produced electrical pulses to the nerve. (K. W. E. Cheng et al., 2004; Fisekovic & Popovic, 2001). Broadly categorised, two methods are used in developing an FES system, including (1) an open-loop system and (2) a closed-loop system.

In an open-loop system, the stimulator operation does not consider any changes in the muscle performance, such as muscle fatigue or muscle response, and lacks adaptive FES parameters control (Li et al., 2018). Such a system only receives the stimulation command from the controller to the stimulator for delivering electrical pulses to the muscle via a pair of stimulating electrodes. In this case, there is no feedback on muscle performance to improve the FES system performance in an open-loop FES system. This technique was used in earlier designs due to its comparative ease of design, implementation, and use (Ibitoye, Hamzaid, Abdul Wahab, Hasnan, & Davis, 2020a; Jezernik, Wassink, & Keller, 2004; Li et al., 2016).

Most of the available FES systems operate in open-loop and are used for therapy (Benoussaad et al., 2015; Ibitoye et al., 2020a). However, in the application of this FES technology to rehabilitate persons with SCI, early onset of muscle fatigue is a significant limitation (Ibitoye et al., 2016a; Koutsou, Moreno, Ama, Rocon, & Pons, 2016; Ruslee, Miller, & Gollee, 2019) and this generally characterises artificial muscle stimulation by FES technologies (Buckmire, Arakeri, Reinhard, & Fuglevand, 2018). As the clinical conditions of persons with SCI may deprive them of sensation, they are unable to manually regulate the parameters of the FES system for optimal performance and clinically significant benefits. The open-loop performance can often be worse in the presence of muscle fatigue and/or muscle spasm. The inability to regulate the FES administration manually may lead to muscle damage and other secondary complications (Fouré et al., 2014; Nosaka, Aldayel, Jubeau, & Chen, 2011).

Therefore, for optimal application of FES technology for the rehabilitation of persons with SCI, a closed-loop model of the FES system has been recommended (Lynch & Popovic, 2008). The closed-loop system incorporates feedback or response from the muscle performance to regulate or control the FES system operation (Figure 2.2). The FES parameters can be modified and optimised according to the stimulator's performance response or reference point with this arrangement.

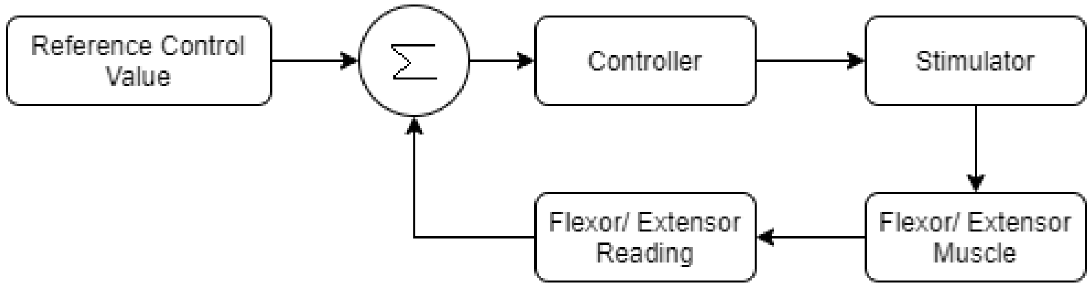

Figure 2.2: A scheme of a closed-loop FES system modified from (Lynch & Popovic, 2008)

2.4.1 Overview of closed-loop FES system

This subsection describes the rationale and strategies for realising a closed-loop FES control system applicable to the current research field. The closed-loop FES system, which is designed to remedy the limitation of open-loop FES systems, is based on the general principle of a closed-loop system. One way to realise a closed-loop FES system is to give feedback on the muscle performance/response signal to regulate the FES parameters. The significant advantage of this approach is that individual muscle responses, which may differ from one person to another, will be used to regulate the FES operation. Therefore, efficient muscle performance monitoring using an accurate and reliable muscle performance proxy would be beneficial to achieving this system (Ibitoye et al., 2016a). The muscle performance proxy should be robust enough to discriminate among different muscle states based on the type of activities under consideration. The muscle performance proxy should identify the fresh muscle contractions and differentiate this from fatiguing muscle contractions using an appropriate classifier through pattern recognition.

2.4.1.1 FES closed-loop system with non-muscle response feedback

There are several approaches to realised closed-loop control of FES systems, and these can be categorised into non-muscle and muscle response feedback systems. Extensive research efforts have been expended on applying the biopotential of muscle origin (i.e., sEMG and MMG) proxy for muscle performance. Specifically, there have been many ongoing research studies for SCI to control the FES-evoked muscle contractions during fresh and muscle fatigue contractions for optimal rehabilitation outcomes. The main objective of a closed-loop FES system is performance optimisation and elimination of manual control methods whereby the only muscle response indicator is the feedback to control the FES system. Many approaches have been investigated in the literature to realise the feedback control signal.

One way to realise this had been previously investigated (Gwo-Ching et al., 1997), where knee joint control was used to control knee activity during a knee exercise on a Cyber 350 dynamometer. These authors designed a neuro-controlled system to control knee joint position using FES stimulation of quadriceps muscles in a person with paraplegia and a healthy volunteer. The experiment was conducted on a Cybex 350 isokinetic dynamometer (Gwo-Ching et al., 1997). The control algorithm used consisted of a proportional-integral differential (PID) and neuro-PID controller in series with a nonlinear function that related PID output (i.e., the muscle force needed for the desired knee angle maintenance) (Figure 2.3) to the stimulation pulses' duration. The performance of their designed controller was evaluated by applying a disturbance that caused the study's participants to bend at the hip. After that, the speed of disturbance rejection by the controller was recorded for assessment. The result showed that for the healthy subject, the tracking RMS error was 7.24º for the neuro-PID controller, 8.15º for the neural controller alone, and 17.86º reported for the PID controller alone. While for paraplegic neural controllers alone and neuro-PID controller tracking, RMS error was 9.57° and 7.18° subsequently. The performance of the PID controller alone was significantly less than the other two controllers.

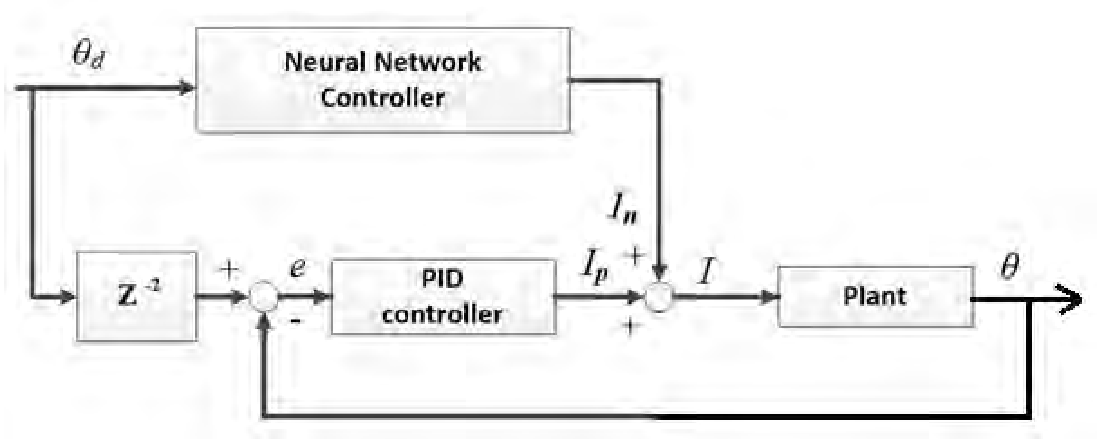

Figure 2.3: The block diagram of a neuro-PID control system. Reproduced with permission from the publisher (Gwo-Ching et al., 1997)

As the patient's safety is essential, designing a safe FES control study protocol has been an exciting research objective. The nature and characteristics of the study participants and the target population should be considered in the experimental setup to preclude the adverse effect of the controller's response during testing as the action may be from the controller or whether the participant's stabilisation is voluntary with a support bar. One standard controller that is frequently used in the FES closed-loop system is the PID controller. A servo potentiometer was also used to measure the joint angle as feedback to the controller (Wood & Dunkerley, 1999). Their results showed that the PID controller aided paraplegic standing, though with some reported physiological complications due to the setting of parameters. The authors suggested that the experimental setting may require better stimulator parameter tuning to prevent muscle spasms and other related physiological abnormalities.

In another study, PID controller was used in closed-loop control of the standing-up movement of paraplegic individuals (Yu, Chen, & Ju, 2001) and compared knee end-velocity (KEV) with open-loop and on/off control methods. Two paraplegic subjects were included in the standing control experiment. The result showed that KEV was 164.63 deg/s (minimum) and 223.71 deg/s (average) in four different ramp-up values, while average KEV was very minimal compared to open-loop is 13.41 deg/s in on/off control method. On the other hand, PID controller KEV was 11.37 deg/s, near the on/off control system. The authors suggested that the closed-loop control system can delay muscle fatigue.

One research group Hunt, Jaime, and Gollee (2001), proposed another FES controller's approach based on H∞ to control ankle moment (Figure 2.4). The H∞ controller ensures stability, especially when the nominal models of the plant and the uncertainties in the system are accurate and can compensate for the included perturbations in the plant model. This study showed that the tracking of the ankle moment and the disturbance-rejection tests were adequately maintained by the H∞ in healthy volunteers. Testing FES controllers' performance on healthy subjects may be challenging as they might inadvertently contract their muscles voluntarily. Therefore, the results obtained for able-bodied people may differ from the outcomes expected from persons with SCI.

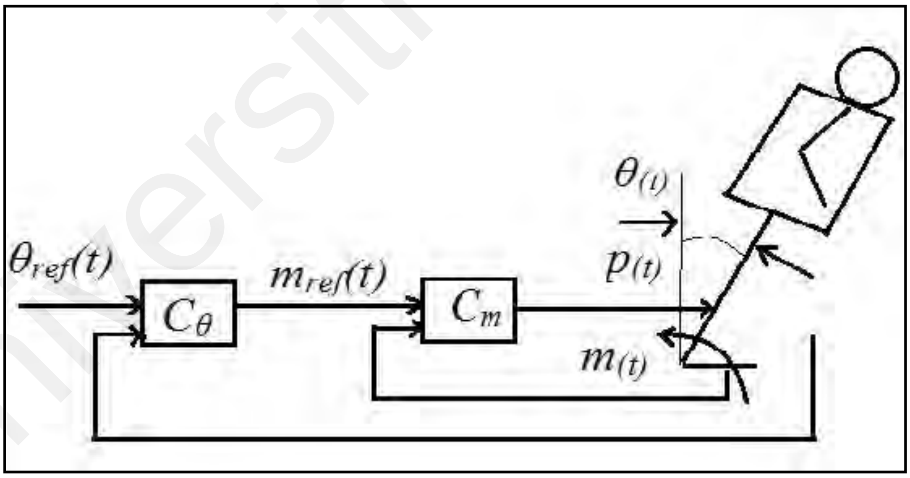

Figure 2.4: Nested-loop control structure. Reproduced with permission from the publisher (Hunt et al., 2001)

Furthermore, Ferrarin, Palazzo, Riener, and Quintern (2001), conducted a study on two trained persons with SCI using four controllers based on knee angle measurement with the electrogoniometer as feedback. When tracking a sinusoidal reference, the RMS errors for each controller after 2 min of adaptation were (i) 11.7^0, (ii) 6.0^0, (iii) 4.6^0, and (iv) less than 10^0 for open-loop, closed-loop PID controller, feed-forward feedback controller, and adaptive controller subsequently (Figure 2.5). In addition, the average lag for the same tracking task was reported as (i) 0.18 s, (ii) 0.29 s, and (iii) 0.18 s. However, the lag was not reported for the adaptive controller because the lag changed during the adaptation process. These results showed that the performance of the combined feedforward feedback controller was the best. Additionally, the imperfection of the inverse model could also be noted as it neglected the "noninvertible model components" (i.e., time delays and saturation effects), which could significantly degrade the feedforward-feedback controller's performance.

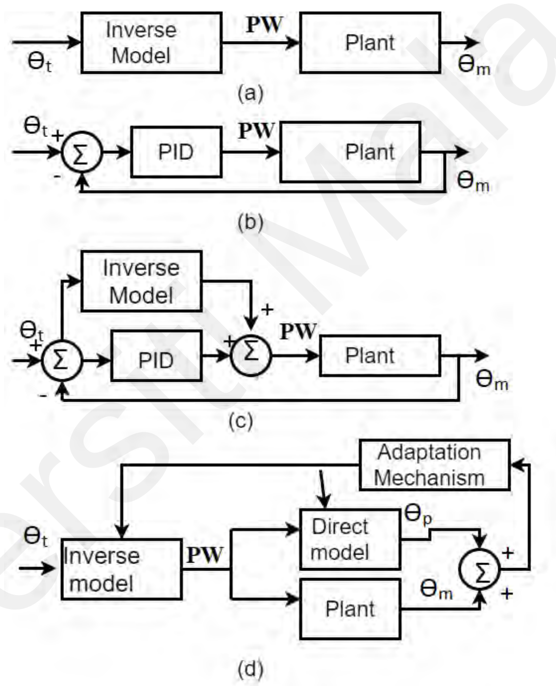

Figure 2.5: The control systems evaluated in (Ferrarin et al., 2001)'s study. (a) Open-loop controller. (b) Closed-loop PID controller (c) Combination feed-forward feedback controller. (d) Adaptive controller

Chen et al. (2001) proposed a real-time closed-loop control FES system developed using a position sensor as the feedback to the stimulator. This sensor could be automatically adjusted during gait training, which was evident in the hemiplegic patient recruited for their study (Chen et al., 2001). The results obtained showed significant improvement in the patient's "mean velocity, cadence, stride length, active ankle motion range, and functional ambulation category.". This outcome was encouraging despite only one subject was recruited for this closed-loop study which may be considered low number of participants.

In another study (Jezernik et al., 2004), a novel FES closed-loop system was designed using a mathematical neuromuscular skeletal model (Figure 2.6). The study was based on a computer simulation and experimental study with six healthy volunteers and two individuals with SCI. Their results revealed that the RMS tracking errors of knee angle were 2.92º and 4.33º, respectively, for the computer simulation and experimental studies. These values could encourage and promote optimisation (Gwo-Ching et al., 1997) for FES control systems. However, physiological muscle conditions, including muscle fatigue, muscle spasm, and others, may warrant additional features to be analysed to design a robust FES control system. Nonetheless, other researchers Ebrahimpour and Erfanian (2008), observed the limitation of this FES control design. Their observation had to do with the approximation in the derivation of the control law that may violate the reaching condition, which could introduce some parasitic unmodeled dynamics in the sliding-mode control loop.

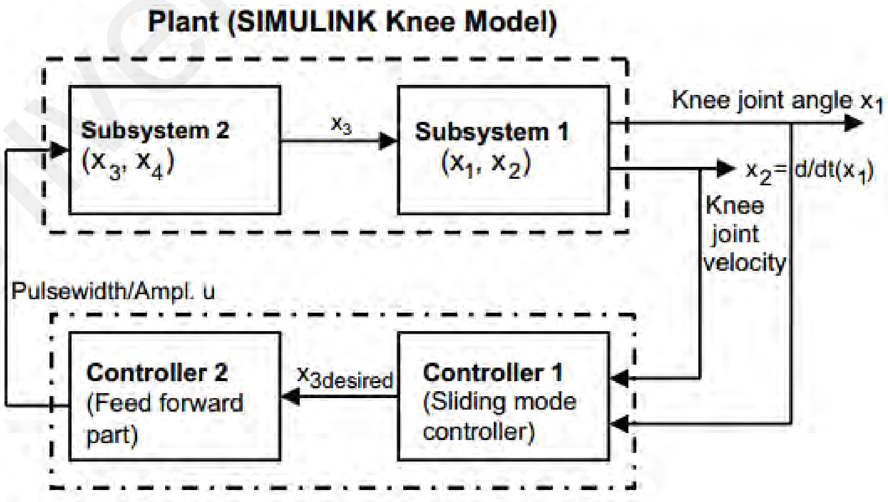

Figure 2.6: FES sliding mode controller. Reproduced with permission from the publisher (Gwo-Ching et al., 1997)

To improve the performance of some notable controllers, Previdi, Ferrarin, Savaresi, and Bittanti (2005) designed a closed-loop FES system to support standing up and sitting down using FES with the flexion goniometer as the response feedback (Figure 2.7). In the control of this strategy, two loops were used. The first loop consisted of a PID controller to make the system stable, and the second loop was the outer loop virtual reference feedback tuning (VRFT) used to deal with the linear and nonlinear control behavior. The simulation results showed that the proposed method was effective within the tracking deviation range of ±0.6 to the nonlinear test. However, the controller response was not tested on humans, which might have a different outcome.

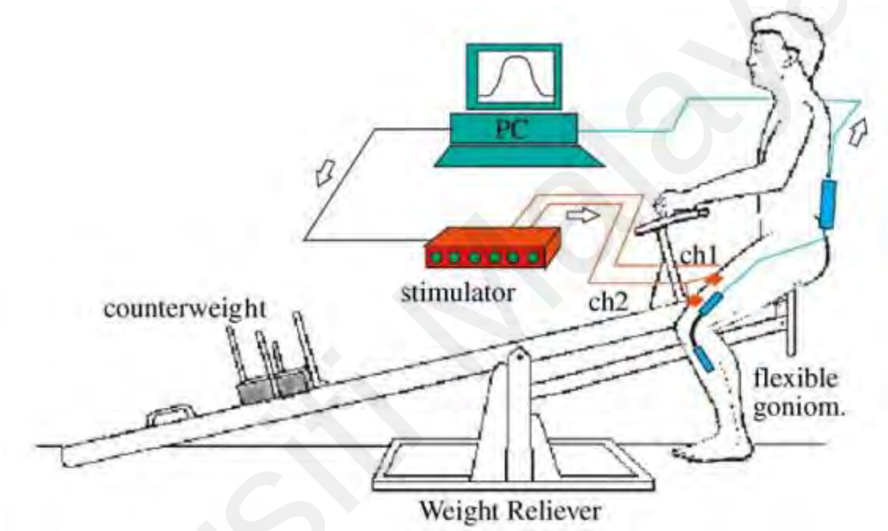

Figure 2.7: Schematic of the experimental setup. Reused with permission from the publisher (Previdi et al., 2005)

Lynch and Popovic (2012) investigated three different closed-loop control systems for FES applications. These controllers are PID control (Re, Krans, Schultheiss, & Gerber, 1994), gain scheduling control (GSC), and sliding mode control (SMC). These controllers were used to control the knee movement when the FES was applied on the quadriceps muscle of three individuals with SCI and one able-bodied volunteer. After introducing naturally occurring disturbances (i.e., muscle spasm, muscle fatigue, and other muscle responses due to muscle retraining) in the simulation, all the tested controllers demonstrated significant degradation. The authors suggested fine-tuning the control methods and algorithms for better performance, especially in real-world situations.

In another study, Itakura, Fujita, Kubo, Iguchi, and Minamitani (1988) applied the Kitamori controller to control FES-evoked muscle contractions. This controller was unstable with the unavoidable change in muscle response to FES during contractions. This situation could be improved by introducing an adaptable stimulation parameter system (i.e., to vary the stimulation parameter based on the muscle properties during contractions). However, the adaptive system was less stable when compared to the Kitamori controller. The results of the simulation conducted by the authors revealed a better control system that included an adaptive controller and a hybrid PI (proportional-integral). Popov, Đozić, Stanković, Krajoski, and Stanišić (2015) also designed an FES-closed-loop system using Proportional-Integral (PI) controller method using the flexion angle to control the joint torque. While keeping the pulse amplitude and frequency constant and controlling the stimulation by varying the pulse width, the authors concluded that the PI controller can control joint torque based on the results obtained.

Downey, Bellman, Kawai, Gregory, and Dixon (2015) developed an FES closed-loop controller for asynchronised stimulation to reduce the early onset of muscle fatigue using knee angle feedback measurement. Four healthy volunteers were recruited to test the performance of the controller. The method applied in their study (Downey et al., 2015) included four channels of asynchronous stimulation with the conventional single-channel stimulation strategy. This control system was designed to avoid the complex "knee-shank tracking" of the desired trajectory instead of a switching simulation channel to reduce muscle fatigue (Downey et al., 2015; McDonnall, Clark, & Normann, 2004). Their results showed that the applied asynchronous stimulation prolonged the stimulation duration, which could be used for feedback control to the stimulator.

2.4.1.2 FES closed-loop system with muscle response feedback

This subsection discusses the closed-loop FES systems that use muscle feedback sensors in the control system. Zhang and co-authors (Zhang, Hayashibe, & Azevedo-Coste, 2013) proposed biopotential of muscle origin based on sEMG signal as an input signal to control the FES closed-loop system. The artificial neural network implemented this to control joint torque (Figure 2.8). The experimental study was conducted on two able-bodied volunteers. Their results showed that the average RMS error with torque was <4.5%, while the sEMG-based RMS error was <10.5% without the torque. These results could be ajudged satisfactory for use in FES closed-loop systems. However, the application of this method of control in persons with SCI was not verified.

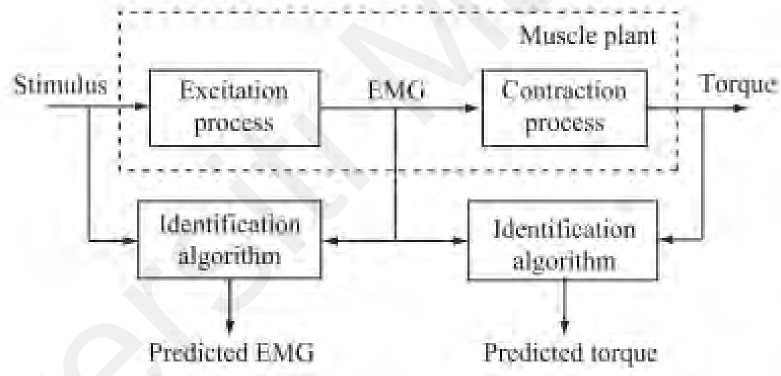

Figure 2.8: The structure of the stimulated muscle model for model identification. Note that the muscle contraction dynamics model relates sEMG to torque and the excitation dynamics model relates stimulation to sEMG. Reproduced with permission from the publisher (Zhang et al., 2013)

It is important to test the controller in isolation of voluntary muscle contractions to ensure that the controller's performance is efficient. This practice will ensure that any muscle contraction results from FES-evoked contractions via the FES controller and not by the voluntary effort of the subject. This exercise can be achieved by recruiting individuals with a motor complete SCI. Once the efficacy of a closed-loop FES controller is established this way, the controller can apply to other types of FES closed-loop systems for efficient stimulation of individuals who have different types of SCI either affecting only their sensory, only their motor, or both functions.

Another closed-loop FES system was proposed by Yusoff and Hamzaid (2014). This study was designed to measure the voltage (Figure 2.9) across the muscle during FES-evoked muscle contractions in four able-bodied volunteers to find the pattern of relationships between the FES-evoked contractions and the generated voltage from contracting muscle based on Ohm's law.

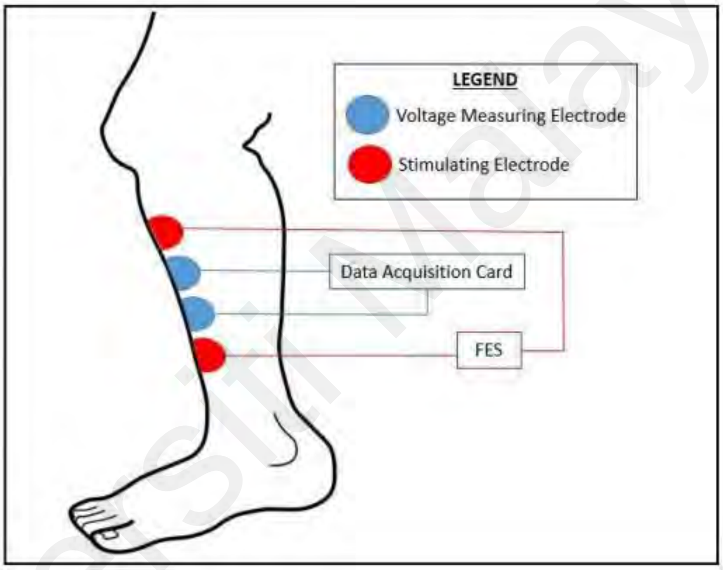

Figure 2.9: Example of stimulation electrodes and voltage measuring electrode placements. Reproduced with permission from the publisher (Yusoff & Hamzaid, 2014)

The study (Yusoff & Hamzaid, 2014) showed that the range of measured voltage least affected by noise was above 0.1 V at room temperature. It was observed that the recorded voltages satisfied Ohm's law with the recorded voltage that had a stimulating current relationship that was positively linear ($r = 0.98$). However, complex muscle behavior such as muscle fatigue and spasm that often characterise FES-evoked muscle contractions were not investigated.

Li, Hayashibe, Andreu, and Guiraud (2015) conducted a study to control muscle activation through online modulation of FES pulse width (Figure 2.10) using eEMG feedback system. The experimental study was conducted on one able-bodied volunteer, and four reference points were given to validate the FES closed-loop system. RMSE error of 0.05 ± 0.01 and the mean value account for (VAF) 92.70 ± 2.33 (%) were obtained.

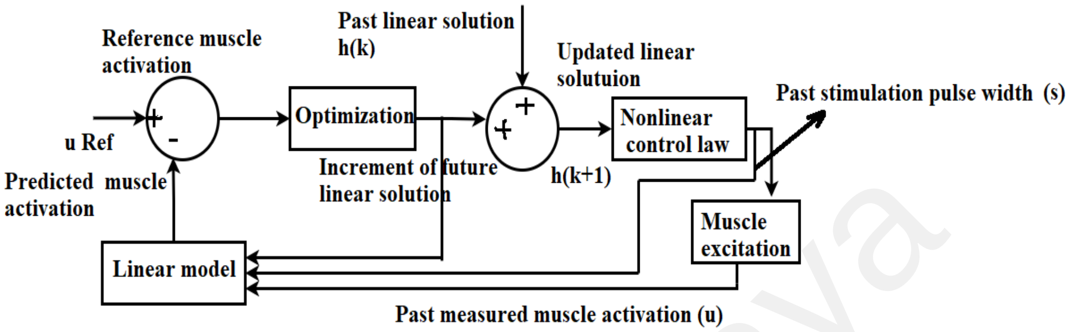

Figure 2.10: Process of predictive model control of FES-muscle activation. Reproduced with permission from the publisher (Li et al., 2015)

A pilot study by (Braz et al., 2016) presented a novel motion sensor-driven FES closed-loop system for gait control. The authors applied four miniaturized motion sensors as kinetic feedback sensors with finite-state controlled method in two persons with complete paraplegia. The proposed system controlled the knee extension using quadriceps and gluteus muscle stimulation during stance. When evaluated against the conventional open-loop FES system during leg swing, the results showed that the closed-loop FES system performed more efficiently. However, some adjustments were suggested for significant improvement of this method on the traditional open-loop FES methods.

Another closed-loop study was conducted by Li et al. (2017) using eEMG sensor as feedback for a real-time closed-loop FES system to control muscle activation by modulating stimulation pulse width on triceps surae and tibialis muscle group. The experiment was performed on five SCI and three able-bodied volunteers. The sEMG signals were acquired by the Biopac data acquisition system and processed in the closed-loop controller as a reference point to produce muscle activation patterns by sending computed pulse width signals to the stimulator using the basic access network controller. The muscle activation control result for healthy volunteer average variance (VAF) was 90.71% ± 5.10 with an average root mean square error of 6.59% ± 2.60%. While for SCI volunteers average, VAF and RMSE were 81.40% ± 6.44% and 8.08% ± 4.80% subsequently. However, the resulting outcome was computed with unequal trial sets for both healthy and SCI volunteers, which might have affect the results.

From the literature discussed so far, most of the available closed-loop systems depended on the joint angle, torque (i.e., often difficult to assess directly during muscle contractions), or sEMG, which is a reliable signal with muscle response during FES-evoked muscle contraction, remains debatable due to stimulation artefacts. On the other hand, researchers are currently exploring in developing other FES closed-loop systems using MMG as a feedback signal. MMG relationship with muscle response has been applied to control both lower and upper limbs prostheses (Hong-liu, Sheng-nan, & Jia-hua, 2010; Wilson & Vaidyanathan, 2017) during static and dynamic muscle actions (Antonelli, Zobel, & Giacomin, 2009; Silva et al., 2005; Xie et al., 2009). Unlike sEMG, MMG is not affected by factors such as sweat or skin impedance (Wilson & Vaidyanathan, 2017; Woodward, Stokes, Shefelbine, & Vaidyanathan, 2019) and is insensitive to stimulation artefacts during FES-evoked contractions (Woods, Subramanian, Shafti, & Faisal, 2018). MMG-based closed-loop FES system in cycling was proposed using pedal force and MMG sensor to control cycling speed. The system was prepared to adjust stimulation parameters to maintain the desired cycling speed based on the PID controller's feedback. However, due to encoder angle measurement error, the MMG sensor was not used in the closed-loop algorithm.

The application of the MMG as a reliable muscle performance indicator was investigated previously during voluntary and FES-evoked contractions (Ibitoye et al., 2014b; Orizio et al., 1999). Dzulkifli, Hamzaid, Davis, and Hasnan (2018) where artificial neural network (ANN) was used to monitor knee torque production during FES-assisted knee extension and standing in persons with SCI. The average correlation of 0.87 and 0.84 was reported between the knee extension and generated torque with root mean square (RMS)-MMG amplitude only and with RMS and zero-crossing (ZC)-MMG. Another study (Ibitoye et al., 2016c) estimated the FES-evoked knee extension torque using MMG in eight able-bodied volunteers. Support vector regression modeling technique was used to predict torque from the MMG. The torque prediction accuracy reaching up to 94% has been reported. As these observations could not be used to infer the model response of FES-evoked contractions in persons with SCI due to lack of motor function, researchers (Ibitoye et al., 2020b) assessed the support vector modeling performance using persons with complete motor SCI. Prediction accuracy of up to 94% and RMSE of not more than 9.82% was reported by Ibitoye et al. (2020b).

2.5 Procedure for FES parameter optimisation to support standing

Physical activity restoration following SCI is a priority for an individual with a physical disability due to SCI. FES-supported activities are one way to achieve independence after SCI. Earlier researchers (Andrews, 1988; Bajd, Kralj, & Turk, 1982) also implemented FES-supported standing exercises to improve the quality of life of paraplegic individuals by assisting standing and walking. Muscle fatigue limits FES standing due to synchronised high-frequency stimulation on the quadriceps (Andrews, 1988). However, FES performance depends on how efficiently its parameters could be optimised for efficient utilisation for standing support. Previous studies (Bijak et al., 2005; Cameron & Alo, 1998; Rouhani, Rodriguez, Bergquist, Masani, & Popovic, 2017) have explored several methods of FES parameters optimisation (i.e., to prevent rapid onset of muscle fatigue which could preclude the optimal performance of FES) for function restoration. As a significant limitation of FES for application in neuroprosthesis

(Rouhani et al., 2017), rapid onset of muscle fatigue could be put under control with efficient FES parameter optimisation procedures (Ibitoye et al., 2016a; Karu, Durfee, & Barzilai, 1995; Thrasher et al., 2005). Among the commonly used methods for efficient FES parameter optimisation are stimulation patterns (Gorgey et al., 2015; Karu et al., 1995) modification and stimulation electrode positioning optimisation (Downey et al., 2015; Popovicc & Malesevic, 2009).

Rouhani et al. (2017) introduced a pulse amplitude and pulse duration optimisation algorithm for a current-controlled FES system to minimise muscle fatigue and achieve a set ankle joint torque level. This procedure facilitated the fatigue reduction by an average of 22.5% and 6.6% based on the fatigue-time and torque-time integral, respectively. Bijak et al. (2005) aimed to achieve natural leg movement during gating by optimising the delivery of stimulation parameters using eight different stimulation channels. Unfortunately, with this approach, while an improved knee trajectory could be achieved, the participants' demand for safety that warranted overstimulation led to the early onset of muscle fatigue.

Based on the discussed literature information and the previous knowledge on muscle assessment, exploration of MMG signal as an indicator of muscle response during FES-evoked contractions, especially during physical task execution such as cycling and standing, needs further investigation. This current thesis aims to answer this question and advance the MMG application as a feedback signal for real-time control of closed-loop FES systems during cycling and standing in persons with SCI. Table 2.2 summarises the findings of FES systems using different control algorithms and stimulator parameters in their experiments for the desired outcomes.

Table 2.2: Literature review summary of FES systems and their control parameters

Author and year	FES control parameter	Muscle fatigue consideration	Feedback control system	Control type (algorithm)	Number of subjects
(Gwo-Ching et al., 1997)	Amplitude (0-80 mA)	Yes	Isokinetic dynamometer (angle)	PID	One AB and one paraplegic
(Wood & Dunkerley, 1999)	Not specified	No	Knee angle	PID	One paraplegic
(Yu et al., 2001)	Amplitude (40-120 mA)	No	Knee end-velocity	PID, on/off	Two SCI
(Hunt et al., 2001)	Pulse width (0-500 µs)	Yes	Ankle moment	Nested loop control	One AB male
(Ferrarin et al., 2001)	Pulse width (0-520 µs)	Yes	Electrogonimeter/knee angle	Open-loop, PID, feed-forward feedback, and adaptive control	Two SCI subjects
(Y. L. Chen et al., 2001)	Amplitude (0 -100 mA)	No	Foot switch/Position sensor	N/A	One hemiplegic
(Jezernik et al., 2004)	Pulse width (0-600 µs) and Amplitude (0-125 mA)	Yes	Knee angle	N/A	Six AB and two SCI
(Previdi et al., 2005)	Pulse width and frequency (not specified)	No	Goniometer (joint angle)	PID and VRFT	One paraplegic
(Lynch & Popovic, 2012)	Pulse width (0-250 µs)	Yes	Knee angle	PID, GSC, SMC	One AB and three SCI

Table 2.2: Continued

Author and year	FES control parameter	Muscle fatigue consideration	Feedback Control Variables	Control type (algorithm)	Number of subjects
(Itakura et al., 1988)	Amplitude (4-10 mA)	No	Ankle force	Adaptive PI	N/A
(Popov et al., 2015)	Pulse width (200-300 µs)	No	Wrist torque	PI	Three AB
(Downey et al., 2015)	Amplitude (0-126 mA) and pulse width (20-500 µs)	Yes	Knee angle	Asynchronized stimulation	Four AB
(Zhang et al., 2013)	Pulse width (0-450 µs)	No	EMG (joint torque)	GPC and Closed-Loop Implementation of the Dual Predictive Controller	Two AB
(Yusoff & Hamzaid, 2014)	Amplitude (23 -43 mA)	No	Voltage measure using Ohm's law	N/A	Four AB
(Li et al., 2015)	Pulse width (0-200 µs)	No	EMG (muscle activation)	Adaptive Model Predictive Controller	One AB
(Braz et al., 2016)	Amplitude (0-180 mA)	Yes	Motion sensor (walking)	Finite-state controller	Two SCI paraplegic
(Li et al., 2017)	Pulse width (0-450 µs)	Yes	EMG (muscle activation)	Adaptive model predictive controller	Five SCI and three AB
(Woods et al., 2018)	Amplitude (0-50 mA) and pulse width (0-250 µs)	No	Crank encoder angle/MMG	PID	One AB

Table 2.2: Continued

Author and year	FES control parameter	Muscle fatigue consideration	Feedback Control Variables	Control type (algorithm)	Number of subject
(Ibitoye et al., 2016a)	N/A	No	MMG and torque	N/A	Six SCI
(Ibitoye et al., 2020b)	N/A	No	MMG and torque	N/A	Eight SCI
(Rouhani et al., 2017)	Amplitude (30-50 mA) and pulse width (150-450 µs)	Yes	Torque sensor	Parameter optimisation	Three AB
(Bijak et al., 2005)	Amplitude (0-50 V)	Yes	Foot position	Parameter optimisation	Twelve SCI

* AB = able bodied / healthy subject, N/A = not applicable

CHAPTER 3: MECHANOMYOGRAPHY-BASED MUSCLE FATIGUE DETECTION DURING ELECTRICALLY-ELICITED CYCLING IN PATIENTS WITH SPINAL CORD INJURY

3.1 Introduction

Spinal cord injury (SCI) could lead to partial or complete paralysis of the upper and/or lower limbs, depending on the level and severity of the injury. SCI causes complications including pressure sores (Liu et al., 2014), muscle spasticity (Elbasiouny et al., 2010), loss of muscle strength, cardiovascular disease (Julio & Michael, 2008), and osteoporosis (Tan et al., 2013). Functional electrical stimulation (FES)-evoked cycling can improve health benefits, including increased muscle strength, volume, insulin sensitivity, glucose metabolism, and endurance (G. M. Davis, Hamzaid, & Fornusek, 2008). In all FES applications, however, fast muscle fatigue is apparent due to the inverse recruitment of motor units (Chou & Binder-Macleod, 2007). It has also been reported that overloading the stimulated muscle might lead to muscle damage (Fouré et al., 2014). These drawbacks limit the FES functional capacity which needs be overcome to optimise the training and functional benefits of FES. As a result, monitoring muscle condition during FES-evoked cycling is required when training the muscle for a longer period.

Physiologically, muscle fatigue is defined as the drop of muscle force during a continuous steady muscle contraction (Wigmore, Befroy, Lanza, & Kent-Braun, 2008). Several methods evaluate muscle fatigue, including torque response (Kent-Braun, Callahan, Fay, Foulis, & Buonaccorsi, 2014) and joint angle measurement (Weir, McDonough, & Hill, 1996). Surface electromyography (EMG) is another non-invasive method to evaluate FES-evoked muscle contraction and fatigue. However, this technique is not well adopted practically due to the interference from the electrical stimulus and motion artefacts or the surrounding noise. Incorporating additional circuits can help to avoid amplifier saturation and blank stimulation artefacts. Nevertheless, the complexity of these circuits (Islam, Sundaraj, Ahmad, & Ahamed, 2013) may lead to challenging fatigue evaluation.

Mechanomyography (MMG), a technique that measures mechanical muscle response, including muscle vibration, has been used to evaluate muscle activities (Islam et al., 2013) and muscle fatigue (Tarata, 2003) involuntary contractions (Xiaogang, William, & Nina, 2014). Dynamic muscle contractions, including concentric and eccentric contractions, produce force (Mohamad, Hamzaid, Davis, Abdul Wahab, & Hasnan, 2017). Such contractions, which are caused by the recruitment of motor units (MU) in response to the MU firing rate, can be monitored using MMG. Several studies have reported the correlation of MU recruitment and firing rate of the muscle fibers with MMG amplitude during motor nerve stimulation (Barry & Cole, 1990; Orizio, 1992; Orizio, Liberati, Locatelli, Grandis, & Veicsteinas, 1996). MMG parameters in time, frequency (Ryan et al., 2008b), and joint time-frequency (TF) (Al-Mulla & Sepulveda, 2014) domains were analysed during isometric FES-evoked contractions. However, given the inconsistent loading and non-stationary nature of muscle contraction during FES cycling (Bonato et al., 2001) MMG responses in the time and/or frequency domains of dynamic evoked-muscle force patterns were reported to be nonlinear (Hong-Bo et al., 2009). This nonlinearity may be due to several factors, including changes in the muscle fiber length, the number of active motor units, firing rates, and thickness of the tissue between muscles (Bonato et al., 2001; Cramer et al., 2005).

In order to analyse the non-stationary MMG signals, wavelet transform (WT), short-time Fourier transform (STFT), and Wigner-Ville transform as joint TF signal processing techniques were proposed (Akataki et al., 2004; Barry & Cole, 1990; Xie et al., 2009). The wavelet transform has been used in several kinds of research to describe non-stationary MMG signals produced during dynamic muscle contractions. Beck et al. (2009) proposed a new wavelet analysis method where 11 non-linearly scaled wavelet filter banks were used to analyse MMG signals. The intensity of the MMG signals was proposed to be used in statistical pattern identification of dynamic muscle contractions.

Furthermore, Ryan et al. (2008b) compared short-time Fourier transform (STFT) with continuous wavelet transform (CWT) for MMG signal analysis and showed that these two were similar in response. Xie et al. (2009) proposed several features such as STFT, short wavelet transform (SWT), wavelet packet transform (WPT), and S-transform joined with singular value decomposition to classify different hand motion patterns including wrist flexion, extension, open and grasp using MMG signals for prosthetic control that achieved 89.7% accuracy.

A work by Silva et al. (2004) acquired MMG signals from a microphone-accelerometer sensor pair to classify two activities of the prosthesis to control wrist extension and wrist flexion using the RMS feature. The classification accuracy achieved from the two subjects was around 70% based on their cross-validation tests. However, this work focused on the RMS feature and did not consider any time-frequency domain features. Subsequently, in another work, Silva et al. (2005) improved the RMS-based MMG signal classification accuracy of muscle activity for opening and closing the prosthesis by coupling the accelerometer-microphone sensor and MMG socket to eliminate the interference of the recorded signal. The experiment was performed on two subjects, and the improved accuracies attained were 88% and 71% for each subject, respectively. However, the number of recruited subjects was relatively low for classification.

Alves et al. (2010) used a Genetic Algorithm for MMG signal feature extraction based on a linear discriminant analysis (LDA) classifier to determine the effect of the single-site forearm accelerometer location. It was reported that the placement of five accelerometers on a single-site forearm achieved group accuracy of nearly 73% for all three classes of muscle actions. However, the classifiers were vulnerable to the changes in forearm position and longitudinal and transverse displacements of the sensors.

Many researchers have extracted features from MMG signals using genetic programming, genetic algorithms (Al-Mulla & Sepulveda, 2014; Kattan et al., 2009), statistical analysis (Al-Mulla & Sepulveda, 2010; Al-Mulla, Sepulveda, Colley, & Al-Mulla, 2009), and wavelet transform (Beck et al., 2005b). However, to date, Mel Frequency Cepstral Coefficients (MFCC) feature has not been introduced to perform MMG signal analysis of dynamic muscle contraction.

The most prevalent and widely used MFCC feature was in automatic sppech recognition applications. In speech recognition, uttered speech is considered dynamic due to its frequency changes with each speech signal. Similarly, muscle generates low frequency (5-50 Hz) vibration (Silva et al., 2005). Additionally, several researchers have reported that MMG frequency (mean power frequency, median frequency) signal pattern changes when the muscle is artificially stimulated (Esposito, Orizio, & Veicsteinas, 1998; Kouzaki, Shinohara, & Fukunaga, 1999; Orizio, 1992; Peters & Fuglevand, 1999). One related work by Doulah and Fattah (Doulah & Fattah, 2014) proposed the MFCC feature application to classify normal and neuromuscular diseased muscles using EMG. The researchers employed the MFCC feature with motor unit action potential rather than the direct MFCC feature of an EMG signal by template matching decomposition method. The MFCC feature achieved a total classification accuracy of up to 92.50%.

This study hypothesized that dynamic muscle force response of eccentric and concentric contractions (muscle length changes) during FES-evoked cycling can be extracted directly from the muscle surface using MMG-derived MFCC feature and evaluated with a Support Vector Machine (SVM) and that the MMG signals can be classified as “non-fatigued” and “fatigued.” The proposed MFCC classification accuracy was compared to RMS features. The accuracy of fatigue prediction among subjects using MFCC in comparison to the generally adopted RMS feature was analysed.

3.2 Methods

3.2.1 Participants

Five individuals with SCI with American Spinal Injury Association Impairment Scale (ASIAIS) classification A and B, implying no voluntary motor control (Kirshblum et al., 2011), were recruited from the University of Malaya Medical Centre, Kuala Lumpur, Malaysia. Participants volunteered to participate in this study (Table 3.1) after giving their informed consent. This study was granted by the University of Malaya Research Ethics Committee (Approval No: 1003.14 (1)). All participants understood the study protocol. The subjects' exclusion criteria were: subjects with metal implanted in the stimulated limb, cognitive impairment or without tolerance to FES sensation, severe spasticity (Elbasiouny et al., 2010), which is related to muscle tone and stiffness (Moon, Choi, & Park, 2017), and undesirable muscle responses (i.e., muscle spasm) from quadriceps muscle as determined by a certified physician. Participants were asked to abstain from any FES-related exercise at least 48 hours before the testing (Bickel, Slade, VanHiel, Warren, & Dudley, 2004).

Table 3.1: Participant demography

Participants	Gender	Age	Body Mass (kg)	Height (cm)	Level of Lesion	ASIAIS	TAI (y)	BMI (kg/m^2)
1	M	45	82.0	172	T4	B	14	27.7
2	M	49	62.4	171	C7	B	11	21.3
3	M	28	79.6	162	T1	A	3	30.3
4	M	33	71.6	179	C6	B	13	22.3
5	F	47	72.0	165	C6	B	15	26.4
Mean		40.4	73.5	169.8			11.2	25.6
SD		9.3	7.7	6.6			4.8	3.36

Abbreviation: ASIAIS – American Spinal Injury Association Impairment Scale, TAI – Time after injury, F – Female, M – Male, BMI – Body Mass Index, ASIAIS A - Sensory and Motor Complete Impairment, ASIAIS B - Motor Complete Impairment.

3.2.2 FES experimental protocol

All participants were seated in their manual wheelchair comfortably during the FES cycling session with their feet safely secured to the pedals using physiotherapy straps. Each participant underwent a 30 min FES cycling session on an FES cycle ergometer (MOTOmed Viva 2, RECK-Medizintechnik GmbH, Betzenweiler, Germany) interfaced with the RehaMove 2 FES system at a cycling speed of 40 revolutions per minute (rpm). This protocol aimed to induce peripheral muscle fatigue through continuously repetitive muscle contraction. A commercial electrical stimulator (Rehabstim2, HASOMED GmbH, Magdeburg, Germany) that produces biphasic rectangular current-controlled stimulation pulses were synchronized with the motor resisted cycling ergometer. The stimulation (maximum 120 mA, 30 Hz, biphasic, pulse width ± 400 μs) started every time the pedal reached a crank angle of 45° and ended at 135°. At a 40rpm cycling speed, a total rotation of 360° takes 1.5 s (Figure 3.1). The duration of the stimulus pulse train was 0.4 s which contained a total of 12 stimulation pulses. However, as the muscle fatigues, the cycling speed might decrease, increasing stimulus duration.

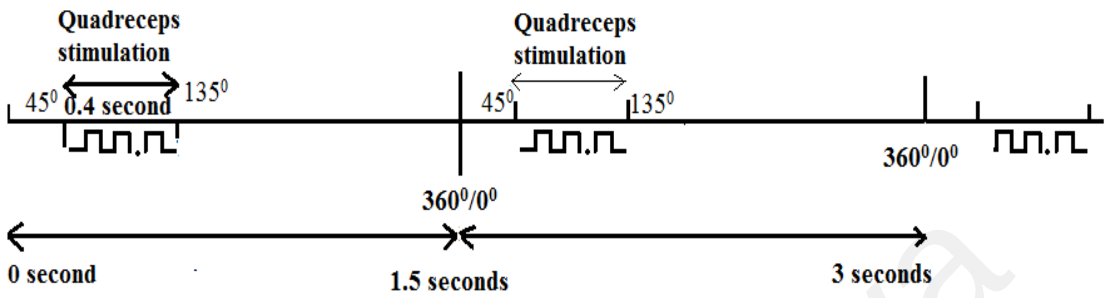

Figure 3.1: Schematic diagram of pulse train synchronized with ergometer pedal angle position in early non-fatigued condition, at 40 rpm

The stimulation parameters were set as follows: biphasic current amplitude adjusted up to 120 mA (peak) or the highest tolerable current of each participant depending on the patient's comfort level; pulse frequency was fixed at 30 Hz, and the biphasic pulse width was set at 400 µs + 400 µs (positive + negative phase). Initially, a 1-minute warm-up session (Fazio, 2014) was initiated using the same stimulation parameters, the current set to produce weak muscle contractions. Electrical stimulation pulses were delivered to the quadriceps, hamstrings, and glutei muscles via self-adhesive electrodes (size 9 cm x 15 cm, RehaTrode, HASOMED, Germany). The first electrode was positioned between 6 and 8 cm near the proximal position of the patellar border, and the second electrode was placed approximately 1/3 of the distance between the region of the inguinal line and the superior patellar border and slightly lateral to the muscle center line to ensure stimulation coverage over the three muscle bellies of vastus lateralis (VL), rectus femoris (RF), and vastus medialis (VM) (Szecsi, Straube, & Fornusek, 2014) (Figure 3.2). The main superficial quadriceps muscles are VL, RF, and VM. Each muscle behavior is different (Ouamer, Boiteux, Petitjean, Travens, & Salès, 1999) and can be detected using external sensors placed on the skin.

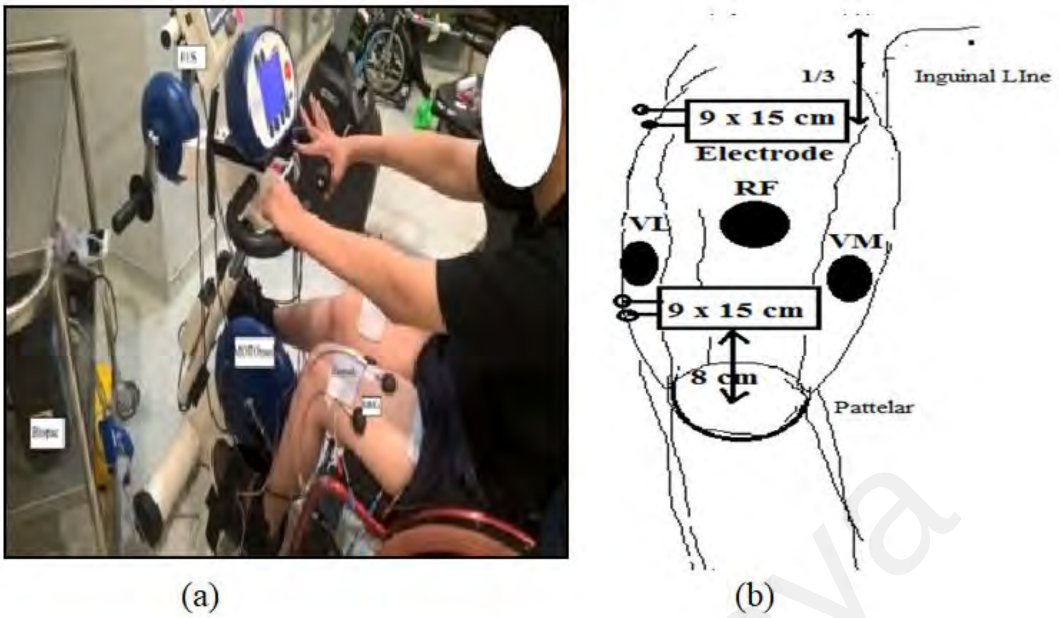

Figure 3.2: (a) Experimental setup, and (b) MMG sensor placement over the muscles (RF: rectus femoris, VL: vastus lateralis, VM: vastus medialis) represented by the solid black circles

3.2.3 MMG signal acquisition

In this research, the sensors were attached to the skin with double-sided adhesive tape over the belly of VL, RF, and VM muscles (Islam et al., 2018). The three MMG sensors used were accelerometer-based Sonostics BPS-IIVMG transducers (frequency range 20 Hz-200 Hz, sensitivity 30 V/g, diameter 32.6 mm, thickness 12.5 mm, mass 10 g). Other researchers described their usage for muscle assessment (Herzog, Zhang, Vaz, Guimaraes, & Janssen, 1994). Sensor locations were marked with a permanent marker to ensure consistent placement. The effect of skin thickness and fat were not considered in this study as it has been reported that no relationship was found between skinfold thickness and MMG RMS (voltage-force correlation) (Cooper, Herda, Vardiman, Gallagher, & Fry, 2014), and no strong correlation was reported between skinfold thickness as well as MMG median and peak frequency (Jaskólska et al., 2004).

3.2.4 Signal processing

MMG sensors were interfaced with a personal computer using the "ACQKnowledge" data acquisition and analysis software package (BIOPAC, Santa Barbara, CA, Inc. USA).

The raw signals were sampled at 2 kHz and band pass filtered (fourth-order Butterworth) at 20-200 Hz to reduce additional noise that might have originated from motion artefacts. The signals were then processed using MATLAB (Version 2013, The Mathworks, Natick, MA) for segmentation and classification. They were segmented by each contraction automatically using a peak detection algorithm whereby only the propulsion phase (0.25 s) of the contraction (minimum 0.4 s) was segmented. The MFCC and RMS features were then extracted from each contraction and used for training and testing the SVM.

3.3 MMG Classification

3.3.1 MFCC Feature

The first stage of the MFCC feature extraction method was to apply STFT analysis (Irino, Minami, Nakatani, Tsuzaki, & Tagawa, 2002; Obuchi, 2004) with window frames of 25 ms to the signal that was considered as stationary (Gil-Pita, lopez-Garrido, & Rosa-Zurera, 2015). The power spectrum was computed for every 25 ms frame with a 10 ms forward shift throughout the 250 ms MMG signal. Typically, window lengths are in the 20 ms-40 ms range because of the consensus that at higher window lengths, the signal may not be stationary while a shorter frame may not have enough information to extract significant signal features (Shang-Ming, Shi-Hau, Jeih-weih, & Lin-Shan, 2001; Wei, Cheong-Fat, Chiu-Sing, & Kong-Pang, 2006). This was followed by the Mel-filterbank equation (3.1) (Gupta, Jaafar, Ahmad, & Bansal, 2013) designed with 26 triangular filters uniformly spaced on the mel scale between lower and upper-frequency limits. The Mel scale is defined as a perceptual scale of frequency when measured at its original frequency.

To calculate filterbank energies (FBEs) (26 filters per frame), the filterbank was applied to the magnitude spectrum values. The 26 log filterbank energies consisting of compressed FBEs were then de-correlated using the discrete cosine transform (DCT) equation as given in equation (3.2) (Young et al., 2002). The *Cn* of the MFCC feature calculated from Equation 3.2 was fed into Equation 3.3 as the feature vector x, as expressed in Equation 3.3. From the results, 13 out of the 26 DCT coefficients were discarded from our application based on common practice from the literature (Gupta et al., 2013; Jong-Hwan, Ho-Young, Te-Won, & Soo-Young, 2000; Wahyuni, 2017). The reasons include that fast changes in the filterbank can degrade recognition performance and computational cost (Wahyuni, 2017).

$$mel(f) = 1127 \ln\left(1 + \frac{f}{700}\right) \qquad (3.1)$$

$$C_n = \sqrt{\frac{2}{N}} \sum_{j-1}^{N} m_j \cos\left(\frac{\pi i}{N}(j - 0.5)\right) \qquad (3.2)$$

where *N* is the number of the filter banks, m_j is the log filter bank amplitudes.

The MFCC process flow is presented in Figure 3.3. The selected 13 out of the 26 DCT coefficients were used to train the SVM classifier.

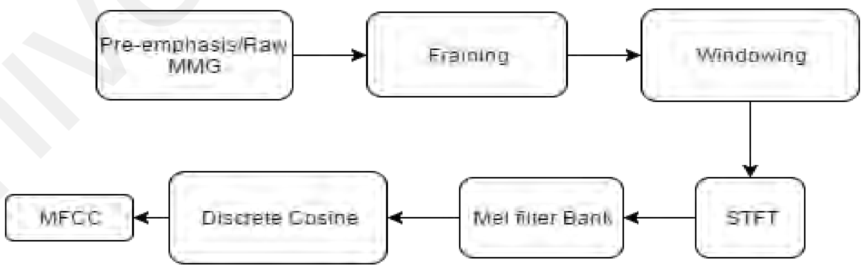

Figure 3.3: Block diagram of the MFCC algorithm

Figure 3.4 shows typical non-fatigued (a) and fatigued (b) MMG signals recorded from the three localized sensors of RF, VL, and VM. The fatigued signals in (b) have generally smaller amplitudes than (a), and the duration of contraction is longer in (b) compared to (a) because fatigued muscle requires more time to complete a single contraction cycle.

Significant differences in MMG signals among RF, VL, and VM can also be observed in Figure 3.4.

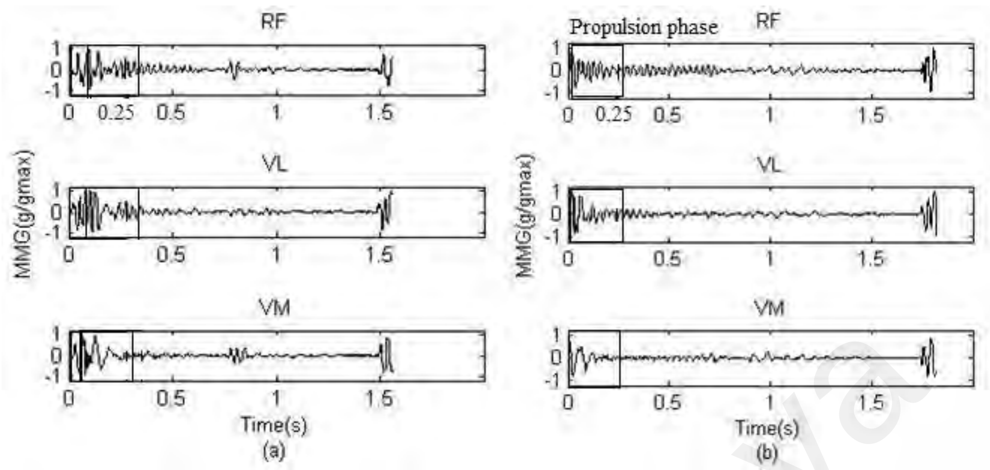

Figure 3.4: Typical normalized (to gmax) MMG signals during one revolution of cycling: (a) non-fatigued and (b) fatigue muscle contractions from sensors placed at RF (top), VL (mid), and VM (bottom)

The MFCC generates only frequency coefficients from the time series of MMG signals (250 ms) as shown in Figure 3.5; Figure 3.6 shows the MMG recognition steps from the input MMG signals to the training and recognition of MMG signals.

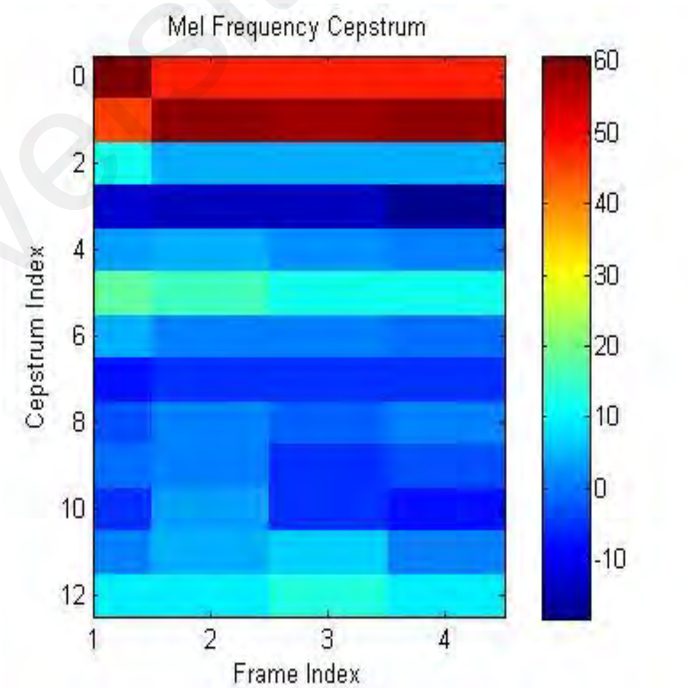

Figure 3.5: Time series of MFCC Cepstrum index plot in frame index of 0.25s MMG signal

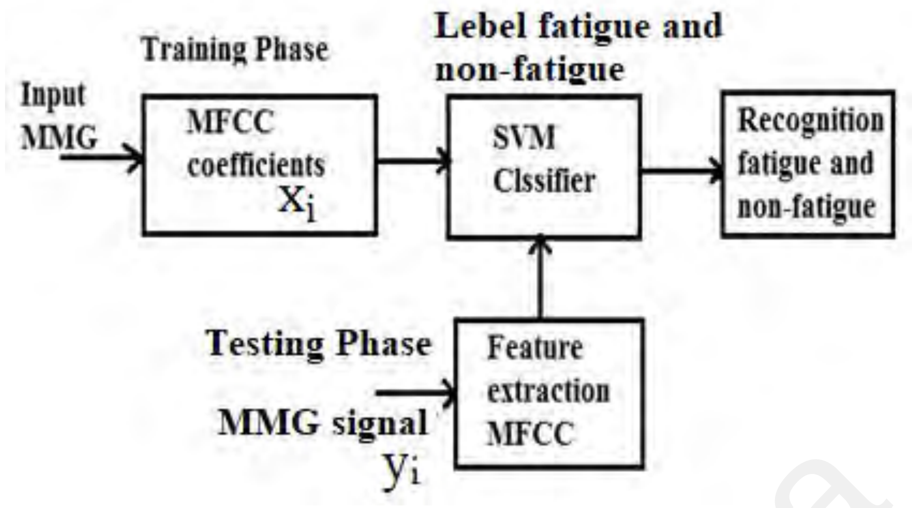

Figure 3.6: Block diagram of MMG signal training and recognition method

For each test subject, their corresponding MMG responses as described above were recorded for 30 minutes. Data from each subject's MMG signals captured from RF, VL, and VM muscles were separated into two groups. Out of all data, 75% of the total contraction signals were used as training data, while 25% were used for testing. For the training data, the MMG signals were partitioned into two categories: non-fatigued muscle contractions and fatigue muscle contractions. Grouping the two muscle conditions was based on the assumption that the first 10 minutes of the cycling session represent the responses of a non-fatigued muscle and the last 10 minutes of a fatigued muscle (Islam et al., 2018). From the recorded data, 400 non-fatigued contraction and 400 fatigued contraction samples were extracted from each RF, VL, and VM MMG response, respectively, totaling 1200 samples for fatigue and non-fatigued each.

Results were validated with the k-fold cross-validation (Xu & Liang, 2001) method in which out of each muscle's 400 contractions set, 300 contractions were used for training and 100 for testing. Therefore, a total of 900 non-fatigued and 900 fatigued contractions from the three sensors (RF, VL, VM) were used to train in the SVM classifier and later tested with 300 contractions. Figure 3.7 illustrates the contraction training and testing methods from one sensor.

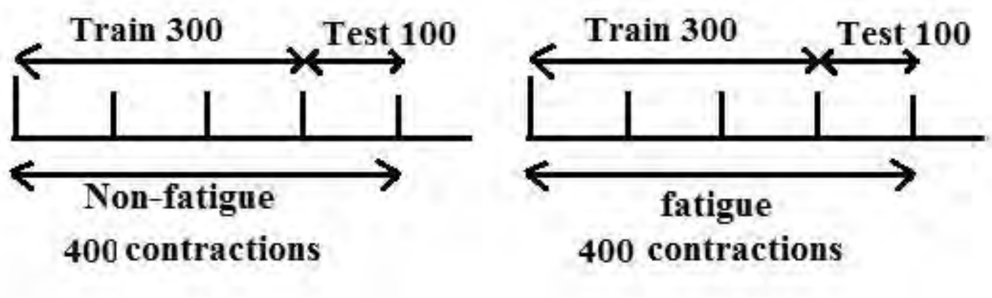

Figure 3.7: Selection of contractions used for training and testing from a cycling session

3.3.2 Support vector machine (SVM)

In the application of biomedical signal classification, Support Vector Machine (SVM) is a widely used machine learning technique (Subasi, 2013). SVM consists of an optimal hyperplane with a margin that separates the two data classes with a maximum distance between them (Cutajar, Gatt, Grech, Casha, & Micallef, 2013). Therefore, the boundary partition between the two classes of information was maximized. The optimal placement of the hyperplane was dependent on the portion of the training data, referred to as support vectors, which lies near the hyperplane. The optimal hyperplane is described in Equation (3.3).

$$w^T.x + b = 0 \qquad (3.3)$$

where *w* is the weight vector, *x* is the input vector from input space, and *b* is the bias. During the training phase, the data from class 1 were labeled as +1, and class 2 were labeled as -1 (Figure 3.8). At the classification detection phase the data was classified as +1 if $w^T.x+b >= +1$ and when $w^T.x+b <= -1$ it was classified as -1.

For testing stage classification, equation 3.4 can be written as

$$f(y) = w^T.x + b \qquad (3.4)$$

$$hence, w^T = \sum_{i=1}^{N} \alpha_i k(x_i y_i)$$

Equation 3.4 can be written as

$$f(y) = \sum_{i=1}^{N} \alpha_i k(x_i y_i) + b \qquad (3.5)$$

K(x,y) is the kernel function that calculates the dot product of two vectors x and y in high-dimensional feature space. Where y_i is the tested vector of MMG signal, x_i is the support vectors (Figure 4.8) calculated from the training data set, and α_i is their weights, and constant bias is b. The radial basis function (RBF) kernels (Equation 3.6) were considered due to their better performance than the linear kernel.

$$K_{RBF}(x, y) = \exp\left(-\gamma \left|\left|x - y\right|\right|^2\right) \qquad (3.6)$$

where γ is a control parameter (kernel width) and ||.|| denotes the Euclidean norm.

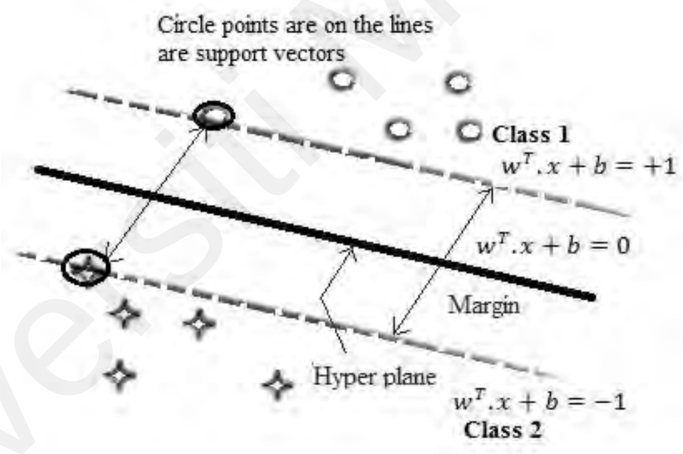

Figure 3.8: SVM hyper plane separated by Support Vectors (Hashem & Mabrouk, 2014)

In Figure 3.8, SVM classification with a hyperplane that maximizes the separating margin between two classes is indicated by "◊" and "O" and support vectors are the elements of the training set that lies on the boundary hyperplane between the two classes (Akay, 2009). However, in a real case scenario, there could be more than one hyperplane. In our case, two classes of muscle contractions of non-fatigued (Class 1) and fatigued (Class 2) were considered for the training and testing subgroups.

3.3.3 Muscle fatigue prediction among subjects

During electrical stimulation throughout the FES cycling exercise among the SCI individuals, their muscle fatigue responses may be similar yet distinct in different individuals to a certain extent. This may suggest different individual training and performance accuracy compared to training and prediction algorithms using cumulative subject data. Therefore, inter-subject prediction accuracy was generated to determine the accuracy when one subject's trained model was tested with the other subjects' non-fatigue and fatigue contraction signals.

Furthermore, results were validated using 4-fold cross-validation methods where all the data was used for training and testing the classifier. The prediction accuracy was calculated in 3 different models used: the MFCC feature, the RMS, and the combined MFCC and RMS features. Individual muscle prediction accuracy performance was also analysed.

3.4 Result and analysis

Over the 30 minutes cycling period, the cycling speed (measured with the built-in speed monitor) was used as an indicator of fatigue, i.e., when the speed drops significantly compared to the initial speed. From the experiment, the subjects' average cycling speed usually decreased throughout the 30 minutes of training. The duration of an example contraction was 1.43 s from the first 10 minutes and 1.82 s from the last 10 minutes (Figure 3.4).

3.4.1 MFCC and RMS features predicted contractions and accuracy

The predicted and expected results of all participants' muscle contractions using the MFCC feature (Table 3.2) and RMS feature (Table 3.3) are presented as a confusion matrix (Khezri & Jahed, 2007) for the fourth fold of repetition. Hence, the confusion matrix shows the expected and recognized number of contractions diagonally.

The accuracy was calculated by the ratio of the total number of contractions detected correctly to the total number of contractions shows in equation 3.7. Overall, the average prediction accuracy using the MFCC and RMS feature is 92.2% and 75.9%, respectively.

$$Accuracy = \frac{Total\ number\ of\ contraction\ detected\ correctly}{Total\ number\ of\ contraction} \times 100 \qquad (3.7)$$

Table 3.2: Number of Expected and Predicted Contractions sample in confusion matrix and accuracy using MFCC feature. Each subject's first and second row shows expected (first row: expected True, second row: expected False) and predicted number (first row: predict)

Subject	Expected result		Predicted contractions		Accuracy
	Non-Fatigue	Fatigue	Non-fatigue	Fatigue	(%)
1	300	0	293	7	96.3
	0	300	15	285	
2	300	0	295	5	98.8
	0	300	2	298	
3	300	0	276	24	85.5
	0	300	63	273	
4	300	0	289	11	96.3
	0	300	11	289	
5	300	0	218	82	84.0
	0	300	14	286	

Table 3.3: Number of Expected and Predicted Contractions sample in confusion matrix and accuracy using RMS feature. Each subject's first and second row shows expected and predicted number of contractions (first row: expected and predicted True, second row: expect)

Subject	Expected result		Predicted contractions		Accuracy (%)
	Non-Fatigue	Fatigue	Non-fatigue	Fatigue	
1	300	0	299	1	87.5
	0	300	74	226	
2	300	0	300	0	97.6
	0	300	14	286	
3	300	0	280	20	59.6
	0	300	222	78	
4	300	0	163	137	48.3
	0	300	173	127	
5	300	0	278	22	86.5
	0	300	59	241	

Based on Table 3.2, subjects number 1, 2, and 4 obtained more than 95% accuracy based on MFCC features. The highest accuracy was in subject 2, where the maximum number of 298 contractions for fatigued and 295 contractions as non-fatigue were predicted correctly. The same level of accuracy was achieved for subjects 1 and 4 at 96.3%. Subject 1 had the least prediction error of fresh contractions, with two contractions identified as fatigued contraction compared to the other subjects. The lowest accuracy of contractions was for subject 5, at an accuracy of 84%.

Table 3.3, on the other hand, presents the prediction accuracy based on the RMS feature of the MMG signals. Similar to the MFCC feature, subject 2 had the highest accuracy, with all non-fatigue contractions were predicted correctly, but a total of 14 fatigue contractions failed to be predicted. The accuracy obtained for subject 3 was less than 60% and for subject 4 was less than 50%. The lowest number of non-fatigue contractions was predicted for subject 4, which was only 163 contractions over the expected 300 non-fatigue contractions.

3.4.2 Muscle fatigue prediction accuracy among subjects

An inter-subject prediction is when one subject's training data is used to create a model and then tested with another subject’s data which is expected to be non-fatigue or fatigue. The inter-subject prediction accuracy of muscle fatigue using the MFCC feature is presented in Table 3.4, while prediction accuracy based on the RMS feature is shown in Table 3.5.

Table 3.4: Predicted inter-subject accuracy using MFCC feature

Trained subject	Test subject accuracy (%)				
	Subject 1	Subject 2	Subject 3	Subject 4	Subject 5
Subject 1		78	49	50	50
Subject 2	71		49.8	51	44
Subject 3	59.1	68.5		50	50.6
Subject 4	44.1	38.5	50		57.1
Subject 5	49	38	58.1	74.1	

Table 3.5: Predicted inter-subject accuracy using RMS feature

Trained subject	Test subject accuracy (%)				
	Subject 1	Subject 2	Subject 3	Subject 4	Subject 5
Subject 1		97.1	48.1	48.3	85.8
Subject 2	90.6		49.5	47.8	87.1
Subject 3	65.8	67.5		59.8	65.5
Subject 4	89.3	97.3	49.1		87.1
Subject 5	88.8	97.3	48.8	48.1	

If one subject's test data was fed into the other subject's training data, and vice versa, the inter-subject correlation assumed high prediction accuracy. This was demonstrated in Table 3.4, whereby when test data of subject 2 was fed into subject 1 trained data, it achieved the highest accuracy of 78% and 71% vice versa, using the MFCC features. This was again demonstrated in Table 3.5 when both subjects 1 and 2 displayed high accuracy based on each other's training and testing data using the RMS feature.

3.4.3 Cross-validation of the combined results of three sensors (RF, VL, and VM)

For results validation, all the non-fatigue and fatigue contractions samples were used for training and testing. Four-fold cross-validation used a total of 1200 contractions (three sensors), of which 75% were used for training and 25% for testing.

Table 3.6: Accuracy results for MFCC features with four repetitions

Subject	Repetition accuracy (%)				Mean ± SD
	First	Second	Third	Fourth	
1	93.3	88.8	85	96.3	90.8 ± 4.9
2	96.5	95.1	81.6	98.8	93.0 ± 7.7
3	96.3	83.6	72.6	85.5	81.7 ± 9.7
4	100	100	85	96.3	92.8 ± 7.1
5	94.1	94.3	86.8	84	89.8 ± 5.2
Mean ± SD	96.0 ± 2.6	92.4 ± 6.3	82.2 ± 5.6	92.1 ± 6.8	

Table 3.7 indicated that, when compared to RMS, MFCC performed better overall with all four repetitions in Table 3.6. However, the mean accuracy of four repetitions for subjects 1 and 2 was higher (93.9% and 98.9%) in RMS than MFCC (90.8% and 93%). The RMS of subjects 3 and 4 depicts the lowest performance compared to MFCC. However, the effect of repetition standard deviation for the MFCC feature was below 10%. On the other hand, the standard deviation of the RMS feature reached 13.2% for subject 4, and for subject 5 it reached 19.8%.

Table 3.7: Accuracy results for RMS features

Subject	Repetition accuracy (%)				Mean ± SD
	First	Second	Third	Fourth	
1	97.1	100	91.3	87.5	93.9 ± 5.6
2	99.3	99.8	99.1	97.6	98.9 ± 0.9
3	59.3	66.83	57.8	59.6	60.8 ± 4.0
4	40.1	22.83	53.1	48.3	41.0 ± 13.2
5	92.5	84.3	48.6	86.5	77.9 ± 19.8
Mean ± SD	77.66 ± 26.5	74.752 ± 32	69.98 ± 23.4	75.9 ± 20.8	

Table 3.8: Accuracy for combined MFCC and RMS features

Subject	Repetition accuracy (%)				Mean ± SD
	First	Second	Third	Fourth	
1	90.6	96.1	83.8	80.8	87.8 ± 6.8
2	100	99.8	75.6	98.8	93.5 ± 11.9
3	97	85	73	78.5	83.1 ± 10.3
4	96.5	95.1	81.1	95.3	92.0 ± 7.2
5	93.6	95.1	81.5	80.1	87.5 ± 7.8
Mean ± SD	95.5 ± 3.5	94.2 ± 5.5	79 ± 4.5	86.7 ± 9.5	

Table 3.8 demonstrates that the combined MFCC and RMS features reached a maximum mean accuracy of up to 93%, while the lowest was 83%, and the standard deviation reached a maximum of about 12%. Results also show that the first and second repetitions have higher accuracy than the third and fourth repetitions.

3.5 Discussion

Classification of non-fatigue and fatigue muscle contractions using the MFCC feature was hypothesized to have a higher prediction ability among subjects than the generally adopted RMS feature. Hence, the overall performance of MFCC might be higher because the MFCC feature incorporates inherent calculations of frequency components and power spectrum of MMG signals in the time and frequency domain.

However, the average inter-subject correlation prediction accuracy of MFCCs was around 50%, which was a deficient performance in classification measurement. Interestingly, the overall inter-subject accuracy based on the RMS feature resulted in better performance than the MFCC feature. However, in both MFCC and RMS features, there was insufficient prediction consistency observed among subjects.

Results revealed that FES muscle fatigue classification of dynamic FES cycling using the MFCC feature projected better accuracy than the RMS feature. The number of correctly identified contractions as non-fatigued and fatigued was higher in MFCC when compared to RMS. Some non-fatigued muscle contractions overlapped with other fatiguing contractions using both MFCC and RMS features. This might be due to the inaccurate assumption that the muscles were not fatigued in the first 10 minutes when the muscles might be undergoing early muscle fatigue within the first 10 minutes of cycling. This is backed by the research findings that suggested that electrical muscle activation is responsible for faster muscle fatigue than voluntary contractions (Marsolais & Edwards, 1988). This is also related to the inability to modulate motor units' firing frequency or recruitment pattern (Bickel, Gregory, & Dean, 2011) and the "inverse recruitment."

Moreover, the captured muscle responses might contain motion artefacts (Ibitoye et al., 2014b) since the subjects in the sitting position on the wheelchair were not completely fixed, and their limbs were moving during cycling.

Furthermore, different muscle properties of RF, VL, and VM and variations in the placement of MMG sensors may have also affected the signals. Table 3.9 shows each of the three individual VM, VL, and RF muscle performance accuracy of MFCC and RMS features. The mean accuracy of the MFCC feature is higher than the RMS feature in RF, VL, and VM muscles. When compared to MFCC on subjects 1 and 5, the RMS feature shows higher accuracy in the three muscle groups. The standard deviation accuracy of three muscles in each subject was higher in MFCC, yet the overall mean accuracy of RMS was lower than MFCC. It is interesting to highlight that inter-individual and intra-individual sensors for each patient have different accuracy in detecting muscle fatigue due to the geometry of each muscle structure (Orizio, 1993). Using the MFCC feature, it could be suggested that one sensor on RF muscle can quantify the whole quadriceps muscle assessment.

Table 3.9: Individual three muscles performance accuracy of RF, VL, and VM.

Subject	MFCC feature accuracy%			Mean ± SD	RMS feature Accuracy %			Mean± SD
	RF	VL	VM		RF	VL	VM	
1	77	90	66.5	77.8 ± 11.7	94	100	99.5	97.8 ± 3.3
2	100	98	99	99.0 ± 1.0	97	98.5	100	98.5 ± 1.5
3	94	78	62.3	78.1 ± 15.8	61	63	56	60 ± 3.6
4	98	99.5	89	95.5 ± 5.6	12	75	42	43 ± 31.5
5	88	86.5	65	79.8 ± 12.8	92	98.5	90	93.5 ± 4.4
Mean± SD	91.4 ± 9.2	90.4 ± 8.7	76.3 ± 16.5		71.2 ± 36.1	87 ± 16.9	77.5 ± 26.7	

Several studies have documented the change in MMG mean power frequency (Esposito et al., 1998; Orizio, 1992; Peters & Fuglevand, 1999) and median frequency (Kouzaki et al., 1999) over the stimulation time due to the inverse recruitment of motor units. These were the basis on which MFCC features could retrieve frequency components from the muscle contractions.

Many studies have been conducted to investigate muscle contraction classification and prosthetic control based on MMG signals using various feature extraction methods such as the RMS, wavelet transform, SWT, and STFT, as well as genetic algorithms (Al-Mulla & Sepulveda, 2014; Silva et al., 2005; Xie et al., 2009).

Two types of muscle contractions for wrist extension and flexion were investigated by Saliva et al., which used the RMS feature, while Xie et al. (2009) studied the STFT, SWT, WPT, and S-transform features to classify hand motion patterns (Silva et al., 2005; Xie et al., 2009). However, in their work, the classification accuracy achieved was below 90%. Alves et al. (2010) reported that the classification accuracy of three classes of movement of MMG signal wrist flexion, wrist extension, and semi-pronation of the single-site forearm based on sensor placement was about 73%. The authors conveyed that accuracy degradation might be influenced by several factors, including sensor placement, classifier complexity, training method, signal feature, and muscle architecture.

Another recent study (Al-Mulla & Sepulveda, 2014) has implemented wavelet transform and modified pseudo-wavelet by using SVM classifier to investigate non-fatigue and fatigue contractions and achieved approximately 80.63% accuracy, though during the experiment a very small number of trials (73 trials) were used for training compared to this study. Madeleine, Hansen, and Samani (2014) suggested that linear and nonlinear analyses of the MMG signal of the wrist extensor could be assessed using average rectified values (ARV) of the MMG output or RMS linear feature with variations in sensor load, location, contraction type, and time. Their results show that a higher ARV value was observed in load variations compared to variations in location and contraction type, while the variance ratio in the percentage of recurrence and percentage of determinism was 22.8% and 0.1%, respectively. Variations in location revealed that ARV was lowest with 31.2 ms^{-2} and, 9.9% recurrence and 43.6% determinism, while varying the time revealed ARV of 89.4 ms^{-2}, with 27% recurrence and 6.6% determinism.

However, this research focused on ARV or RMS features only. Sarlabous et al. (2013) used the dog model to quantify the stochastic nature of MMG signals to estimate muscle force using ARV or RMS parameters based on the Lempel-Ziv algorithm. Both studies emphasized that non-linear analyses are found promising when analyzing muscle fatigue or muscle force. In this study, RMS and MFCC features of the MMG signal were classified using the SVM classifier with the RBF kernel to map the data in higher dimensions for non-linear MMG data separation.

The MFCC feature represents the short-term power spectrum of a signal based on a linear cosine transform of a logarithmic power spectrum on a nonlinear Mel scale of frequency. Therefore, the non-linear MMG signal feature during cycling was deemed to be more suitable for MFCC than classical STFT in dynamic muscle contraction classification. Moreover, the computational costs of short wavelet transform or wavelet packet transform are higher than MFCC, which plays an important role in real-time applications.

The total accuracy for the MFCC feature of the MMG signal achieved up to 96% accuracy for non-fatigue and fatigue classification for the first fold repetition, and the average accuracy of 4-fold was 90.7%. The combined MFCC and RMS feature with an average accuracy of 88.8% did not significantly improve accuracy. Studies on FES and fatigue-related exercise can benefit from our findings by implementing MFCC feature extraction of the MMG signal.

The results of fatigue detection correlation among subjects illustrate a good correlation between subjects 1 and 2 in both MFCC and RMS. However, generally, higher accuracy was found in RMS feature adoption. The relationship between these two subjects could be a similarity in muscular behavior during stimulation (Vromans & Faghri, 2018). These results may suggest the possibility of using identified similarly performing muscles, as in subjects 1 and 2, to pool the other subjects' data to improve their fatigue prediction learning and ability or to use one subject's trained algorithm to predict another's. The RMS feature showed better-correlated accuracy among the subjects, but the results were not consistently high in all subjects. Therefore, more investigation of muscle responses is required during stimulation to find out the correlation among subjects.

A new method of MFCC feature extraction for MMG signal classification during FES cycling has been successfully implemented using the SVM classifier. The outcomes of this study, however, were limited by the number of trials within each subject due to challenges in multiple subject recruitment and sessions. Thus, increasing the repetition of trials, in the long run, would positively influence the accuracy of the results (Alves et al., 2010). However, the effect of different window lengths of MMG signals on accuracy could be an exciting topic for future researchers.

3.6 Conclusions

This study is the first to demonstrate the adoption of the MFCC feature, which had been primarily applied in the "Automatic Speech Recognition" domain, for MMG classification of fatigued and non-fatigued contractions throughout dynamic FES cycling. The MFCC feature showed better accuracy, up to 90.7%, compared to the RMS feature, with an accuracy of 74.5%. Thus, the proposed features can be used in muscle fatigue prediction in dynamic and cyclical evoked muscle contraction as long as the system is trained with data from the monitored subject. Inter-subject prediction accuracy is inconsistent and has low accuracy, indicating the need to have a larger pool of training data. Further investigations will help understand the nature of the MMG signals better and influence factors such as physiological properties and physical milieu. The method introduced in this study could be implemented in FES systems to monitor muscle fatigue to increase patient safety and optimise patient training by adapting the FES parameters during electrically-evoked contractions in individuals with motor complete SCI.

CHAPTER 4: DEVELOPMENT OF FES SYSTEM WITH MECHANOMYOGRAPHY FEEDBACK FOR COMPLETE SPINAL CORD INJURY STANDING

4.1 Introduction

Spinal cord injury (SCI) may lead to partial or complete paralysis depending on the level of injury in the spinal cord region (Weld & Dmochowski, 2000). As a result of thoracic or cervical levels of SCI, affected individuals may be unable to move their lower limbs to perform functional activities of daily living such as standing, walking, and related functional activities. Several methods promote functional activity recovery following SCI to improve the victims' quality of life. One popular rehabilitation method is through the use of functional electrical stimulation (FES) technology.

FES applies modulated and tolerable electrical pulses to specific muscles via motor points or nerves to energize paralyzed muscles using a pair of surface electrodes to activate the nerves to affect muscle contractions. FES provides pulses to generate artificial muscle contractions missing in people with motor paralysis following SCI. Several studies (Mushahwar, Jacobs, Normann, Triolo, & Kleitman, 2007; Popovic, Curt, Keller, & Dietz, 2001) have shown that FES-related exercises have functional benefits for the people with motor paralysis, such as standing and walking. To achieve such functional benefits, a complex control method of stimulation of different muscle groups may be required. While open-loop FES administration has limited functional applications (Jezernik et al., 2004; Sinkjaer, Haugland, Inmann, Hansen, & Nielsen, 2003), the closed-loop FES system alternative has been widely promoted for neuromuscular stimulation, particularly for improved muscle condition monitoring and prevention of overstimulation to prevent tissue damage (Cogan et al., 2016). Over-stimulation can be prevented by monitoring muscle response as a feedback indicator in the closed-loop FES systems. Therefore, selecting sensors to capture the useful muscle response information/biopotentials is vital in a closed-loop control system for real-time FES applications based on cost, size, and reliability in the presence of external interference. One good option is mechanomyography (MMG) (Beck et al., 2007; Ebersole et al., 1999; Orizio et al., 1999), considering the cost, size, and reliability in the presence of electrical stimulation artefacts.

The MMG signal represents a mechanical representation of low-frequency muscle contraction signals that could be obtained non-invasively (Beck et al., 2007; Orizio, 1993; Yoshitake & Moritani, 1999). Using proprietary FES systems in open-loop mode, previous studies have promoted the application of this signal in tracking muscle contraction patterns during muscle extension/flexion exercise (Ibitoye et al., 2020a; Ibitoye et al., 2016b) and standing tasks (Dzulkifli et al., 2018) in people with SCI. In the present study, this research aimed to develop a real-time functional electrical stimulation (FES) system to support functional, efficient, and secure physical exercise, including standing and monitoring muscle conditions in people with SCI.

4.2 Design of proposed FES system

A portable two-channel Bluetooth-controlled FES device was designed using a voltage step-up circuit and H bridge circuit, and each channel’s stimulation parameters were able to be controlled by the microcontroller independently. This study mainly tests the closed-loop system responses from the graphical user interface and MMG to visualize muscle responses with standing support and fatigue detection in relation to knee angle drop. For the test of the developed FES system to monitor muscle using the MMG sensor, parameters change in four phases when knee-buckling begins. In addition, the developed FES system also has features to integrate other sensors, such as goniometer for modulation and optimisation. This study's main objective is to develop an FES system to generate sufficient muscle power to support standing for SCI individuals and monitor muscle condition using an MMG sensor.

4.2.1 Block diagram of the proposed closed-loop system

Figure 4.1 shows the block diagram of the developed FES system. This system consists of four sections: (1) the stimulator which generates electrical pulses to stimulate the muscle, (2) the stimulation electrodes and muscle of interest for the task to be performed, (3) the MMG sensor arrangement and data acquisition system for signal acquisition and processing, (4) the control interface that uses the information from section (3) to modulate and optimise the performance of the stimulation device.

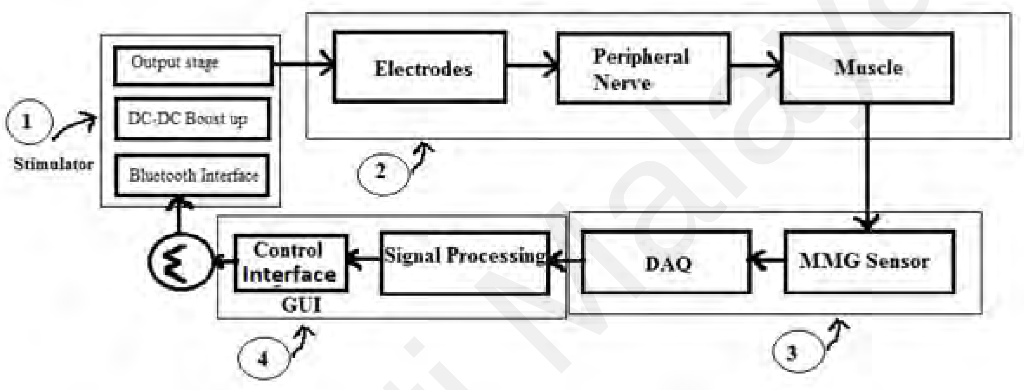

Figure 4.1: Block diagram of the proposed closed-loop system

4.2.2 Stimulator

The stimulator consists of a step-up power controller and output stage controller for each channel of stimulation. A rechargeable 3.7 V lithium-ion battery powers the stimulator. Initially, the battery voltage is stepped up to 5 V using a dc-dc boost converter circuit to supply power to the microcontroller and stimulator power circuit. To step up the battery voltage from 3.7 V to 5V, an MT3608 chip is used, which is most commonly used for a 5 V DC supply. A sliding-type switch is used to turn on the power of the stimulator. The stimulator control signal is supposed to be received by Bluetooth serial communication. Figure 4.2 represents the voltage step-up circuit diagram (block diagram section 1) for the stimulator.

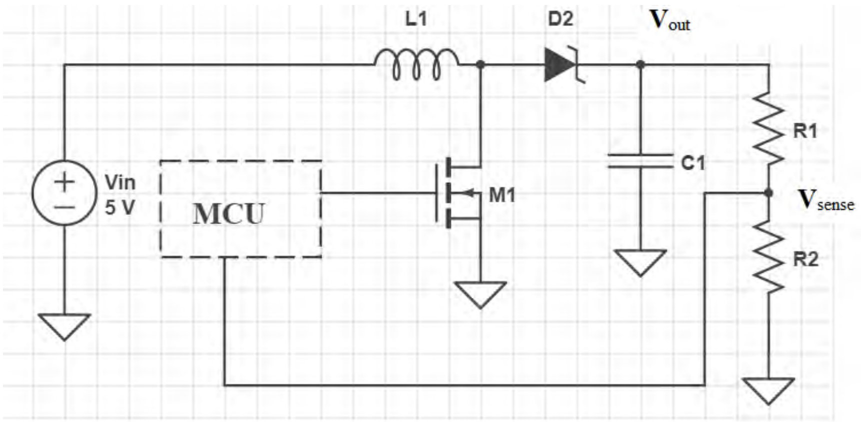

Figure 4.2: Voltage step-up circuit

Voltage step-up for the circuit (Figure 4.2), the input voltage was 5 V, and the output voltage could achieve up to 120 $V_{p\text{-}p}$ maximum for a 1 kOhm load resistor. To output voltage control in a step of 1 V, 8-bit digital-to-analog converter (DAC) values are used to control pulse width modulation (PWM) to regulate voltage from Microcontroller (ATmega328) Unit (MCU). The components' values of this circuit were selected based on test and trial methods as follows: inductance (L), capacitance (C), resistor R1, and resistor R2 were 220 μH, 4.7 μF, 10 MΩ, and 10 KΩ, respectively.

The voltage output stage of the biphasic square pulses was designed to be generated from the H-bridge circuit configuration (Figure 4.3). The stimulation frequency and pulse width were controlled by on/off transistor switches, while the amplitude was controlled by the pulse width modulated signals from the microcontroller. The four switches of the H-bridge circuit are T1, T2, T3, and T4, which were precisely controlled by the MCU's digital output pins DO1, DO2, DO3, and DO4 that determined the time duration of each pulse (Figure 4.3).

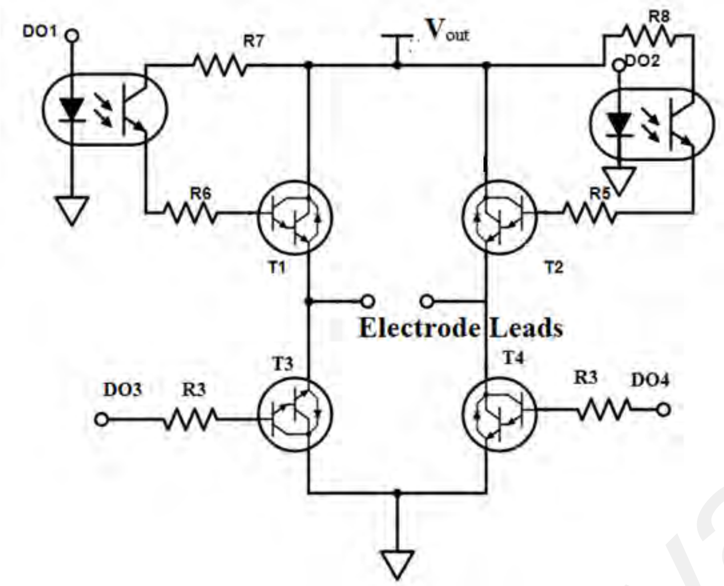

Figure 4.3: Circuit diagram of the output stage

All the transistors used in this device could handle high voltage and large currents. The pattern generation table closely followed the operation of the output stage in Figure 4.4. In the table depicted in Figure 4.4, turning off T1 and T4 determined the positive output voltage while T2 and T3 determined the negative output voltage.

DO1	DO2	DO3	DO4	State
0	0	0	0	Off
1	0	0	1	V1
0	1	1	0	V2

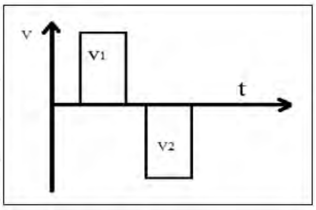

Figure 4.4: Stimulation pattern generation table

The stimulator pulse width ranges from 50 µs to 600 µs, while the frequency range is between 10 Hz to 200 Hz. These values were meant to generate both low and high muscle contractions. Figure 4.5 depicts the biphasic square wave pulse generated across 1 kOhm resistor load.

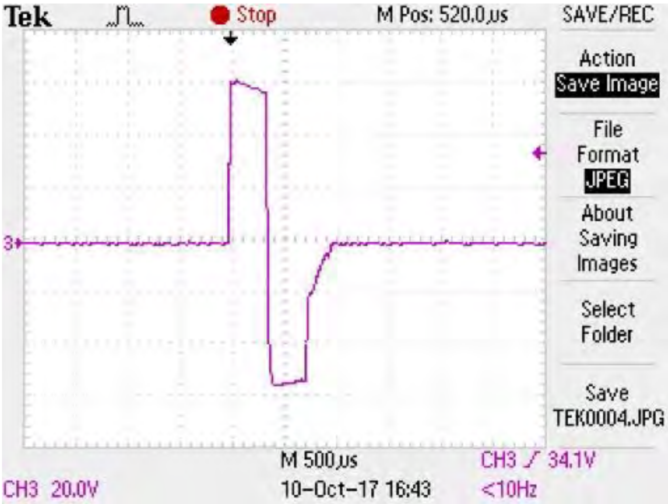

Figure 4.5: Biphasic square wave output across 1K Ohm resistor

The fourth section of this design includes the graphical user interface (GUI), sets the stimulator parameter, and sends the control signal to the stimulator. This section is mainly controlled by the processed MMG signal after processing and feature extraction.

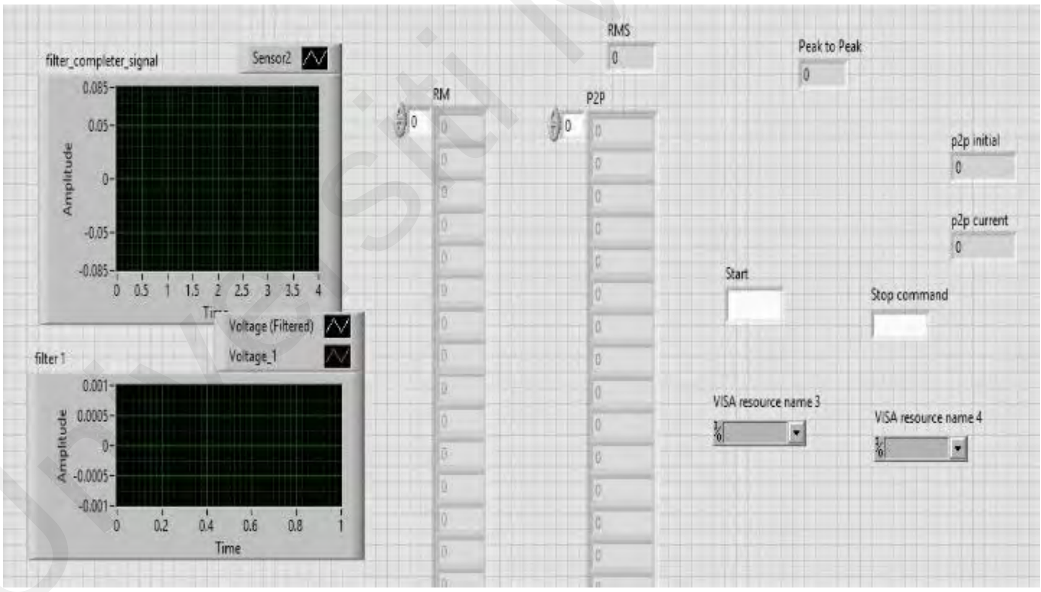

Figure 4.6: Graphical User interface to send control signal and to process MMG signal

The LabView program (Figure 4.6) was used in this fourth section to design a GUI for user compatibility and interaction. The National Instrument data acquisition card was used for the applied MMG features to record the raw MMG signal in the GUI. The GUI system displays the processed raw MMG signals, the filtered MMG signal, and useful extracted features saved in a file for further usage.

4.2.3 MMG Sensor

An accelerometer sensor (ADXL335, Figure 4.7) was used to collect the MMG signals. The accelerometer can collect data along with the x, y, and z-axis of vibration. For this experiment, only the x-axis is used to acquire the MMG signals. The dimension of the accelerometer was 18 mm × 15 mm × 2 mm, including its PCB board. A custom-designed 3D printed plastic casing of 30 mm diameter in the depth of 4 mm (inside to outer surface thickness of 1 mm) was used to house the sensor to obtain maximum muscle vibration from the skin surface.

Figure 4.7: MMG sensor setup

4.3 FES experiment during standing

4.3.1 Subject

Two experienced FES users volunteered to participate in this experiment. However, following clinical assessment and physical examination, one subject was excluded from the experiment because he was found unfit. The included SCI participant (one male) was classified in American Spinal Injury Association (ASIA) impairment scale as A. The participant was aged 35 years with 72 kg body weight and 15 years post-injury for the experiment.

The participant was found to be physically and psychologically fit for the experiment. A consent form was given to the participant to endorse before the experiment. The experimental procedure used in this study was approved by the University of Malaya ethical committee with approval No: MECID.NO: 20164 – 2366.

4.3.2 Apparatus

The customed-developed (two-channel) pair of wireless FES stimulators were used in this study to stimulate quadriceps and gluteus maximus muscles to support the standing exercise using surface electrodes with size (i.e., 9 cm x 15 cm, RehaTrode, HASOMED, Germany). LabView software was used to communicate with the stimulator through Bluetooth serial communication.

An accelerometer MMG sensor (ADXL335) was placed over the volunteer's rectus femoris muscle belly to collect the muscle responses for analysis and application. The MMG signals were recorded in the LabView environment using the National Instrument data acquisition card model USB-6343 (Austin, TX, USA), and a fourth-order bandpass filter filtered the signals at 5 - 100 Hz (Perry et al., 2001) with a sampling rate of 2 kHz. The participant was passively supported by the Biodex harness (Biodex Offset Unweighing System) to prevent sudden falls. For stabilization of the upper body, the subject had access to the sidebars provided by the harness system (Figure 4.8). The sidebars could be held as desired by the participant. This experiment did not consider force from the upper limb or partial weight-bearing support force. A goniometer was used to measure knee flexion angle. A 30° knee flexion indicated standing failure due to muscle fatigue and the stimulation was terminated at the time. At 30°, knee flexion showed standing failure due to muscle fatigue and stop stimulation.

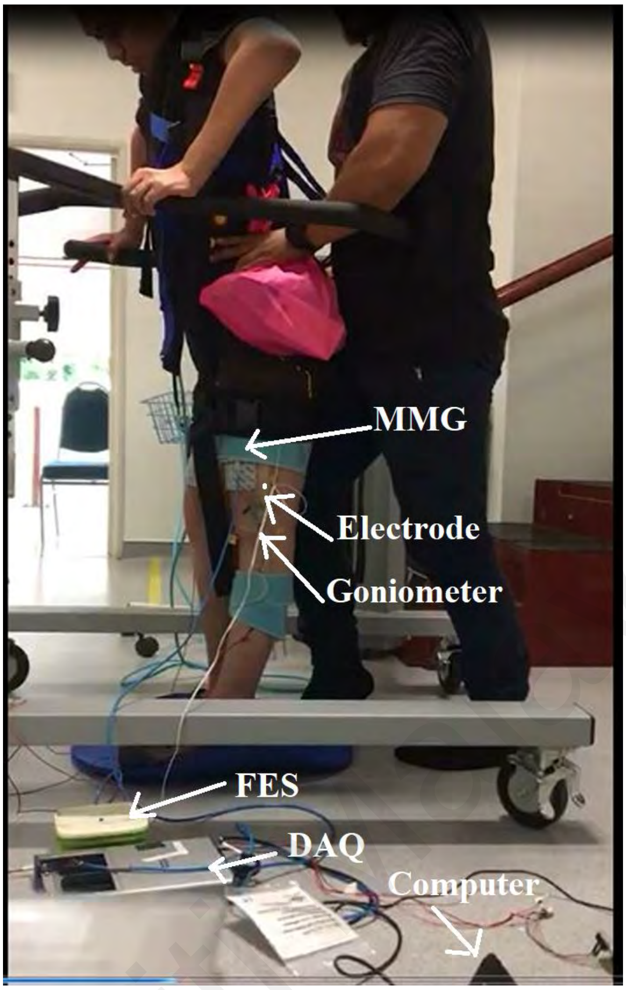

Figure 4.8: FES supported standing

4.3.3 Protocol

The FES standing exercise was conducted in two days to achieve 4 trials in all. Before the commencement of the experiment, the stimulation amplitude was slowly increased to set the starting amplitude for a full knee extension. On the first day, the first trial began with fixed stimulation parameters (i.e., amplitude: 80 V_{p-p}, pulse width: 350 µs, and frequency: 35 Hz). After completing the first trial, the participant was made to rest for 30 minutes to allow the muscle to recover from fatigue. After the recovery time, the second trial commenced with parameter optimisation settings by visual observation of the goniometer's knee angle drops to 30° as a total standing failure.

The stimulation parameters were optimised in four phases; in each phase of transition, stimulation voltage was increased by 20% and frequency reduced by 10% from the initial set parameters (i.e., 80 V_{p-p}, and frequency of a 35 Hz). This referred to when each phase transition happens, the amplitude of the initial 80 Vp-p increases 20%, and frequency reduces 10% from the initial set value of 35 Hz. These four phases are implemented by visual inspection of the knee angle that starts to drop, then immediately increases current and reduces the frequency in the stimulator by receiving a command from the LabView program. Whereas in the last phase, when the knee angle drop was more than 30°, the stimulator was switched off to avoid overstimulation. For muscle fatigue recovery from the first-day trial, the second-day trial was separated by 48 hours. To avoid bias in the second-day trial, the first trial of the day was with parameter optimisation, and similarly, 30 minutes of recovery time for the second trial was allowed between trials.

4.4 Result and discussion

The standing duration of the two days' trials was found to be as follows: for the first-day trial with fixed stimulation parameters, the standing duration was 17 s, while for the second trial that used optimised parameters, the standing duration was up to 39 s. The second-day optimised standing trial duration of 81 s was comparatively higher than the standing duration for the fixed stimulation parameter trial of 48 s only.

Figure 4.9 (A) showed the fixed-parameter MMG signals when the knee angle dropped to 30°, and the stimulation was switched off. The MMG signal pattern after 15 s of stimulation indicated muscle fatigue. In Figure 4.9 (B), which is the MMG signal pattern during the parameter optimisation session, after the initialization of the stimulation, the MMG signal pattern after 15 s showed a drop simultaneously with the knee angle reduction. This was closely followed by the second phase of the set parameters with increased amplitude. This second phase's standing duration climbed up to 24 s from 16 s, while the third phase was activated from 24 s and continued to about 12 s, and the final phase continued only for 3 s as the muscle power generation was unable to sustain standing further.

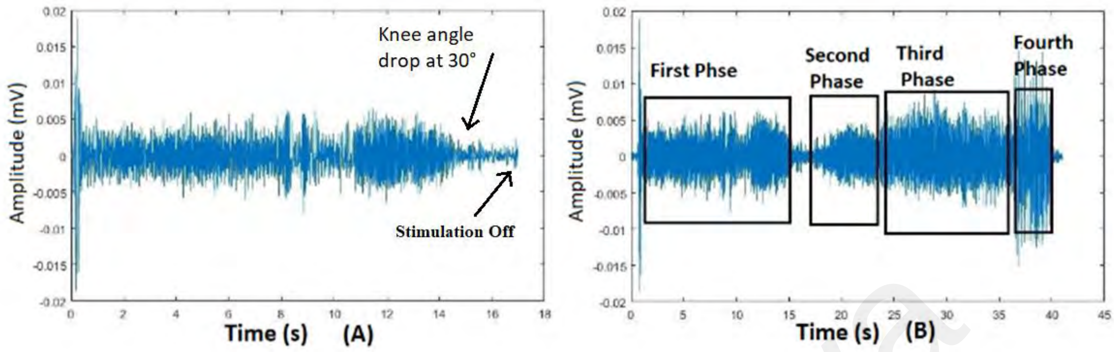

Figure 4.9: (A) MMG signal in fixed-parameter (B) MMG signal in parameter optimization

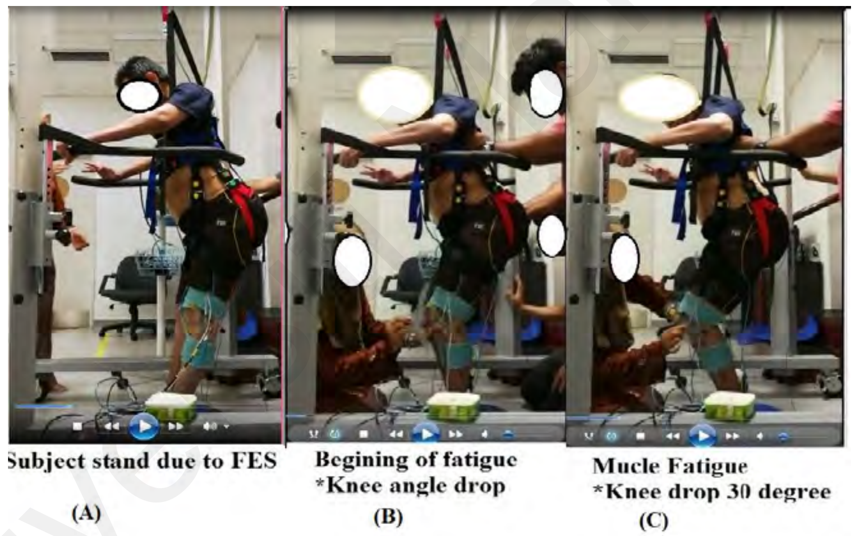

Figure 4.10: A shows the subject started to stand by FES, B shows the knee angle started to drop, and C clearly shows that the knee angle drops to 30°

The shorter average standing duration of the first-day trial, compared to the second-day trials, might be due to the fast-twitch muscle fibers becoming fatigued on an earlier day and later-day muscle becoming the fatigue-resistant cause of delay (Thrasher et al., 2005). That could cause the second standing session with a fixed parameter trial of up to 48 s. As the high frequency promotes the rapid onset of muscle fatigue (Rongsawad & Ratanapinunchai, 2018), the parameter optimisation method in different stimulation phases increases stimulation amplitude to reduce the stimulation frequency for a long-standing duration. Open-loop FES standing studies usually adopt high amplitude (Dzulkifli et al., 2018; Ibitoye et al., 2020a), leading to maximum muscle power generation. With this approach, once muscle begins to fatigue, it becomes difficult to prevent it. High stimulation amplitude also promotes high knee joint velocity that may be challenging to manage using control algorithms (Davood & Andrews, 1998). For optimised stimulation, the experiment started with a minimum stimulation amplitude that could support standing, while the other two parameters (i.e., frequency and pulse width) were set as found in the common FES standing studies (Braz et al., 2015; Ibitoye et al., 2020a). As hypothesized, iterative changes in stimulation parameters promoted longer standing duration when compared to the fixed-parameter stimulation trials. One limitation of this pilot experiment is based on the use of only one person with SCI. Also, although the stimulation parameters were updated manually, this could be implemented in the LabView algorithm using the MMG feedback signal. This is evident as recent studies (Dzulkifli et al., 2018; Ibitoye et al., 2016b) have shown a strong positive correlation between FES-induced isometric torque and MMG-RMS feature during fresh and fatiguing muscle contractions.

Future work may further explore the prolongation of FES-supported standing duration using MMG amplitude feature such as MMG root mean square as a feedback signal in the control algorithm. This will employ parameter modulation using stimulation amplitude, frequency, or pulse width in the stimulator. However, this study successfully implemented FES parameter optimisation based on knee angle and MMG signals to support the prolonged standing exercise.

4.5 Conclusion

This work presented the development and implementation of a closed-loop FES system, and stimulation parameter optimisation could be used to prolong FES standing duration. The study has also discovered that the stimulation parameter optimisation that was based on the MMG signal was also related to the standing duration and muscle fatigue as indicated by knee buckle measurement. Another important message from this research study is that MMG could be used alone as a feedback signal in the closed-loop FES standing exercise to monitor muscle fatigue and optimise FES parameters.

CHAPTER 5: ELECTRICAL STIMULATOR WITH MECHANOMYOGRAPHY-BASED REAL-TIME MONITORING, MUSCLE FATIGUE DETECTION, AND SAFETY SHUT-OFF: A PILOT STUDY

5.1 Introduction

Functional electrical stimulation (FES) is a neuroprosthetics technique to assist individuals with spinal cord injury (SCI) to train and strengthen their paralyzed muscles (Krajl, Bajd, Turk, & Benko, 1986; Kralj & Bajd, 1989; Veltink & Donaldson, 1998). In general, the electrical stimulation parameters, i.e., pulse amplitude, width, and frequency, are preset before the stimulation training begins (Newham & Donaldson, 2007) and can be changed manually throughout the session to achieve a certain amount of muscle output. In an open-loop stimulation system such as FES cycling, these parameters may not be changed automatically even if the muscle output drops as a result of muscle fatigue. Systems that monitor the output in some ways and adopt the parameters accordingly are generally referred to as "closed-loop systems".

Various types of feedback sensory have been used in previous studies, e.g., electromyography (EMG) signals (Ibitoye et al., 2014a), kinematic sensors to detect movement (Taylor, Picard, & Widrick, 2011), user-controlled buttons (Newham & Donaldson, 2007), and position sensor for gait control (Y. L. Chen et al., 2001). (Y. L. Chen et al., 2001). Sensors such as proximity (Hodkin et al., 2018), kinetic (Simonsen, Spaich, Hansen, & Andersen, 2016), motion (Braz et al., 2016), and stretch (Shimada et al., 2001) sensors have been reported to be used in closed-loop systems or to monitor the FES evoked activities online. Even though there has been research on several closed-loop FES systems, they have not been extensively applied in clinical applications (Ibitoye et al., 2016c). Evoked-EMG is one of the most popular methods for closed-loop FES systems because it correlates relatively well with the muscle contraction force.

Alternatively, a mechanomyography (MMG) sensor can be used to record the mechanical activities of the muscle.

Zhang et al. (2013) developed a closed-loop FES system to control knee joint torque with real-time feedback of the evoked-electromyography (eEMG) on able-bodied volunteers using EMG-feedback predictive control (EFPC) to control joint torque. Results showed adequate torque tracking with an RMS error of approximately 2.2 N m. However, their techniques for removing stimulation artefacts from the eEMG signal remain unclear, and the experiment was limited to able-bodied volunteers and did not consider muscle fatigue.

Li et al. (2016) proposed an eEMG controlled real-time closed-loop FES system to estimate induced joint torque and muscle activation on both healthy and SCI volunteers. Results showed that joint torque prediction and muscle activation tracking and control of FES were satisfactory. However, a large number of subjects could vary the results of muscle activation tracking and joint torque prediction accuracy using the Kalman filter neural network. Another EMG-based real-time closed-loop control FES system was proposed by Li et al. (2017) to control four muscle activation patterns in triceps surae and tibialis muscle by adjusting the pulse width. Three able-bodied and five SCI patients were investigated. Results showed satisfactory tracking of the muscle activation by pulse width modulation and EMG feedback. However, the researcher did not consider muscle fatigue in the experiment and any detection technique. An alternative to the EMG signal can be the MMG signal (Tanaka, Okuyama, & Saito, 2011). The MMG sensors have been reported to quantify muscle fatigue during FES muscle contractions (Ebersole et al., 1999). Furthermore, the MMG signal is not influenced by stimulation artifacts. Studies on MMG applications in FES systems have found a strong correlation between MMG parameters and FES induced torque (Hill et al., 2016; Ibitoye et al., 2016b).

Krueger, Scheeren, Nogueira-Neto, Button, and Nohama (2017) used two MMG features, RMS and mean frequency (MF), to investigate a possible relationship between healthy volunteers and SCI patients in their rectus femoris and vastus lateralis. The result showed that RMS and MF were not consistent between healthy volunteers and SCI patients due to differences in slow and fast-twitch muscle fiber composition and responses. Moreover, RMS and MF were inversely correlated, which could be due to the usage of monophasic pulses and the charge imbalance at the activated nerve. The researcher focused on off-line analysis but suggested implementing an MMG sensor in a closed-loop application. Ibitoye et al. (2016b) estimated NMES-evoke knee extension (KE) torque using the MMG signal and a Support Vector Regression (SVR) model with a kernel function. Results of eight healthy volunteers showed that the knee torque prediction accuracy achieved was up to 94% and 89% for actual and predicted torque values, respectively, in a cross plot of training and testing data set.

Wu, Wang, Huang, and Gao (2018) introduced real-time voluntary knee motion recognition using a multichannel mechanomyography signal from MMG sensors, attached to clothes. Eight able-bodied subjects were selected to classify six knee motions with the support vector machine (SVM) using four features, namely the mean standard deviation (STD), autoregressive coefficients (AR(3)), the difference in mean absolute value (DMAV), and power spectral density (PSD). The mean accuracy achieved was 88%. The system's accuracy increased up to 91% with the proposed DMAV feature. However, MMG knee motion classification in real-time closed-loop FES induced knee motion can be challenging.

Most of the closed-loop studies in real-time applications use EMG sensors to monitor or control the contraction strength of the muscle. MMG sensor applications in the FES system have been mostly used to perform muscle assessment or torque estimation.

However, based on the literature, researchers have not yet reported any MMG sensor-based real-time FES system that monitors SCI patients' muscle performance and prevents overstimulation. Muscle fatigue is one of the limitations of FES applications and must be monitored to avoid overstimulation of the muscles. This pilot study proposed a novel MMG sensor-based FES system that uses the MMG-RMS feature in real-time to detect muscle fatigue. The proposed FES system was configured to automatically terminate the stimulation session, depending on the fatigue-related drop of the MMG-RMS signal. To validate the system, isometric torque was measured throughout the experiment.

5.2 Experiment Protocol

5.2.1 Participants:

This pilot study was conducted in the Department of Rehabilitation, University of Malaya Medical Centre. Three subjects with motor complete SCI were included, according to the American Spinal Injury Association (ASIA) impairment scale (AIS) A and B, implying complete motor loss. The SCI subjects were 30, 47, and 51 years of age with a level of injury at T4, C7, and T1 and time post-injury 5, 13, and 15 years. AIS scale B for the first two and AIS scale A for the last one. Before starting the experiment procedure, each subject signed the consent form as approved by the University Malaya Medical Centre ethics committee (Approval No: 1003.14 (1)). All subjects were experienced FES users.

5.2.2 Experiment setup

A constant voltage, wireless controlled stimulator (custom developed) was used in this experiment. The stimulator waveform was a biphasic charged balanced square wave. The amplitude was set according to the patients' maximum tolerable current to reach maximum possible muscle contraction (Ibitoye et al., 2016b), and amplitude was adjusted (80-90 Vp-p) for each individual to generate a complete unloaded knee extension prior to the experiment (Krueger, Scheeren, Nogueira-Neto, Button, and Nohama 2017). However, the maximum tolerable amplitude level was limited to the patient's comfort when high stimulation current contracts the muscle.

The frequency and pulse width were fixed at 35 Hz and 350 μs according to the recommendations of Vargas Luna José, Krenn, Cortés Jorge, and Mayr (2013). Two 9 x 15 cm self-adhesive skin surface electrodes (RehaTrode, HASOMED, Germany) were placed proximally 7-10 cm above the patella and the second one 7-10 cm higher in the proximal distance (Gargiulo et al., 2008; Gobbo, Maffiuletti, Orizio, & Minetto, 2014; Kralj & Bajd, 1989). Figure 5.1 illustrates the experimental setup.

The subject is seated on the Biodex chair for isometric torque recording. Stimulation electrodes are attached on the quadriceps muscle. The MMG sensor was mounted on the skin surface over the rectus femoris muscle belly. Signals are recorded using a DAQ card and then processed on a laptop computer using LabView Software.

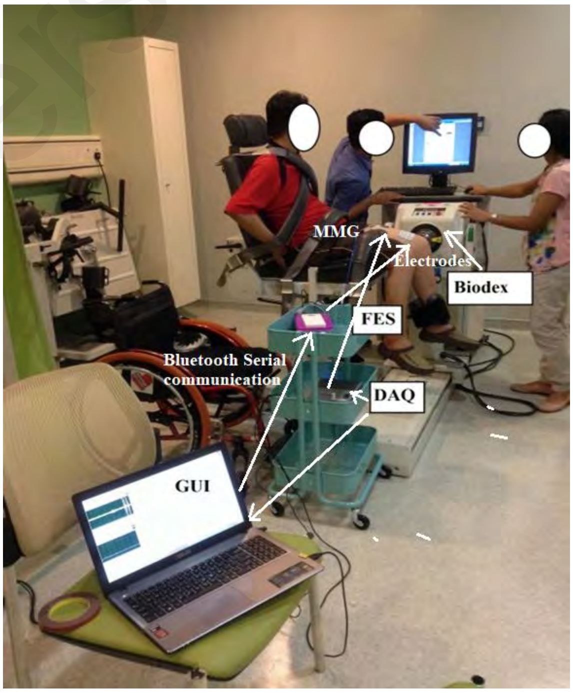

Figure 5.1: Experimental setup for the proposed real-time monitoring FES system

5.2.3 Instrumentation

Isometric torque was measured with the Biodex dynamometer System 4 (Biodex Medical Systems, Shirley, NY, USA) and concurrently recorded with muscle MMG signal. The MMG sensor was connected to the National Instruments (Austin, TX, USA) Multifunction I/O Device USB-6343, which is connected via USB to a laptop computer running LabView (National Instruments, Austin, TX, 2014) for further data processing and controlling the stimulator remotely via serial port.

5.2.3.1 MMG measurement

An accelerometer sensor (ADXL335) was used to collect MMG signals (Islam et al., 2014). (Islam et al., 2014). The dimension of the accelerometer on the PCB board is 18 mm × 15 mm × 2 mm. A plastic casing of 30 mm diameter and 4 mm height (inside to outer surface thickness 1 mm) was used to obtain maximum muscle vibration from the skin surface. The sensor sensitivity was 300 mV/g. The MMG sensor was placed on the muscle belly over the rectus femoris using double-sided tape to ensure gentle placement on the skin (Ryan et al., 2008a). The knee joint angle was set to 30° using the Biodex knee attachment module (Mohamad, Hamzaid, Davis, Abdul Wahab, & Hasnan, 2017).

During the electrically evoked muscle contraction, the MMG signals were acquired at a 1 kHz sampling rate. To reduce movement-related noise and artifacts (Beck et al., 2009; Madeleine, Bajaj, Søgaard, & Arendt-Nielsen, 2001) the acquired raw signal was digitally filtered with a zero-phase 4th order Butterworth bandpass filter with cut-off frequencies of 5Hz and 100Hz. Data was recorded in three trials for left and the right legs with 15 minutes of rest between each trial per day. The resting period ensures that the muscles are completely recovered at the beginning of each trial. Each SCI individual participated in three sessions, with a minimum duration of 48 hours between session days (Kesar & Binder-Macleod, 2006).

The recorded data was processed in real-time using a LabView program for extracting the RMS feature of the MMG signals. The MMG-RMS feature was calculated every second and compared with its initial RMS value starting from the third seconds (avoiding the first two seconds to allow sensor readings to stabilize). The FES-evoked muscle fatigue was defined as the percentage drop in MMG-RMS value compared to the initial value and was compared with the drop in isometric torque. Three threshold values were defined; 50% (thr50), 60% (thr60), and 70% (thr70) drop from initial MMG-RMS value. A custom-written algorithm (Figure 5.2) was incorporated in the LabView software to automatically terminate the stimulation session when the MMG-RMS value dropped to the threshold value. Isometric torque, measured with the Biodex dynamometer, was additionally recorded for offline analysis and to validate the MMG response.

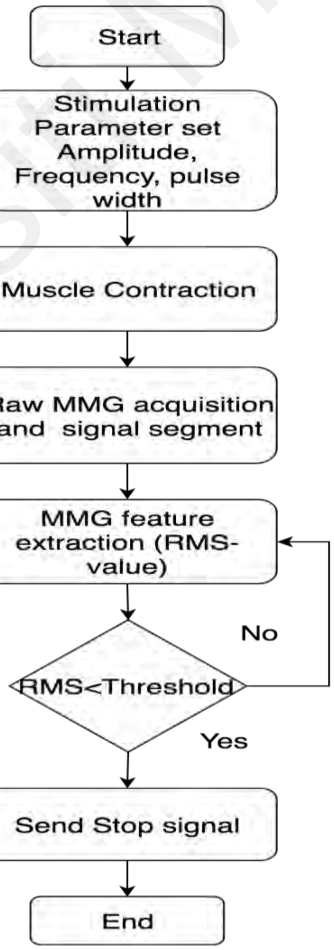

Figure 5.2: Flow chart of the FES system with MMG-based real-time fatigue monitoring and safety shut off.

5.3 Results and analysis

Figure 5.3 and 5.4 show the mean and standard deviation of the MMG-RMS and the isometric torque for 3 trials at different threshold values. The threshold level thr70 shows longer stimulation time as well as MMG-RMS and torque drop the lowest from its initial value. It can be seen from Figure 5.4 that the torque dropped below 9 N-m from the maximum mean torque of 18 N-m. When stimulation starts to reach the peak torque as displayed on the Biodex-system, the response time is higher, while the MMG-RMS response is instantaneous (less than a second).

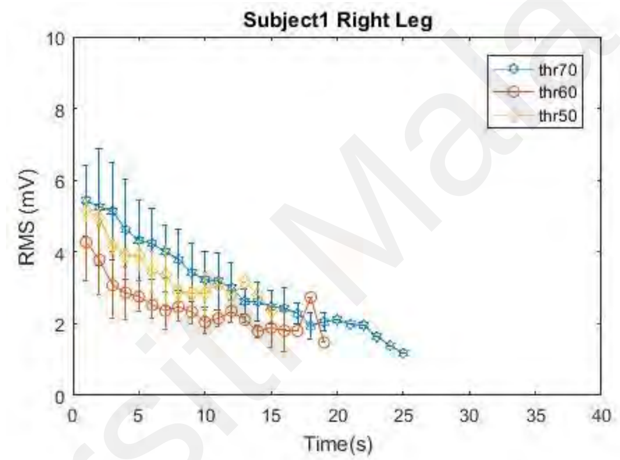

Figure 5.3: MMG-RMS over stimulation time of three trials with safety-shutoff at thr50, thr60 and thr70 for Subject 1, right leg

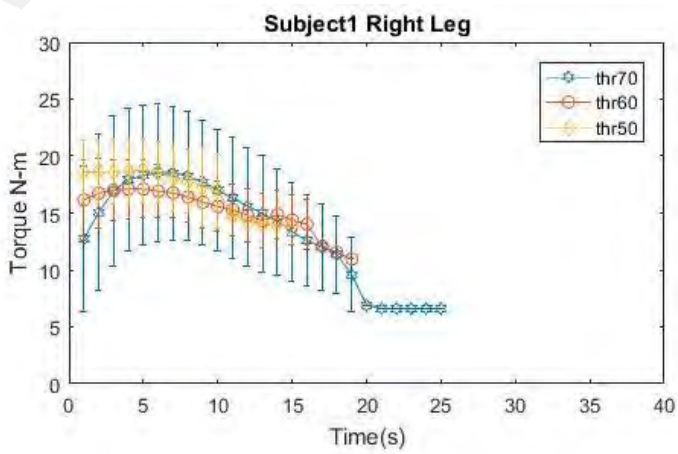

Figure 5.4: Isometric torque over stimulation time with safety-shutoff at thr50, thr60, and thr70 drop for Subject 1, right leg

Table 5.1 shows the mean auto-termination time of all trials for all 3 subjects in both legs for RMS threshold levels thr50, thr60, and thr70. The stimulation time of thr70 is significantly longer than thr50 (p=0.01).

Table 5.1: Average stimulation time for different RMS threshold drops.

RMS Threshold Level	Trials^	time, s (Mean , SD)
thr50	18	22.7 ± 9.9
thr60	18	25.6 ±11.2
thr70	18	31.2 ± 8.7*

* Indicates a significant difference. ^ Each leg 3 trials in 1 day, 3 days 9 trials for one leg, both legs 18 trials.

The stimulation times to reach the threshold thr50 and thr60 are statistically not different (p=0.38) as well as the stimulation times to reach thr60 and thr70 (p=0.09).

Overall, the stimulation time increased as the threshold level decreased. Table 5.2 summarises the mean stimulation time for all 3 subjects for both legs. Subjects 1 and 2 had their mean stimulation time increased when the MMG-RMS was allowed to drop to a lower threshold, i.e., 11 s to 20.6 s when dropping from thr50 to thr70 (Subject 1, right leg). For subject 3, thr60 and thr70 showed a similar time of about 39 s with a lower stimulation time of 28 s at thr50.

Table 5.1: Stimulation end time (s) at different RMS threshold drop

Subject	Number of trials	Stimulation end time, s					
		thr50		thr60		thr70	
		Left	Right	Left	Right	Left	Right
1	3	27.3 ± 2.5	11 ± 3.6	21.6 ± 6.5	16 ± 3.0	28.6 ± 3.0	20.6 ± 3.7
2	3	19.3 ± 6.4	13.3 ± 1.5	18 ± 5.2	18 ± 4.3	34 ± 6.5	23.6 ± 2.0
3	3	37 ± 4.3	28.3 ± 3.5	41 ± 1.7	39.3 ± 1.1	42.6 ± 2.5	38 ± 5.2
Total	9	27.8 ± 8.8	17.5 ± 9.3	26.8 ± 12.3	24.4 ± 13	35 ± 7.0	27 ± 9.3
Time (%)		79.4	50	76.5	69.7	100	77.1

*Data in Mean ± SD

The stimulation time in the left leg did not show a consistent increment from thr50 to thr60 for all subjects. However, for subjects 1 and 2, their stimulation time significantly increased by about 7 s and 16 s for threshold thr60 to thr70 in the left leg. On the other hand, in subject 3's left leg, the mean stimulation time remained in the range of 37 s – 42 s for all threshold levels.

5.4 Discussion

A real-time MMG-RMS-based FES system that automatically terminates an electrical stimulation session when critical muscle fatigue occurs was successfully implemented on 3 SCI individuals on both legs. This study focused on muscle monitoring using an MMG sensor to detect muscle fatigue using the RMS feature of MMG. One of the most important features for monitoring muscle condition is the RMS feature of MMG. Two studies reported a linear relationship between RMS and isometric torque prediction (X. Chen et al., 2012). In our study, muscle fatigue was evaluated using a Biodex torque measurement device, while MMG-RMS values were computed every second. The mean stimulation time for both legs increased as the threshold decreased, as expected, and manifested by the longer stimulation time before safety shutoff occurs. Overall mean stimulation times in thr50 and thr60 were reportedly similar, suggesting that any future deployment of MMG-RMS as feedback in a closed-loop system should only consider thr70 MMG-RMS drop for critical fatigue detection.

The monitoring of muscle fatigue to prevent tissue damage during an isometric electrical stimulation training session was demonstrated. In future projects, MMS-RMS monitoring might be considered to prolong dynamic training sessions like FES cycling, which usually continues up to one hour (de Sousa, Harvey, Dorsch, Leung, & Harris, 2016). However, it must be considered that FES cycling employs periodic stimulation of different muscle groups, so the reliability of the sensor must be proven for such dynamic movement. The significantly longer time to fatigue in FES cycling (1 hour) compared to the stimulation time in this study (less than 1 min) is explained by the on-off stimulation regime in cycling, other than the simple continuous knee extension as presented in this study.

MMG-RMS thr50 and thr70 were significantly different (p=0.013) in stimulation time that indicates the thr70 MMG-RMS drop prolongs the stimulation time and influences the torque drop below 50% of initial torque, which indicates critical muscle fatigue (Yoshitake, Ue, Miyazaki, & Moritani, 2001). The produced torque (out of 18 trials) did not drop to 50% at MMG-RMS thr50 (drops 3 out of 18) and thr60 (drops 5 out of 18) as compared to thr70 (drops 14 out of 18). Therefore, a thr70 selection can be used as a muscle fatigue monitoring indicator, which is the proxy of the external torque measurement.

Considering that a drop of muscle torque to 50% of the initial value indicates the beginning of critical muscle fatigue (Cheng & Rice, 2010; Enoka & Duchateau, 2008), thr70 is the related threshold to stop stimulation. Therefore, thr70 combines the advantages of the longest stimulation duration with timely safety shutoff.

Results also indicated longer stimulation time in the left leg compared to the right leg (Table 5.2), meaning, the right leg tends to get fatigued more quickly than the left leg. Interestingly, stimulation times for thr50, thr60, thr70 did not change significantly for subject 3 in the left leg (Table 5.2). This could be due to physiological changes in the muscle properties and blood oxygenation (Hasnan et al., 2018; Hunt et al., 2006) that changed differently in both legs during stimulation (Laubacher et al., 2019), which affected muscle fatigue. In addition, psychological factors of an individual during FES exercise may also affect on early muscle fatigue. In (Belza, 1994), the authors defined muscle fatigue as a complex physiological and psychological phenomenon. As demonstrated in this study, the longest stimulation time was at the thr70 and shortest at thr50.

Moreover, total auto-termination time (all trials) for subjects 1 and 3 in between both their legs was significant (subject1 $p=0.0071$, subject2 $p=0.05$). On the other hand, subject 3 shows no significant changes in the performance of both legs ($p=0.145$). This indicates that the same stimulation parameter could have different effects on different legs of the same individual (Laubacher et al., 2019), which could be an effect of side dominance, whereby one side maybe naturally stronger than the other. The results confirm that the set-up of stimulation parameters should be adjusted individually before starting any long-duration exercise such as FES cycling.

This study was limited to monitoring muscle fatigue only using the threshold of the MMG-RMS feature. As the number of subjects in this study is small, it is difficult to generalize the inter-subject's correlation of muscle fatigue time based on MMG-RMS as the stimulation shut-off source. Further investigations of the real-time MMG might qualify the sensor to be included in closed-loop systems that can vary in real-time any FES parameters to control muscle contraction and simultaneously monitor muscle fatigue. This study shows that MMG-based real-time closed-loop application may replace additional fatigue-monitoring torque measurement systems, reducing the amount of equipment and the effort for manual monitoring. In combination with the results of this study, MMG demonstrated its potential to serve as a feedback signal in real-time control of FES applications such as FES standing (Dzulkifli, Hamzaid, Davis, & Hasnan, 2018).

5.5 Conclusion

In conclusion, this study presented a real-time fatigue monitoring FES system, based on the MMG-RMS feature. Each SCI subject's mean stimulation time depends on the MMG-RMS drop from its initial stimulation time. MMG-RMS thr70 drop allowed a longer stimulation time compared to thr50 and thr60 and was able to successfully detect muscle fatigue, as defined by the 50% drop in torque. Besides, this study found that each muscle performs differently, even in the same SCI individual. However, due to the dynamic muscle responses which affect each individual's fatigue time, further investigation is required to use features of the MMG sensor to monitor FES-related exercise or training sessions. FES-evoked activities such as cycling, hand dynamometry, and standing for SCI patients could be performed safer, and more conveniently with minimal manual intervention.

CHAPTER 6: SIMULATION OF DIFFERENT MODES OF USER CONTROL STRATEGY TO SUSTAIN STANDING DURATION WITH SCI TO PREVENT MUSCLE FATIGUE WITH MMG FEEDBACK

6.1 Introduction

Functional electrical stimulation (FES) has been widely used to restore lost motor function after spinal cord injury (SCI). FES standing is an essential exercise since it could stimulates lower limb muscles and bones, including increasing the muscle force production following sufficient training (Gordon & Mao, 1994). This exercise also has the advantage of improving physiological and musculoskeletal outcomes (Abreu, Cliquet, Rondina, & Cendes, 2008; Previdi et al., 2005; Riener, Ferrarin, Pavan, & Frigo, 2000).

The main limitations to achieving these benefits and other positive outcomes of the FES standing exercise are the complexity of motor unit recruitment and firing frequency and the consequent rapid muscle fatigue onset. The literature (Ibitoye et al., 2016a) indicates that rapid muscle fatigue impedes prolonged FES standing as muscle fatigue cannot be eliminated from FES induced contractions. Ongoing research efforts to attenuate muscle fatigue effects to prolong the FES standing exercise duration using different control methods and controllers are being undertaken. Common control methods include the proportional integral derivative (PID) controller, fuzzy logic controller, neural network (NN) controller, and the on-off controller. These methods were mainly used for FES parameters optimisation for better control in muscle contraction. For example, a computer simulation-based reinforcement machine learning method (Davood & Andrews, 1998) was used by implementing a fuzzy logic controller in FES to support the sit-to-stand exercise. In (Davis, Houdayer, Andrews, & Barriskill, 1999), a complex implanted stimulator to prolong FES closed-loop standing exercise was implemented on two paraplegic people. At a 10° knee angle drop, this study presents a control system for knee angle correction using goniometer feedback sensing. The implanted stimulation and knee angle feedback showed that people with paraplegia could maintain an upright stance for ≥ 60 min. Before this study, Davis, Houdayer, Andrews, Emmons, and Patrick (1997) also applied FES-closed-loop using surface electrodes to achieve uninterrupted standing for ≤ 30 min. However, in this experiment, the application of the muscle fatigue monitoring system was not considered, hence, no reporting on the standing duration.

In another study by Yu et al. (2001), a PID controller was applied to FES in standing to control knee-end velocity (Yu et al., 2001). The experiment was implemented by stimulating quadriceps and hamstring muscles and compared with an open-loop and on/off control system in people with SCI. The study employed an electrogoniometer to capture knee angular velocity as a feedback signal in the PID control system. The controller performed best in reducing knee extension velocity rate when compared to the other two stimulation methods based on open-loop control of stimulation. Another FES closed-loop study on smooth standing outcome was reported by Jaime, Matjacic, and Hunt (2002). Their experiment was conducted in real-time by varying stimulator parameters (i.e., amplitude, pulse width, and frequency) modulation to control standing balance using a force plate as a reference track in a person with paraplegia.

Bijak and co-researchers (Bijak et al., 2005) conducted an FES-supported standing and stepping study in SCI patients by stimulation parameters optimisation. The authors (Bijak et al., 2005) reported a smooth upward movement in standing by stimulation onset duration between 0.2-0.4 s for quadriceps and gluteus muscle activation. This study did not consider the limiting influence of muscle fatigue. Generally, none of those above studies applied signals of muscle origin that are immune to stimulation artefacts (Ibitoye et al., 2014b), such as our proposed method that utilizes an MMG signal that is sent as a feedback signal to optimise the stimulation parameters and at the same time monitors muscle performance during the standing exercise.

Dzulkifli et al. (2018) conducted an FES standing study to predict FES induced torque using MMG-RMS and RMS-zero crossing as a feedback signal for artificial NN controller in individuals with SCI. However, the NN controller was trained with a very small number of data sets, which may have affected the accuracy of their study. Additionally, optimisation of stimulation parameters was not considered to prolong standing duration in their study. In a recent experimental study by (Ibitoye et al., 2020a), MMG amplitude was identified as a proxy of muscle fatigue during standing exercise in people with SCI. These studies did not consider the importance of the stimulation parameters selection criterion for extending standing time or reducing fatigue time. In this study, stimulation of different modes is simulated in control of standing by an SCI user by pressing a button to increase the amplitude.

6.2 Methodology

This study was in two stages. In the first stage of the study, an FES standing experiment was conducted on SCI individuals to collect MMG signals from their rectus femoris (RF), vastus lateralis (VL), and vastus medialis (VM). This was done to obtain the MMG-RMS values for application, such as feedback signal for FES standing optimisation to attenuate the effect of the early onset of unavoidable muscle fatigue. In the second stage of this study, a simulation environment was created using a python programming language with the experimental MMG-RMS values representing standing duration and contraction strength. Each participant with SCI underwent two experimental trials separated by 48 hours following the standard procedure to check the muscle fatigue effect.

6.2.1 Study population

Five experienced FES users with SCI (four male and one female) voluntarily participated in this experiment. All the participants had motor-complete SCI and were unable to do voluntarily contract their lower limb muscles. Their injury levels were A and B (i.e., according to AIS (Fawcett et al., 2007); injury levels were between C6 and T4; age: 40 ± 9 years; body mass: 73 ± 7 kg; postinjury duration: 11 ± 5 years; and body height: 171 ± 6 cm. The participants were made to stand with Biodex harness support for safety. The following exclusion criterion for the participants' recruitment is (1) severe contractures, (2) pressure sores, and (3) severe spasticity, which could have prevented smooth and upright standing posture. Throughout the experimental sessions, participants were continuously being monitored, especially their blood pressure and heart rate, by a rehabilitation physician to ensure their medical fitness. Each participant endorsed a written informed consent form before participation. The experimental procedure was approved by the University of Malaya ethical committee with approval No: MECID.NO: 20164 – 2366.

6.2.2 FES set up and MMG signal acquisition

In the standing experiment, two different stimulation frequencies of 20 Hz and 35 Hz were chosen to vary the muscle fatigue onset time (Eser, Donaldson, Knecht, & Stussi, 2003; Ibitoye et al., 2016a). Based on an earlier proof of concept study that was published in our laboratory (Ibitoye et al., 2020a), stimulation was stopped manually when the observed knee buckle angle was up to 30°. This was in accordance to the study of Braz et al. (2015), which identified this knee position as the point of critical muscle fatigue measured by a goniometer. The stimulation pulse width was fixed at 300 μs in both frequencies' trials. Stimulation current was delivered via current-controlled neuromuscular stimulator (RehaStim™, Hasomed GmbH, Magdeburg, Germany) through pairs of surface electrodes (9 cm × 15 cm; Hasomed GmbH, D-39114

Magdeburg, Germany) and were placed on quadriceps and gluteal muscles (Ibitoye et al., 2020a) (Figure 6.1). It is important to note that the delivered/selected stimulation currents vary depending on the individuals based on their muscle size and tolerance, ranging between 80 mA and 120 mA, for quadriceps, while the gluteal current was 20% less compared to the quadriceps as recommended in (Braz et al., 2015).

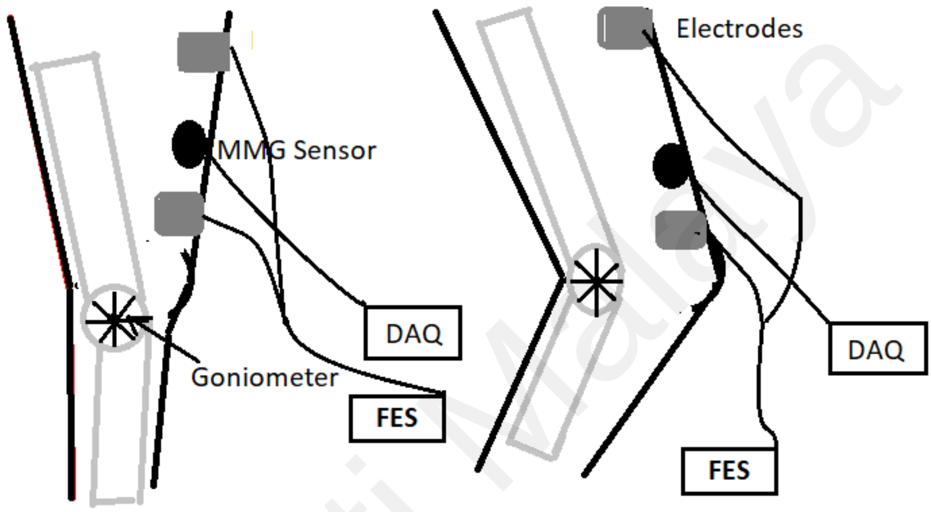

Figure 6.1: The experimental setup for FES supported standing, one MMG sensor showing at the lateral side only

The MMG signals were collected and recorded at a 2 kHz sampling rate using the BIOPAC system (MP150, BIOPAC Systems Inc., Goleta, CA, USA), and the signals were digitally filtered between 20 Hz and 200 Hz as recommended in (Dzulkifli et al., 2018). Furthermore, the MMG-RMS values were extracted from the processed MMG signals at every second in the FES five modes of simulation stage, which is the second stage of this study.

6.2.3 FES five modes of simulation

The simulation environment was created using a python script. The simulation environment was designed to emulate actual SCI user activity, such as manually pressing a button using one's hand to increase stimulation current and preset settings to sustain longer standing duration. The simulation environment was separated into five settings: (i) open-loop; (ii) single press increase at 5 s; (iii) single press at 10 s; (iv) double; and (v) triple press increase.

In the open-loop setting, the stimulation parameter (i.e., current) remains unchanged for all users. For the single press 5 s setting mode, the current increases on the 5th, 10th, and 15th seconds. The single press 10 s setting raises current values on the tenth, twentieth, and thirtieth seconds. While the double press and triple setting modes, as shown in Figure 6.2, increase current at the 10th, 20th, and 30th second twice and three times.

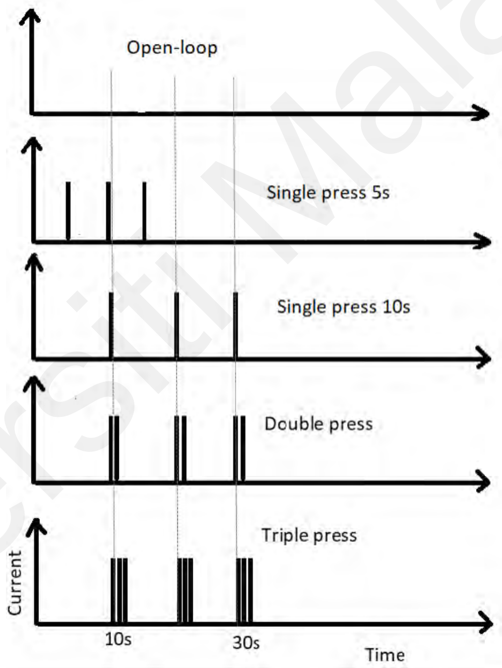

Figure 6.2: Five settings for simulation environment adopted in this study

For the simulation, the input signal was MMG-RMS values. Three sensors' MMG-RMS values were combined (i.e., affixed to RF, VL, VM) to get a single MMG-RMS value in the combination of sensors (RF-VL, RF-VM, VL-VM) to randomize the simulation. The increment and decrement of MMG-RMS values in different settings (i.e., single, double, and triple press) were simulated randomly to avoid bias in simulation results. Every single button press gives the effect of the current increase to reflect in the MMG-RMS increase up to 10-20% from the maximum MMG-RMS value depending on individual participant muscle responses. The rate of increment of MMG-RMS in the double and triple press settings is made to be lower than the preset of the single press for the simulation to reflect the dynamic response from the user. Conversely, the effect the simulated decrement rate after increment in the MMG-RMS values was also random. This was because when multiple presses occur, the rate of decrement is usually faster, and this could be caused by muscle fatigue in random as muscle may not be able to sustain a long time due to the quick increment (Braz et al., 2015).

The simulation stopped automatically when MMG-RMS values dropped by 80% from the initial value, which indicated critical muscle fatigue. The threshold value was selected to confirm that all the trials become fatigued in actual torque measurement. The analysis ignored the first two seconds of MMG-RMS values due to signal instability during stimulation onset. To analyse and compare simulated and standing data, the IBM SPSS software (version 20, IBM SPSS for Windows, Armonk, NY, USA) was used to find the relationship between the trials, participants, and simulated setting mode. Statistically significant ($p \leq 0.05$) was set as the acceptance level.

6.3 Result

Figure 6.3 depicts the results of the simulated output for all five settings when the MMG-RMS dropped below 80% for a subject at 20 Hz frequency. From the figure, it can be seen that the MMG-RMS value dropped quickly for the double and triple press settings. In the figure, actual-RMS depicts computed MMG-RMS from experiment data. The highest simulation time was achieved in the 10 s setting compared to other setting modes. The single press 10 s setting simulation time was near the actual standing time, which could be referred to as the point of 30° knee buckle or critical muscle fatigue (Dzulkifli et al., 2018; Ibitoye et al., 2020a).

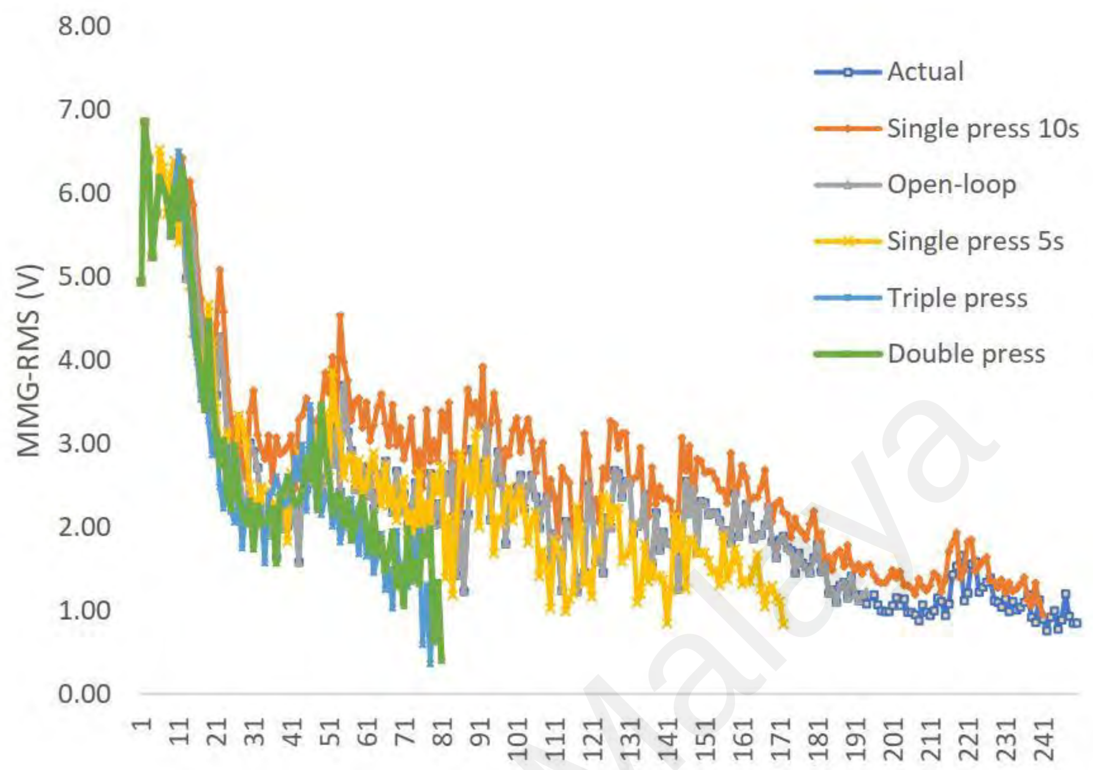

Figure 6.3: Simulated MMG-RMS output of 20 Hz for five settings of subject 2 as a representative case

Furthermore, since the simulation time also depends on each participant due to different dynamic muscle responses when electrical stimulation is applied (Lynch, Graham, & Popovic, 2011), the average simulation times observed for the five subjects were 64 ± 40 s, 125 ± 63 s, 80 ± 43 s, 51 ± 21 s, 45 ± 15 s for participants one to five, respectively. A summary of the simulated standing time for the two stimulation frequencies is given in Table 6.1.

From the table, the average standing time was higher for the 20 Hz frequency when compared to the 35 Hz frequency because higher frequency results in a faster onset of muscle fatigue (Ibitoye et al., 2020a). The recorded first trial stimulation time was higher than the second trial simulation. This could be due to inadequate fatigue recovery time for the same muscle group resulting in earlier fatigue onset on the second trial, preventing longer standing duration (Ibitoye et al., 2020b). Overall, the standing duration between the low frequency 20 Hz and high frequency 35 Hz stimulation was statistically significantly different ($p \leq 0.001$).

Table 6.1: Average simulation time of sensors combinations in 20 and 35 Hz frequency in five subjects

Subject No.	20 Hz		35 Hz	
	Trial1 time (s)	Trial2 time (s)	Trial1 Time (s)	Trial2 Time (s)
1	128 ± 72	98 ± 62	68 ± 43	52 ± 30
2	156 ± 65	98 ± 19	58 ± 34	47 ± 16
3	83 ± 67	96 ± 73	94 ± 58	64 ± 20
4	58 ± 25	64 ± 20	53 ± 22	35 ± 5
5	51 ± 12	53 ± 14	70 ± 25	36 ± 3

The different simulation setting modes (i.e., the manually controlled settings) also affected the standing duration and muscle fatigue time, as shown in Table 6.2. In the open-loop mode for participants 1, 3, 4, and 5, the average standing duration was below 70 s, while for participant 2, the standing duration was about double the values recorded for open-loop, which indicated the fatigue duration differences for these two cases. Compared to the single press 5 s setting, the double press, and the triple press settings, the standing duration was also lower. However, the highest standing duration of 10 s was found in single press mode. For the 10 s mode, the stimulation current increased in a single unit at a time, then the muscle stayed in the resting position compared to other setting modes.

Table 6.2: Average simulation time of three sensor combinations for the different five setting modes

Subject No.	Open-loop duration (s)	Single press mode	Single press mode	Double press mode	Triple press mode
		10s	5s	10s	10s
1	62 ± 37	153 ± 58	110 ± 57	62 ± 35	44 ± 12
2	98 ± 67	141 ± 67	91 ± 48	61 ± 25	57 ± 25
3	66 ± 27	174 ± 61	91 ± 28	47 ± 7	43 ± 8
4	48 ± 14	81 ± 24	52 ± 19	42 ± 7	36 ± 7
5	47 ± 11	74 ± 29	56 ± 12	42 ± 9	42 ± 7

Statistically, there were significant differences between setting modes. The open-loop mode is only significantly different in standing time ($p \leq 0.001$) from the single press 10 s mode only, while other setting modes did not show any statistical significance in terms of the p-value of 0.315 for the open-loop single press (5 s), and p-value of 0.748 for the open-loop-double press, and p-value of 0.088 for the open-loop-triple press. Furthermore, the single press 5 s was not significantly different ($p > 0.005$) compared to the single press 10 s, while other modes are significantly different.

On the other hand, double press and triple press mode were significant to single press 10 s and single press 5 s mode. All in all, statistical analysis shows that single press 10 s mode systems performance was better in extending the FES standing exercise duration when compared to other setting modes. These results also show that the application of the MMG signal may be useful in monitoring muscle fatigue during standing exercise. Although the single press 10 s setting showed good performance in the designed simulation environment, further practical FES supported standing in a wider population may be needed to generalize the good performance obtained in this study, and this may also influence statistical inferences.

6.4 Discussion

Muscle fatigue prevents FES users from continuing standing exercises for a long duration. In FES-supported standing, in some situations, users may desire to control the level of stimulation current 'strength' by themselves during standing. However, due to the users' lack of understanding of muscle fatigue and stimulation intensity relations, the standing durations can be significantly affected when stimulation parameters are manually controlled by the SCI users or by a physiotherapist who may also be due to the unavailable or inaccessible appropriate feedback measure during FES-assisted standing. In general, standing stimulation operates in an open-loop where the stimulation parameters are fixed, and fatigue can happen faster when parameters do not fit the SCI individuals. Available literature showed a strong correlation between MMG-RMS and muscle fatigue (Ibitoye et al., 2019). Thus, this research shows how muscle fatigue can affect standing duration in different settings modes of stimulation in a simulation environment.

The open-loop stimulation requires very laborious attention to monitor muscle fatigue by visual inspection when the knee buckle occurs and stop stimulation at the right time. Having a feedback system to the stimulator helps to monitor SCI individuals accurately when muscle fatigue happens. Figure 6.3 shows that in the open-loop mode, the standing duration reaches about 191 s while the actual standing duration is about 242 s. This shows that muscle fatigue occurs much earlier than assumed when no intervention was made during the standing session. The single press 10 s mode standing duration reached a duration close to the actual experimental standing duration from stage 1 because of stimulation amplitude changes in a controlled manner, which delayed fatigue time rather than the fixed amplitude parameter settings in open-loop.

Muscle fatigue was also compared between trials and two frequencies in Table 6.1. Higher stimulation frequency causes muscle fatigue to happen faster than lower frequency (Kesar & Binder-Macleod, 2006). For subjects 1, 2, and 4, with lower frequency (20 Hz), the average standing durations in all trials are higher than 35 Hz. On the other hand, for subjects 3 and 5, their standing duration only fit the hypothesized frequency strategy in the second trial. The outcome of this finding suggests that the selection of stimulation frequency plays an important role in standing duration. Importantly, through this simulation exercise, the result shows that muscle fatigue detection by MMG-RMS threshold and thus termination of FES standing occur earlier than all the experimental trials done through observation of knee buckles.

Table 6.2 shows the simulated standing time in five modes of settings for each individual. The user control modes significantly affect the standing time by pressing a button multiple times to increase the stimulation power. Simulated modes were assumed to have a layperson understanding of FES current control effect and are not advanced in understanding control stimulation parameters by themselves and also do not have direct access to the state of their muscle fibers, thus being uninformed about their muscles' fatiguability prospect. The simulation modes were also considered stressful situations such as FES-evoked standing body imbalance and heightened security demand during standing, and they could press the ‘current increase’ button multiple times to increase the current amplitude. Thus, in the simulated environment, the effect of multiple presses (double and triple press) modes on the standing duration becomes shorter than in open-loop for all subjects. This is very likely due to the fact that multiple presses cause more increases in amplitude, and consequently, the muscles fail to sustain a long-standing duration. The most recommended strategy in terms of prolonged standing duration would be a preset 10 s single amplitude increment, which could deliver the highest standing duration (mean 124 s) compared to all other modes (open-loop: 64 s, single press 5 s: 80 s, double press 10 s: 51 s, and triple press 10s: 44 s). These results show that the application of the MMG signal may be useful in monitoring muscle fatigue during standing exercise. The single press 10 s setting showed good performance in the designed simulation environment; further trials on FES supported standing in a wider SCI population may be needed to generalize the favorable performance obtained in this study, which may also influence its statistical inferences. Although this study did not develop an adaptive stimulation parameter controller, these different modes of settings will help researchers to design a closed-loop MMG based electrically evoked standing system and conduct experiments more efficiently.

6.5 Conclusion

In clinical applications of FES-supported standing, safety is of high priority and is always desirable for objective clinical deployment. Because of random button pressing, unnecessary current increase, and thus faster fatigue onset, manually-controlled standing using stimulation button pressing may promote over-stimulation and, as a result, faster knee buckle. In this research, five modes of stimulations are simulated for optimal parameter selection purposes for standing exercises. The double press and triple press settings tended to shorten the standing duration and induced faster muscle fatigue. The single press 10 s mode proved efficient in achieving a relative maximum standing duration using MMG-RMS feedback. Thus, this research benefits rehabilitation physicians using the FES standing training program to improve the FES-standing protocol of people with SCI.

CHAPTER 7: CONCLUSION AND RECOMMENDATION

This Chapter discusses the conclusion derived from the results obtained following the research studies conducted in this thesis. The Chapter also describes the thesis contributes to knowledge, the limitations of the thesis, and future recommendations of this thesis.

7.1 Conclusion

This thesis focused on developing and implementing a real-time muscle monitoring FES system using mechanomyography as a feedback signal for individuals with spinal cord injury. Following several experimental studies, the results obtained from these studies have answered the research questions in the thesis objectives.

The first thesis objective was to deploy and implement mel-frequency cepstral coefficients (MFCC) feature extraction method to detect muscle fatigue from MMG signals collected from quadriceps muscles in persons with SCI during FES cycling using support vector machine classifiers. This was meant to demonstrate that the MMG signal could be used to track muscle contraction patterns during FES supported physical exercise such as cycling. Chapter 3 of this thesis was published in Medical & Biological Engineering & Computing and showed that MFCC features of the MMG signals were able to classify non-fatiguing contractions and fatiguing contractions during FES supported cycling exercise in individuals with SCI. Specifically, the MFCC feature demonstrated higher accuracy with up to 90.7% in classification than the RMS feature of 74.5% accuracy in RF, VL, VM muscles with SVM classifier.

The average classification accuracy of the three sensors in each subject varied with a small standard deviation, and the outcome suggests that a single sensor may be sufficient to monitor muscle fatigue in quadriceps muscles. The accuracy of the RMS feature was lower than that of the MFCC feature of MMG, however the computation cost was lower in RMS compared to that of MFCC. Overall, the purpose of the first objective was fulfilled by introducing new feature extraction methods for MMG signals to detect muscle fatigue using MFCC.

The second objective of this thesis was the development of a real-time muscle monitoring FES system using MMG sensor. The study conducted on this objective was reported in Chapter 4 of the thesis, and the study is in preparation for publication. This study described the design and development of a stimulator system to monitor muscle condition in real-time using MMG sensor during standing. For implementation, a pair of two-channel Bluetooth controlled FES was used for control communicate to elicit sufficient muscle power to support standing exercise in individuals with SCI. The MMG responses from induced quadriceps muscle contractions showed a clear relationship between the drop in knee angle and MMG signal drops. Furthermore, the control signal responses were instantly sent from the graphical user interface to control stimulator parameter’s when knee-buckling began.

The third thesis objective focused on implementing MMG signal for muscle fatigue detection during isometric muscle contractions evoked by the developed stimulator. This study on MMG-based real-time muscle fatigue detection has been published in the journal Biomedizinische Technik, De Gruyter. The experiment was conducted in a secured and controlled laboratory environment using Biodex Isokinetic Dynamometer to measure isometric knee torque. This was done in order to be able to compare the fresh and fatiguing muscle contraction with the MMG-RMS feature. In the experiment, the stimulation was made to automatically switch off during the isometric knee extension task once there was a drop in MMG-RMS compared to the preset threshold value. It was identified that the thr 70% (i.e., when RMS amplitude dropped to 70% from initial value) setting related to the drop in MMG-RMS had the maximum number of trials matched to detect muscle fatigue time with dynamometer’s torque measurement. In general, this study uniquely provided evidence on the relationship between MMG signal and isometric muscle fatiguing contractions in individuals with SCI using the developed stimulator to evoke muscle contractions.

The fourth objective of this thesis was to simulate different modes of stimulation for standing exercise using MMG-RMS as the feedback signal. This was done to investigate if this practice could objectively prolong standing duration. This study sought to simulate different modes of settings to optimise stimulation parameters from the experimental standing data. The experimental standing data of MMG-RMS was used to simulate five modes of control actions from SCI users. The button press was used to increase amplitude to sustain upright standing. Among the different settings for stimulation control strategies, the single press 10 s mode system supported the maximum simulated standing duration while the other simulated modes led to shortened standing duration. Overall, this thesis has presented the design and development of muscle condition monitoring FES system using MMG as the feedback signal. This was validated to recognize fresh and fatiguing isometric muscle contractions and standing exercise in individuals with SCI.

7.2 Study contributions

The main contribution of this study was to develop an FES device using MMG as the feedback signal. The thesis also investigated the device's performance during isometric knee extension, cycling, and standing exercise. Although this thesis mainly focused on lower limb rehabilitation, the results could also be applied to rehabilitate upper limb functions such as wrist extension and flexion. While the FES system was developed with MMG as the feedback signal, other sensors such as a goniometer, force-sensitive resistor, and similar sensors can be integrated in the future.

Furthermore, while most of the commercially available stimulator's firmware is restricted to the modifying of stimulation parameters by the user, the developed FES system in this thesis stood out with the integrated FES controlled FES algorithm for automatic parameter optimisation. The outcomes of the studies conducted in this thesis also broaden the rehabilitation research application of MFCC for MMG feature analysis and extraction. In addition, the parameter selection criterion in this thesis could also aid our better understanding of how stimulation parameters affect muscle fatigue time when applied in clinical settings. Overall, this thesis has contributed to developing a viable and clinically useful FES system with MMG feedback to promote physical exercises in individuals with SCI.

7.3 Study limitation

One obvious limitation of the studies reported in this thesis under the clinical evaluation of the developed device was the small number of participants due to the unavailability of a suitable clinical population. A larger population may have aided results generalization. This is valid for training artificial intelligence algorithms to use a large pool of training datasets for better results. Another limitation of this thesis is because the developed device used surface electrodes for stimulation. By implication, the strength of the stimulation will always depend on the skin impedance, skinfold, and other anatomical characteristics of the potential users. Implanted electrode for stimulation would have been immune from all these limitations with a better muscle/nerve selectivity. However, most users prefer surface stimulation due to the invasive nature of the implanted stimulation and the fact that the mode of stimulation is also prone to infection if not professionally managed.

7.4 Future work and recommendations

Although the design and development of the FES system using MMG as a feedback signal meet the aim of the thesis as specified by the thesis's objectives, there are still some areas for further improvement.

1. In the developed FES system, the laboratory's processing and analysis of MMG signals require a computer and data acquisition card. For portability, the MMG data acquisition and processing could be implemented in an integrated board such as raspberry Pi to make the system independent.
2. In the different modes of the FES stimulation, only the amplitude parameter of the stimulation was considered for optimisation to prolong standing duration. Parameter optimisation of other stimulation parameters such as frequency and pulse width could also be investigated in the future, with implementation using appropriate artificial intelligence methods for better standing control and safety.
3. Integration of this FES system on the conventional exercise supports and methods such as cycling ergometer, standing and stepping harness, isokinetic dynamometers could also be explored in the future.

REFERENCES

Abreu, D. C. C., Cliquet, A., Rondina, J. M., & Cendes, F. (2008). Electrical Stimulation During Gait Promotes Increase of Muscle Cross-sectional Area in Quadriplegics: A Preliminary Study. *Clinical Orthopaedics and Related Research, 467*(2), 553. doi: 10.1007/s11999-008-0496-9

Akataki, K., Mita, K., & Watakabe, M. (2004). Electromyographic and mechanomyographic estimation of motor unit activation strategy in voluntary force production. *Electromyography and Clinical Neurophysiology, 44*(8), 489-496.

Akataki, K., Mita, K., Watakabe, M., & Itoh, K. (2001). Mechanomyogram and force relationship during voluntary isometric ramp contractions of the biceps brachii muscle. *European Journal of Applied Physiology, 84*(1-2), 19-25.

Akay, M. F. (2009). Support vector machines combined with feature selection for breast cancer diagnosis. *Expert Systems with Applications, 36*(2, Part 2), 3240-3247. doi: http://doi.org/10.1016/j.eswa.2008.01.009

Al-Mulla, M. R., & Sepulveda, F. (2010). Novel feature modelling the prediction and detection of semg muscle fatigue towards an automated wearable system. Sensors, 10(5), 4838-4854.

Al-Mulla, M. R., & Sepulveda, F. (2014). Novel Pseudo-Wavelet function for MMG signal extraction during dynamic fatiguing contractions. *Sensors, 14*(6), 9489-9504.

Al-Mulla, M. R., Sepulveda, F., & Colley, M. (2011). Evolved pseudo-wavelet function to optimally decompose sEMG for automated classification of localized muscle fatigue. *Medical Engineering & Physics, 33*(4), 411-417. doi: http://dx.doi.org/10.1016/j.medengphy.2010.11.008

Al-Mulla, M. R., Sepulveda, F., Colley, M., & Al-Mulla, F. (2009, 17-19 Oct. 2009). *Statistical Class Separation Using sEMG Features Towards Automated Muscle Fatigue Detection and Prediction.* Paper presented at the 2009 2nd International Congress on Image and Signal Processing.

Alves, N., & Chau, T. (2008). Stationarity distributions of mechanomyogram signals from isometric contractions of extrinsic hand muscles during functional grasping. *Journal of Electromyography and Kinesiology, 18*(3), 509-515. doi: https://doi.org/10.1016/j.jelekin.2006.11.010

Alves, N., & Chau, T. (2010a). The design and testing of a novel mechanomyogram-driven switch controlled by small eyebrow movements. *Journal of NeuroEngineering and Rehabilitation, 7*(1), 22. doi: 10.1186/1743-0003-7-22

Alves, N., & Chau, T. (2010b, Aug. 31-Sept. 4 2010). *Recognition of forearm muscle activity by continuous classification of multi-site mechanomyogram signals.* Paper presented at the 2010 Annual International Conference of the IEEE Engineering in Medicine and Biology.

Alves, N., & Chau, T. (2010). Uncovering patterns of forearm muscle activity using multi-channel mechanomyography. *Journal of Electromyography and Kinesiology, 20*(5), 777-786. doi: http://dx.doi.org/10.1016/j.jelekin.2009.09.003

Alves, N., Sejdić, E., Sahota, B., & Chau, T. (2010). The effect of accelerometer location on the classification of single-site forearm mechanomyograms. *BioMedical Engineering OnLine, 9*(1), 23. doi: 10.1186/1475-925X-9-23

Amaral, T. G., Dias, T. G., Wolczowski, A., & Fernão Pires, V. (2012, 13-15 June 2012). *Neural network based identification of hand movements using biomedical signals.* Paper presented at the 2012 IEEE 16th International Conference on Intelligent Engineering Systems (INES).

Andrews, B. J. (1988). Rule Based Control of Hybrid Fes Orthoses. *IFAC Proceedings Volumes, 21*(1), 287-294. doi: https://doi.org/10.1016/S1474-6670(17)57569-2

Antonelli, M. G., Zobel, P. B., & Giacomin, J. (2009). Use of MMG Signals for the Control of Powered Orthotic Devices: Development of a Rectus Femoris Measurement Protocol. *Assistive Technology, 21*(1), 1-12. doi: 10.1080/10400430902945678

Armstrong, W. (2011). *Wavelet-based intensity analysis of mechanomyographic signals during single-legged stance following fatigue* (Vol. 21).

Bajd, T., Kralj, A., & Turk, R. (1982). Standing-up of a healthy subject and a paraplegic patient. *Journal of Biomechanics, 15*(1), 1-10. doi: https://doi.org/10.1016/0021-9290(82)90029-X

Barry, D. T., & Cole, N. M. (1990). Muscle sounds are emitted at the resonant frequencies of skeletal muscle. *IEEE Transactions on Biomedical Engineering, 37*(5), 525-531. doi: 10.1109/10.55644

Barry, D. T., Leonard, J. A., Gitter, A. J., & Ball, R. D. (1986). Acoustic myography as a control signal for an externally powered prosthesis. *Archives of Physical Medicine and Rehabilitation, 67*(4), 267-269.

Basmajian, J. V., & De Luca, C. J. (1985). *Muscles Alive: Their Functions Revealed By Electromyography*. Baltimore: Williams and Wilkins.

Beck, T. W., Housh, T. J., Cramer, J. T., Weir, J. P., Johnson, G. O., Coburn, J. W., . . . Mielke, M. (2005a). Mechanomyographic amplitude and frequency responses during dynamic muscle actions: a comprehensive review. *BioMedical Engineering OnLine, 4*(1), 67. doi: 10.1186/1475-925X-4-67

Beck, T. W., Housh, T. J., Fry, A. C., Cramer, J. T., Weir, J. P., Schilling, B. K., . . . Moore, C. A. (2009). A wavelet-based analysis of surface mechanomyographic signals from the quadriceps femoris. *Muscle & Nerve, 39*(3), 355-363. doi: https://doi.org/10.1002/mus.21208

Beck, T. W., Housh, T. J., Johnson, G. O., Cramer, J. T., Weir, J. P., Coburn, J. W., & Malek, M. H. (2007). Does the frequency content of the surface mechanomyographic signal reflect motor unit firing rates? A brief review. *Journal of Electromyography and Kinesiology, 17*(1), 1-13. doi: http://dx.doi.org/10.1016/j.jelekin.2005.12.002

Beck, T. W., Housh, T. J., Johnson, G. O., Weir, J. P., Cramer, J. T., Coburn, J. W., & Malek, M. H. (2005b). Comparison of Fourier and wavelet transform procedures for examining the mechanomyographic and electromyographic frequency domain responses during fatiguing isokinetic muscle actions of the biceps brachii. *Journal of Electromyography and Kinesiology, 15*(2), 190-199. doi: https://doi.org/10.1016/j.jelekin.2004.08.007

Beck, T. W., Tscharner, V., Housh, T. J., Cramer, J. T., Weir, J. P., Malek, M. H., & Mielke, M. (2008). Time/frequency events of surface mechanomyographic signals resolved by nonlinearly scaled wavelets. *Biomedical Signal Processing and Control, 3*(3), 255-266. doi: http://dx.doi.org/10.1016/j.bspc.2008.01.005

Belza, B. (1994). The impact of fatigue on exercise performance. *Arthritis & Rheumatism: Official Journal of the American College of Rheumatology, 7*(4), 176-180.

Benoussaad, M., Poignet, P., Hayashibe, M., Azevedo-Coste, C., Fattal, C., & Guiraud, D. (2015). Synthesis of optimal electrical stimulation patterns for functional motion restoration: applied to spinal cord-injured patients. *Medical & Biological Engineering & Computing, 53*(3), 227-240. doi: 10.1007/s11517-014-1227-x

Bickel, C. S., Gregory, C. M., & Dean, J. C. (2011). Motor unit recruitment during neuromuscular electrical stimulation: a critical appraisal. *European Journal of Applied Physiology, 111*(10), 2399. doi: 10.1007/s00421-011-2128-4

Bickel, C. S., Slade, J. M., VanHiel, L. R., Warren, G. L., & Dudley, G. A. (2004). Variable-frequency-train stimulation of skeletal muscle after spinal cord injury. *Journal of Rehabilitation Research and Development, 41*(1), 33.

Bijak, M., Rakos, M., Hofer, C., Mayr, W., Strohhofer, M., Raschka, D., & Kern, H. (2005). Stimulation Parameter Optimisation for FES Supported Standing up and Walking in SCI Patients. *Artificial Organs, 29*(3), 220-223. doi: 10.1111/j.1525-1594.2005.29039.x

Bonato, P., Roy, S. H., Knaflitz, M., & Luca, C. J. D. (2001). Time-frequency parameters of the surface myoelectric signal for assessing muscle fatigue during cyclic dynamic contractions. *IEEE Transactions on Biomedical Engineering, 48*(7), 745-753. doi: 10.1109/10.930899

Braz, G. P., Russold, M., & Davis, G. M. (2009). Functional electrical stimulation control of standing and stepping after spinal cord injury: A review of technical characteristics. *Neuromodulation: Technology at the Neural Interface, 12*(3), 180-190.

Braz, G. P., Russold, M. F., Fornusek, C., Hamzaid, N. A., Smith, R. M., & Davis, G. M. (2015). Cardiorespiratory and Muscle Metabolic Responses During Conventional Versus Motion Sensor-Assisted Strategies for Functional Electrical Stimulation Standing After Spinal Cord Injury. *Artificial Organs, 39*(10), 855-862. doi: https://doi.org/10.1111/aor.12619

Braz, G. P., Russold, M. F., Fornusek, C., Hamzaid, N. A., Smith, R. M., & Davis, G. M. (2016). A novel motion sensor-driven control system for FES-assisted walking after spinal cord injury: A pilot study. *Medical Engineering & Physics, 38*(11), 1223-1231. doi: http://dx.doi.org/10.1016/j.medengphy.2016.06.007

Buckmire, A. J., Arakeri, T. J., Reinhard, J. P., & Fuglevand, A. J. (2018). Mitigation of excessive fatigue associated with functional electrical stimulation. *Journal of Neural Engineering, 15*(6), 066004. doi: 10.1088/1741-2552/aade1c

Cameron, T., & Alo, K. M. (1998). Effects of Posture on Stimulation Parameters in Spinal Cord Stimulation. *Neuromodulation: Technology at the Neural Interface, 1*(4), 177-183. doi: 10.1111/j.1525-1403.1998.tb00014.x

Carson, R. G., & Buick, A. R. (2019). Neuromuscular electrical stimulation-promoted plasticity of the human brain. *The Journal of Physiology, n/a*(n/a). doi: https://doi.org/10.1113/JP278298

Chen, X., Zheng, Y. P., Jing, G., Zhu, Z., Chan, S., & Zhang, Z. (2012). *Sonomyographic responses during voluntary isometric ramp contraction of the human rectus femoris muscle* (Vol. 112).

Chen, Y. L., Li, Y. C., Kuo, T. S., & Lai, J. S. (2001). The development of a closed-loop controlled functional electrical stimulation (FES) in gait training. *Journal of Medical Engineering & Technology, 25*(2), 41-48.

Cheng, A. J., & Rice, C. L. (2010). Fatigue-induced reductions of torque and shortening velocity are muscle dependent. *Medicine & Science in Sports & Exercise, 42*(9), 1651-1659.

Cheng, K. W. E., Yan, L., Kai-Yu, T., Rad, A. B., Chow, D. H. K., & Sutanto, D. (2004). Development of a circuit for functional electrical stimulation. *IEEE Transactions on Neural Systems and Rehabilitation Engineering, 12*(1), 43-47. doi: 10.1109/TNSRE.2003.819936

Chou, L.-W., & Binder-Macleod, S. A. (2007). The Effects Of Stimulation Frequency And Fatigue On The Force-Intensity Relationship For Human Skeletal Muscle. *Clinical Neurophysiology: Official Journal of the International Federation of Clinical Neurophysiology, 118*(6), 1387-1396. doi: 10.1016/j.clinph.2007.02.028

Cogan, S. F., Ludwig, K. A., Welle, C. G., & Takmakov, P. (2016). Tissue damage thresholds during therapeutic electrical stimulation. *Journal of Neural Engineering, 13*(2), 021001. doi: 10.1088/1741-2560/13/2/021001

Cooper, M. A., Herda, T. J., Vardiman, J. P., Gallagher, P. M., & Fry, A. C. (2014). Relationships between skinfold thickness and electromyographic and mechanomyographic amplitude recorded during voluntary and non-voluntary muscle actions. *Journal of Electromyography and Kinesiology, 24*(2), 207-213. doi: https://doi.org/10.1016/j.jelekin.2013.12.005

Cramer, J. T., Housh, T. J., Weir, J. P., Johnson, G. O., Coburn, J. W., & Beck, T. W. (2005). The acute effects of static stretching on peak torque, mean power output, electromyography, and mechanomyography. *European Journal of Applied Physiology, 93*(5), 530-539. doi: 10.1007/s00421-004-1199-x

Cutajar, M., Gatt, E., Grech, I., Casha, O., & Micallef, J. (2013, 1-4 July 2013). *Hardware-based support vector machine for phoneme classification.* Paper presented at the Eurocon 2013.

Davis, G. M., Hamzaid, N. A., & Fornusek, C. (2008). Cardiorespiratory, Metabolic, and Biomechanical Responses During Functional Electrical Stimulation Leg Exercise: Health and Fitness Benefits. *Artificial Organs, 32*(8), 625-629. doi: 10.1111/j.1525-1594.2008.00622.x

Davis, R., Houdayer, T., Andrews, B., & Barriskill, A. (1999). Paraplegia: Prolonged Standing Using Closed-Loop Functional Electrical Stimulation and Andrews Ankle-Foot Orthosis. *Artificial Organs, 23*(5), 418-420. doi: https://doi.org/10.1046/j.1525-1594.1999.06368.x

Davis, R., Houdayer, T., Andrews, B., Emmons, S., & Patrick, J. (1997). Paraplegia: prolonged closed-loop standing with implanted nucleus FES-22 stimulator and Andrews' foot-ankle orthosis. *69*(1-4), 281-287.

Davood, R., & Andrews, B. J. (1998). Computer simulation of FES standing up in paraplegia: a self-adaptive fuzzy controller with reinforcement learning. *IEEE Transactions on Rehabilitation Engineering, 6*(2), 151-161. doi: 10.1109/86.681180

de Sousa, D. G., Harvey, L. A., Dorsch, S., Leung, J., & Harris, W. (2016). Functional electrical stimulation cycling does not improve mobility in people with acquired brain injury and its effects on strength are unclear: a randomised trial. *Journal of Physiotherapy,* 62(4), 203-208. doi: https://doi.org/10.1016/j.jphys.2016.08.004

Donaldson, N., Perkins, T. A., Fitzwater, R., Wood, D. E., & Middleton, F. (2000). FES cycling may promote recovery of leg function after incomplete spinal cord injury. *Spinal Cord, 38*(11), 680.

Dorgan, S. J., & O'Malley, M. J. (1997). A nonlinear mathematical model of electrically stimulated skeletal muscle. *IEEE Transactions on Rehabilitation Engineering, 5*(2), 179-194.

Doucet, B. M., Lam, A., & Griffin, L. (2012). Neuromuscular electrical stimulation for skeletal muscle function. *The Yale journal of biology and medicine, 85*(2), 201-215.

Doulah, A. B. M. S. U., & Fattah, S. A. (2014, 10-12 April 2014). *Neuromuscular disease classification based on mel frequency cepstrum of motor unit action potential.* Paper presented at the 2014 International Conference on Electrical Engineering and Information & Communication Technology.

Downey, R. J., Bellman, M. J., Kawai, H., Gregory, C. M., & Dixon, W. E. (2015). Comparing the Induced Muscle Fatigue Between Asynchronous and Synchronous Electrical Stimulation in Able-Bodied and Spinal Cord Injured Populations. *IEEE Transactions on Neural Systems and Rehabilitation Engineering, 23*(6), 964-972. doi: 10.1109/TNSRE.2014.2364735

Dzulkifli, M. A., Hamzaid, N. A., Davis, G. M., & Hasnan, N. (2018). Neural Network-Based Muscle Torque Estimation Using Mechanomyography During Electrically-Evoked Knee Extension and Standing in Spinal Cord Injury. *Frontiers in Neurorobotics, 12*(50). doi: 10.3389/fnbot.2018.00050

Ebersole, K. T., Housh, T. J., Johnson, G. O., Evetovich, T. K., Smith, D. B., & Perry, S. R. (1999). MMG and EMG responses of the superficial quadriceps femoris muscles. *Journal of Electromyography and Kinesiology, 9*(3), 219-227. doi: https://doi.org/10.1016/S1050-6411(98)00036-4

Ebrahimpour, M. M., & Erfanian, A. (2008). Comments on "Sliding Mode Closed-Loop Control of FES: Controlling the Shank Movement. *IEEE Transactions on Biomedical Engineering, 55*(12), 2842-2843. doi: 10.1109/TBME.2008.2003086

Elbasiouny, S. M., Moroz, D., Bakr, M. M., & Mushahwar, V. K. (2010). Management of Spasticity After Spinal Cord Injury: Current Techniques and Future Directions. *Neurorehabilitation and Neural Repair, 24*(1), 23-33. doi: 10.1177/1545968309343213

Enoka, R. M., Amiridis, I. G., & Duchateau, J. (2019). Electrical Stimulation of Muscle: Electrophysiology and Rehabilitation. *Physiology, 35*(1), 40-56. doi: 10.1152/physiol.00015.2019

Enoka, R. M., & Duchateau, J. (2008). Muscle fatigue: what, why and how it influences muscle function. *The Journal of physiology, 586*(1), 11-23.

Enoka, R. M., & Stuart, D. G. (1992). Neurobiology of muscle fatigue. *Journal of Applied Physiology, 72*(5). doi: 10.1063/1.351680

Eser, P. C., Donaldson, N. N., Knecht, H., & Stussi, E. (2003). Influence of different stimulation frequencies on power output and fatigue during FES-cycling in recently injured SCI people. *IEEE Transactions on Neural Systems and Rehabilitation Engineering, 11*(3), 236-240. doi: 10.1109/TNSRE.2003.817677

Esposito, F., Limonta, E., & Cè, E. (2011). Time course of stretching-induced changes in mechanomyogram and force characteristics. *Journal of Electromyography and Kinesiology, 21*(5), 795-802. doi: https://doi.org/10.1016/j.jelekin.2011.07.012

Esposito, F., Orizio, C., & Veicsteinas, A. (1998). Electromyogram and mechanomyogram changes in fresh and fatigued muscle during sustained contraction in men. *European Journal of Applied Physiology and Occupational Physiology, 78*(6), 494-501. doi: 10.1007/s004210050451

Fawcett, J. W., Curt, A., Steeves, J. D., Coleman, W. P., Tuszynski, M. H., Lammertse, D., . . . Short, D. (2007). Guidelines for the conduct of clinical trials for spinal cord injury as developed by the ICCP panel: spontaneous recovery after spinal cord injury and statistical power needed for therapeutic clinical trials. *Spinal Cord, 45*(3), 190-205. doi: 10.1038/sj.sc.3102007

Fazio, C. (2014). Functional electrical stimulation for incomplete spinal cord injury. *Proceedings (Baylor University. Medical Center), 27*(4), 353-355.

Ferrarin, M., Palazzo, F., Riener, R., & Quintern, J. (2001). Model-based control of FES-induced single joint movements. *IEEE Transactions on Neural Systems and Rehabilitation Engineering, 9*(3), 245-257. doi: 10.1109/7333.948452

Fisekovic, N., & Popovic, D. B. (2001). New controller for functional electrical stimulation systems. *Medical Engineering & Physics, 23*(6), 391-399. doi: https://doi.org/10.1016/S1350-4533(01)00069-8

Fouré, A., Nosaka, K., Wegrzyk, J., Duhamel, G., Le Troter, A., Boudinet, H., . . . Gondin, J. (2014). Time Course of Central and Peripheral Alterations after Isometric Neuromuscular Electrical Stimulation-Induced Muscle Damage. *PloS One, 9*(9), e107298. doi: 10.1371/journal.pone.0107298

Frangioni, J. V., Kwan-Gett, T. S., Dobrunz, L. E., & McMahon, T. A. (1987). The mechanism of low-frequency sound production in muscle. *Biophysical Journal, 51*(5), 775-783.

Frigo, C., Ferrarin, M., Frasson, W., Pavan, E., & Thorsen, R. (2000). EMG signals detection and processing for on-line control of functional electrical stimulation. *Journal of Electromyography and Kinesiology, 10*(5), 351-360. doi: http://dx.doi.org/10.1016/S1050-6411(00)00026-2

Frotzler, A., Coupaud, S., Perret, C., Kakebeeke, T. H., Hunt, K. J., Donaldson, N. d. N., & Eser, P. (2008). High-volume FES-cycling partially reverses bone loss in people with chronic spinal cord injury. *Bone, 43*(1), 169-176.

Furlan, J. C., & Fehlings, M. G. (2008). Cardiovascular complications after acute spinal cord injury: pathophysiology, diagnosis, and management. *25*(5), E13.

Galea, M. P. (2012). Spinal cord injury and physical activity: preservation of the body. *Spinal Cord, 50*(5), 344-351. doi: 10.1038/sc.2011.149

Gang, W., Zhiguo, Y., Xiao, H., Hongbo, X., & Zhizhong, W. (2006). Classification of surface EMG signals using harmonic wavelet packet transform. *Physiological Measurement, 27*(12), 1255.

Gargiulo, P., Vatnsdal, B., Ingvarsson, P., Knútsdóttir, S., Gudmundsdóttir, V., Yngvason, S., & Helgason, T. (2008). Restoration of Muscle Volume and Shape Induced by Electrical Stimulation of Denervated Degenerated Muscles: Qualitative and Quantitative Measurement of Changes in Rectus Femoris Using Computer Tomography and Image Segmentation. *Artificial Organs, 32*(8), 609-613. doi: 10.1111/j.1525-1594.2008.00610.x

Giat, Y., Mizrahi, J., & Levy, M. (1993). A musculotendon model of the fatigue profiles of paralyzed quadriceps muscle under FES. *IEEE Transactions on Biomedical Engineering, 40*(7), 664-674.

Gil-Pita, R., lopez-Garrido, B., & Rosa-Zurera, M. (2015). Tailored MFCCs for Sound Environment Classification in Hearing Aids. In H. A. Sulaiman, M. A. Othman, M. F. I. Othman, Y. A. Rahim & N. C. Pee (Eds.), *Advanced Computer and Communication Engineering Technology* (Vol. 315). Cham: Springer.

Gobbo, M., Cè, E., Diemont, B., Esposito, F., & Orizio, C. (2006). Torque and surface mechanomyogram parallel reduction during fatiguing stimulation in human muscles. *European Journal of Applied Physiology, 97*(1), 9-15. doi: 10.1007/s00421-006-0134-8

Gobbo, M., Maffiuletti, N. A., Orizio, C., & Minetto, M. A. (2014). Muscle motor point identification is essential for optimizing neuromuscular electrical stimulation use. *Journal of NeuroEngineering and Rehabilitation, 11*(1), 17. doi: 10.1186/1743-0003-11-17

Gordon, T., & Mao, J. (1994). Muscle Atrophy and Procedures for Training After Spinal Cord Injury. *Physical Therapy, 74*(1), 50-60. doi: 10.1093/ptj/74.1.50

Gorgey, A. S., Dolbow, D. R., Dolbow, J. D., Khalil, R. K., & Gater, D. R. (2015). The effects of electrical stimulation on body composition and metabolic profile after spinal cord injury – Part II. *The Journal of Spinal Cord Medicine, 38*(1), 23-37. doi: 10.1179/2045772314Y.0000000244

Graham, G. M., Thrasher, T. A., & Popovic, M. R. (2006). The effect of random modulation of functional electrical stimulation parameters on muscle fatigue. *IEEE Transactions on Neural Systems and Rehabilitation Engineering, 14*(1), 38-45. doi: 10.1109/TNSRE.2006.870490

Gupta, S., Jaafar, J., Ahmad, W. F. W., & Bansal, A. (2013). Feature extraction using MFCC. *Signal & Image Processing, 4*(4), 101.

Gwo-Ching, C., Jer-Junn, L., Gon-Der, L., Jin-Shin, L., Cheng-Kung, C., Bor-Lin, K., & Te-Son, K. (1997). A neuro-control system for the knee joint position control with quadriceps stimulation. *IEEE Transactions on Rehabilitation Engineering, 5*(1), 2-11. doi: 10.1109/86.559344

Hamid, S., & Hayek, R. (2008). Role of electrical stimulation for rehabilitation and regeneration after spinal cord injury: an overview. *European Spine Journal, 17*(9), 1256-1269. doi: 10.1007/s00586-008-0729-3

Hashem, E. M., & Mabrouk, M. S. (2014). A Study of support vector machine algorithm for liver disease diagnosis. *American Journal of Intelligent Systems, 4*(1), 9-14. doi: http://article.sapub.org/10.5923.j.ajis.20140401.02.html

Hasnan, N., Saadon, N. S. M., Hamzaid, N. A., Teoh, M. X.-H., Ahmadi, S., & Davis, G. M. (2018). Muscle oxygenation during hybrid arm and functional electrical stimulation–evoked leg cycling after spinal cord injury. *Medicine, 97*(43).

Herda, T. J., Housh, T. J., Fry, A. C., Weir, J. P., Schilling, B. K., Ryan, E. D., & Cramer, J. T. (2010). A noninvasive, log-transform method for fiber type discrimination using mechanomyography. *Journal of Electromyography and Kinesiology, 20*(5), 787-794. doi: http://dx.doi.org/10.1016/j.jelekin.2010.01.004

Herzog, W., Zhang, Y. T., Vaz, M. A., Guimaraes, A., & Janssen, C. (1994). Assessment of muscular fatigue using vibromyography. *Muscle & Nerve, 17*(10), 1156-1161.

Hettinga, F. J., Konings, M. J., & Cooper, C. E. (2016). Differences in muscle oxygenation, perceived fatigue and recovery between long-track and short-track speed skating. *Frontiers in Physiology, 7*, 619.

Hill, E. C., Housh, T. J., Camic, C. L., Smith, C. M., Cochrane, K. C., Jenkins, N. D. M., . . . Johnson, G. O. (2016). Effects of velocity on electromyographic, mechanomyographic, and torque responses to repeated eccentric muscle actions. *Journal of strength and conditioning research, 30*(6), 1743-1751.

Hodkin, E. F., Lei, Y., Humby, J., Glover, I. S., Choudhury, S., Kumar, H., . . . Jackson, A. (2018). Automated FES for Upper Limb Rehabilitation Following Stroke and Spinal Cord Injury. *IEEE Transactions on Neural Systems and Rehabilitation Engineering, 26*(5), 1067-1074. doi: 10.1109/TNSRE.2018.2816238

Hong-Bo, X., Yong-Ping, Z., & Jing-Yi, G. (2009). Classification of the mechanomyogram signal using a wavelet packet transform and singular value decomposition for multifunction prosthesis control. *Physiological Measurement, 30*(5), 441.

Hong-liu, Y., Sheng-nan, Z., & Jia-hua, H. (2010). *MMG signal and its applications in prosthesis control*. Paper presented at the Proceedings of the 4th International Convention on Rehabilitation Engineering & Assistive Technology, Shanghai, China.

Hunt, K. J., Ferrario, C., Grant, S., Stone, B., McLean, A. N., Fraser, M. H., & Allan, D. B. (2006). Comparison of stimulation patterns for FES-cycling using measures of oxygen cost and stimulation cost. *Medical Engineering & Physics, 28*(7), 710-718.

Hunt, K. J., Jaime, R. P., & Gollee, H. (2001). Robust control of electrically-stimulated muscle using polynomial H∞ design. *Control Engineering Practice, 9*(3), 313-328.

Ibitoye, M. O., Estigoni, E. H., Hamzaid, N. A., Wahab, A. K. A., & Davis, G. M. (2014a). The Effectiveness of FES-Evoked EMG Potentials to Assess Muscle Force and Fatigue in Individuals with Spinal Cord Injury. *Sensors, 14*(7). doi: 10.3390/s140712598

Ibitoye, M. O., Hamzaid, N. A., Abdul Wahab, A. K., Hasnan, N., & Davis, G. M. (2020a). Quadriceps mechanomyography reflects muscle fatigue during electrical stimulus-sustained standing in adults with spinal cord injury – a proof of concept. *Biomedical Engineering / Biomedizinische Technik, 65*(2), 165-174. doi: https://doi.org/10.1515/bmt-2019-0118

Ibitoye, M. O., Hamzaid, N. A., Abdul Wahab, A. K., Hasnan, N., Olatunji, S. O., & Davis, G. M. (2020b). SVR modelling of mechanomyographic signals predicts neuromuscular stimulation-evoked knee torque in paralyzed quadriceps muscles undergoing knee extension exercise. *Computers in Biology and Medicine, 117*, 103614. doi: https://doi.org/10.1016/j.compbiomed.2020.103614

Ibitoye, M. O., Hamzaid, N. A., Hasnan, N., Wahab, A. K. A., & Davis, G. M. (2016a). Strategies for Rapid Muscle Fatigue Reduction during FES Exercise in Individuals with Spinal Cord Injury: A Systematic Review. *PloS One, 11*(2), e0149024. doi: 10.1371/journal.pone.0149024

Ibitoye, M. O., Hamzaid, N. A., Hasnan, N., Wahab, A. K. A., Islam, M. A., Kean, V. S. P., & Davis, G. M. (2016b). Torque and mechanomyogram relationships during electrically-evoked isometric quadriceps contractions in persons with spinal cord injury. *Medical Engineering & Physics, 38*(8), 767-775.

Ibitoye, M. O., Hamzaid, N. A., Hayashibe, M., Hasnan, N., & Davis, G. M. (2019). Restoring prolonged standing via functional electrical stimulation after spinal cord injury: A systematic review of control strategies. *Biomedical Signal Processing and Control, 49*, 34-47. doi: https://doi.org/10.1016/j.bspc.2018.11.006

Ibitoye, M. O., Hamzaid, N. A., Wahab, A. K. A., Hasnan, N., Olatunji, S. O., & Davis, G. M. (2016c). Estimation of electrically-evoked knee torque from mechanomyography using support vector regression. *16*(7), 1115.

Ibitoye, M. O., Hamzaid, N. A., Zuniga, J. M., Hasnan, N., & Wahab, A. K. A. (2014b). Mechanomyographic Parameter Extraction Methods: An Appraisal for Clinical Applications. *Sensors (Basel, Switzerland), 14*(12), 22940-22970. doi: 10.3390/s141222940

Irino, T., Minami, Y., Nakatani, T., Tsuzaki, M., & Tagawa, H. (2002). *Evaluation of a speech recognition/generation method based on HMM and straight.* Paper presented at the 7th Internatinoal Conference on Spoken Language Processing (ICSLP2002), Denver, Colorado, USA.

Islam, M. A., Hamzaid, N. A., Ibitoye, M. O., Hasnan, N., Wahab, A. K. A., & Davis, G. M. (2018). Mechanomyography responses characterize altered muscle function during Electrical Stimulation-evoked cycling in individuals with spinal cord injury. *Clinical Biomechanics, 58*, 21-27. doi: https://doi.org/10.1016/j.clinbiomech.2018.06.020

Islam, M. A., Sundaraj, K., Ahmad, R. B., & Ahamed, N. U. (2013). Mechanomyogram for Muscle Function Assessment: A Review. *PloS One, 8*(3), e58902. doi: 10.1371/journal.pone.0058902

Islam, M. A., Sundaraj, K., Ahmad, R. B., Sundaraj, S., Ahamed, N. U., & Ali, M. A. (2014). Cross-Talk in Mechanomyographic Signals from the Forearm Muscles during Sub-Maximal to Maximal Isometric Grip Force. *PloS One, 9*(5), e96628. doi: 10.1371/journal.pone.0096628

Itakura, N., Fujita, K., Kubo, K., Iguchi, Y., & Minamitani, H. (1988, 4-7 Nov. 1988). *Evaluation of FES control system employing adaptive and PI controllers.* Paper presented at the Proceedings of the Annual International Conference of the IEEE Engineering in Medicine and Biology Society, New Orleans, Louisiana, USA.

Jaime, R., Matjacic, Z., & Hunt, K. J. (2002). Paraplegic standing supported by FES-controlled ankle stiffness. *IEEE Transactions on Neural Systems and Rehabilitation Engineering, 10*(4), 239-248. doi: 10.1109/TNSRE.2002.806830

Jaskólska, A., Brzenczek, W., Kisiel-Sajewicz, K., Kawczyński, A., Marusiak, J., & Jaskólski, A. (2004). The effect of skinfold on frequency of human muscle mechanomyogram. *Journal of Electromyography and Kinesiology, 14*(2), 217-225. doi: https://doi.org/10.1016/j.jelekin.2003.08.001

Jayaraman, A., Gregory, C. M., Bowden, M., Stevens, J. E., Shah, P., Behrman, A. L., & Vandenborne, K. (2006). Lower extremity skeletal muscle function in persons with incomplete spinal cord injury. *Spinal Cord, 44*(11), 680-687. doi: 10.1038/sj.sc.3101892

Jezernik, S., Wassink, R. G. V., & Keller, T. (2004). Sliding mode closed-loop control of FES controlling the shank movement. *IEEE Transactions on Biomedical Engineering, 51*(2), 263-272. doi: 10.1109/TBME.2003.820393

Jong-Hwan, L., Ho-Young, J., Te-Won, L., & Soo-Young, L. (2000, 5-9 June 2000). *Speech feature extraction using independent component analysis.* Paper presented at the 2000 IEEE International Conference on Acoustics, Speech, and Signal Processing. Proceedings (Cat. No.00CH37100), Istanbul, Turkey.

Julio, C. F., & Michael, G. F. (2008). Cardiovascular complications after acute spinal cord injury: pathophysiology, diagnosis, and management. *Neurosurgical Focus FOC, 25*(5), E13. doi: 10.3171/FOC.2008.25.11.E13

Karu, Z. Z., Durfee, W. K., & Barzilai, A. M. (1995). Reducing muscle fatigue in FES applications by stimulating with N-let pulse trains. *IEEE Transactions on Biomedical Engineering, 42*(8), 809-817. doi: 10.1109/10.398642

Kattan, A., Al-Mulla, M. R., Sepulveda, F., & Poli, R. (2009). *Detecting Localised Muscle Fatigue during Isometric Contraction using Genetic Programming.* Paper presented at the IJCCI, Madeira, Portugal.

Kent-Braun, J. A., Callahan, D. M., Fay, J. L., Foulis, S. A., & Buonaccorsi, J. P. (2014). Muscle weakness, fatigue, and torque variability: Effects of age and mobility status. *Muscle & Nerve, 49*(2), 209-217. doi: 10.1002/mus.23903

Kesar, T., & Binder-Macleod, S. (2006). Effect of frequency and pulse duration on human muscle fatigue during repetitive electrical stimulation. *Experimental Physiology, 91*(6), 967-976. doi: 10.1113/expphysiol.2006.033886

Kesar, T., Chou, L.-W., & Binder-Macleod, S. A. (2008). Effects of stimulation frequency versus pulse duration modulation on muscle fatigue. *Journal of Electromyography and Kinesiology, 18*(4), 662-671.

Khezri, M., & Jahed, M. (2007). Real-time intelligent pattern recognition algorithm for surface EMG signals. *BioMedical Engineering OnLine, 6*(1), 45. doi: 10.1186/1475-925x-6-45

Kirshblum, S. C., Burns, S. P., Biering-Sorensen, F., Donovan, W., Graves, D. E., Jha, A., . . . Waring, W. (2011). International standards for neurological classification of spinal cord injury (Revised 2011). *The Journal of Spinal Cord Medicine, 34*(6), 535-546. doi: 10.1179/204577211X13207446293695

Koutsou, A. D., Moreno, J. C., Ama, A. J., Rocon, E., & Pons, J. L. (2016). Advances in selective activation of muscles for non-invasive motor neuroprostheses. *Journal of NeuroEngineering and Rehabilitation, 13*(1), 56. doi: 10.1186/s12984-016-0165-2

Kouzaki, M., Shinohara, M., & Fukunaga, T. (1999). Non-uniform mechanical activity of quadriceps muscle during fatigue by repeated maximal voluntary contraction in humans. *European Journal of Applied Physiology and Occupational Physiology, 80*(1), 9-15. doi: 10.1007/s004210050551

Krajl, A., Bajd, T., Turk, R., & Benko, H. (1986). Posture switching for prolonging functional electrical stimulation standing in paraplegic patients. *Paraplegia, 24*(4), 221-230.

Kralj, A. R., & Bajd, T. (1989). *Functional electrical stimulation: standing and walking after spinal cord injury*: CRC press.

Krueger, E., Scheeren, E. M., Nogueira-Neto, G. N., Button, V. L. S., & Nohama, P. (2017). *Preliminary evaluation of mechanomyographic signal of rectus femoris muscle between spinal cord injured and healthy subjects.* Paper presented at the 2017 IFESS Conference, London, UK.

Kurzynski, M., Krysmann, M., Trajdos, P., & Wolczowski, A. (2016). Multiclassifier system with hybrid learning applied to the control of bioprosthetic hand. *Computers in Biology and Medicine, 69*, 286-297. doi: https://doi.org/10.1016/j.compbiomed.2015.04.023

Laubacher, M., Aksoez, E. A., Brust, A. K., Baumberger, M., Riener, R., Binder-Macleod, S., & Hunt, K. J. (2019). Stimulation of paralysed quadriceps muscles with sequentially and spatially distributed electrodes during dynamic knee extension. Journal of NeuroEngineering and Rehabilitation, 16(1), 5. doi: 10.1186/s12984-018-0471-y

Lei, K. F., Tsai, W. W., Lin, W. Y., & Lee, M. Y. (2011, 9-12 Oct. 2011). *MMG-torque estimation under dynamic contractions.* Paper presented at the 2011 IEEE International Conference on Systems, Man, and Cybernetics, Anchorage, Alaska, USA.

Leung, K. W., Tong, R. K., Wang, X., Lee, G. T., Pang, P. M., Wai, H. W., & Leung, H. C. (2017). The Effectiveness of Functional Electrical Stimulation (FES) in On-Off Mode for Enhancing the Cycling Performance of Team Phoenix at 2016 Cybathlon. *European Journal of Translational Myology, 27*(4), 7132-7132. doi: 10.4081/ejtm.2017.7132

Levin, O., Mizrahi, J., & Isakov, E. (2000). Transcutaneous FES of the paralyzed quadriceps:: is knee torque affected by unintended activation of the hamstrings? *Journal of Electromyography and Kinesiology, 10*(1), 47-58. doi: https://doi.org/10.1016/S1050-6411(99)00016-4

Li, Z., David, G., David, A., Anthony, G., Charles, F., & Mitsuhiro, H. (2018). Real-Time Closed-Loop Functional Electrical Stimulation Control of Muscle Activation with Evoked Electromyography Feedback for Spinal Cord Injured Patients. *International Journal of Neural Systems, 28*(06), 1750063. doi: 10.1142/s0129065717500630

Li, Z., Guiraud, D., Andreu, D., Fattal, C., Gelis, A., & Hayashibe, M. (2016). A Hybrid Functional Electrical Stimulation for Real-Time Estimation of Joint Torque and Closed-Loop Control of Muscle Activation. *European Journal of Translational Myology, 26*(3), 6064-6064. doi: 10.4081/ejtm.2016.6064

Li, Z., Guiraud, D., Andreu, D., Gelis, A., Fattal, C., & Hayashibe, M. (2017). Real-Time Closed-Loop Functional Electrical Stimulation Control of Muscle Activation with Evoked Electromyography Feedback for Spinal Cord Injured Patients. *International Journal of Neural Systems, 28*(06), 1750063. doi: 10.1142/S0129065717500630

Li, Z., Hayashibe, M., Andreu, D., & Guiraud, D. (2015, 22-24 April 2015). *Real-time closed-loop FES control of muscle activation with evoked EMG feedback.* Paper presented at the 2015 7th International IEEE/EMBS Conference on Neural Engineering (NER), Montpellier, France.

Liu, L. Q., Moody, J., Traynor, M., Dyson, S., & Gall, A. (2014). A systematic review of electrical stimulation for pressure ulcer prevention and treatment in people with spinal cord injuries. *The Journal of Spinal Cord Medicine, 37*(6), 703-718. doi: 10.1179/2045772314Y.0000000226

Lynch, C. L., Graham, G. M., & Popovic, M. R. (2011). A generic model of real-world non-ideal behaviour of FES-induced muscle contractions: simulation tool. *Journal of Neural Engineering, 8*(4), 046034. doi: 10.1088/1741-2560/8/4/046034

Lynch, C. L., & Popovic, M. R. (2005). *Closed-loop control for FES: Past work and future directions.* Paper presented at the 10th Annual Conference of the International FES Society, Montreal, Canada.

Lynch, C. L., & Popovic, M. R. (2008). Functional Electrical Stimulation. *IEEE Control Systems Magazine, 28*(2), 40-50. doi: 10.1109/MCS.2007.914689

Lynch, C. L., & Popovic, M. R. (2012). A Comparison of Closed-Loop Control Algorithms for Regulating Electrically Stimulated Knee Movements in Individuals With Spinal Cord Injury. *IEEE Transactions on Neural Systems and Rehabilitation Engineering, 20*(4), 539-548. doi: 10.1109/TNSRE.2012.2185065

Madeleine, P., Bajaj, P., Søgaard, K., & Arendt-Nielsen, L. (2001). Mechanomyography and electromyography force relationships during concentric, isometric and eccentric contractions. *Journal of Electromyography and Kinesiology, 11*(2), 113-121. doi: https://doi.org/10.1016/S1050-6411(00)00044-4

Madeleine, P., Hansen, E. A., & Samani, A. (2014). Linear and nonlinear analyses of multi-channel mechanomyographic recordings reveal heterogeneous activation of wrist extensors in presence of delayed onset muscle soreness. *Medical Engineering & Physics, 36*(12), 1656-1664. doi: https://doi.org/10.1016/j.medengphy.2014.09.003

Maffiuletti, N. A., Minetto, M. A., Farina, D., & Bottinelli, R. (2011). Electrical stimulation for neuromuscular testing and training: state-of-the art and unresolved issues. *European Journal of Applied Physiology, 111*(10), 2391. doi: 10.1007/s00421-011-2133-7

Malek, M. H., & Coburn, J. W. (2012). The Utility of Electromyography and Mechanomyography for Assessing Neuromuscular Function: A Noninvasive Approach. *Physical Medicine and Rehabilitation Clinics of North America, 23*(1), 23-32. doi: http://dx.doi.org/10.1016/j.pmr.2011.11.005

Marsolais, E. B., & Edwards, B. G. (1988). Energy costs of walking and standing with functional neuromuscular stimulation and long leg braces. *Archives of Physical Medicine and Rehabilitation, 69*(4), 243-249.

Martin, R., Sadowsky, C., Obst, K., Meyer, B., & McDonald, J. (2012). Functional electrical stimulation in spinal cord injury:: from theory to practice. *Topics in spinal cord injury rehabilitation, 18*(1), 28-33. doi: 10.1310/sci1801-28

McDonnall, D., Clark, G. A., & Normann, R. A. (2004). Interleaved, multisite electrical stimulation of cat sciatic nerve produces fatigue-resistant, ripple-free motor responses. *IEEE Transactions on Neural Systems and Rehabilitation Engineering, 12*(2), 208-215. doi: 10.1109/TNSRE.2004.828425

McQueen, J. M., Norris, D., & Cutler, A. (2006). The Dynamic Nature of Speech Perception. *Language and Speech, 49*(1), 101-112. doi: 10.1177/00238309060490010601

Merletti, R., Knaflitz, M., & DeLuca, C. J. (1992). Electrically evoked myoelectric signals. *Critical Reviews in Biomedical Engineering, 19*(4), 293-340.

Mohamad, N. Z., Hamzaid, N. A., Davis, G. M., Abdul Wahab, A. K., & Hasnan, N. (2017). Mechanomyography and Torque during FES-Evoked Muscle Contractions to Fatigue in Individuals with Spinal Cord Injury. *Sensors, 17*(7), 1627.

Moon, S.-H., Choi, J.-H., & Park, S.-E. (2017). The effects of functional electrical stimulation on muscle tone and stiffness of stroke patients. *Journal of Physical Therapy Science, 29*(2), 238-241. doi: 10.1589/jpts.29.238

Mushahwar, V. K., Jacobs, P. L., Normann, R. A., Triolo, R. J., & Kleitman, N. (2007). New functional electrical stimulation approaches to standing and walking. *Journal of Neural Engineering, 4*(3), S181-S197. doi: 10.1088/1741-2560/4/3/s05

Naeem, J., Amelia, W. A., Sheroz, K., & Yasir, M. M. (2013). *An investigation of fatigue phenomenon in the upper limb muscle due to short duration pulses in an FES system.* Paper presented at the IOP Conference Series: Materials Science and Engineering, Kuala Lumpur, Malaysia.

Newham, D. J., & Donaldson, N. d. N. (2007). FES cycling. In D. E. Sakas, B. A. Simpson & E. S. Krames (Eds.), *Operative Neuromodulation: Volume 1: Functional Neuroprosthetic Surgery. An Introduction* (pp. 395-402). Vienna: Springer Vienna.

Nosaka, K., Aldayel, A., Jubeau, M., & Chen, T. C. (2011). Muscle damage induced by electrical stimulation. *European Journal of Applied Physiology, 111*(10), 2427. doi: 10.1007/s00421-011-2086-x

Obuchi, Y. (2004). *Delta-cepstrum normalization for robust speech recognition.* Paper presented at the Proc. ICA.

Orizio, C. (1992). Soundmyogram and EMG cross-spectrum during exhausting isometric contractions in humans. *Journal of Electromyography and Kinesiology, 2*(3), 141-149. doi: https://doi.org/10.1016/1050-6411(92)90011-7

Orizio, C. (1993). Muscle sound: Bases for the introduction of a mechanomyographic signal in muscle studies. *Critical Reviews in Biomedical Engineering, 21*(3), 201-243.

Orizio, C., Diemont, B., Esposito, F., Alfonsi, E., Parrinello, G., Moglia, A., & Veicsteinas, A. (1999). Surface mechanomyogram reflects the changes in the mechanical properties of muscle at fatigue. *European Journal of Applied Physiology and Occupational Physiology, 80*(4), 276-284. doi: 10.1007/s004210050593

Orizio, C., Liberati, D., Locatelli, C., Grandis, D., & Veicsteinas, A. (1996). Surface mechanomyogram reflects muscle fibres twitches summation. *Journal of Biomechanics, 29*(4), 475-481. doi: http://dx.doi.org/10.1016/0021-9290(95)00063-1

Ouamer, M., Boiteux, M., Petitjean, M., Travens, L., & Salès, A. (1999). Acoustic myography during voluntary isometric contraction reveals non-propagative lateral vibration. *Journal of Biomechanics, 32*(12), 1279-1285. doi: https://doi.org/10.1016/S0021-9290(99)00132-3

Perry-Rana, S. R., Housh, T. J., Johnson, G. O., Bull, A. J., Berning, J. M., & Cramer, J. T. (2002). MMG and EMG responses during fatiguing isokinetic muscle contractions at different velocities. *Muscle & Nerve, 26*(3), 367-373. doi: 10.1002/mus.10214

Perry, S. R., Housh, T. J., Weir, J. P., Johnson, G. O., Bull, A. J., & Ebersole, K. T. (2001). Mean power frequency and amplitude of the mechanomyographic and electromyographic signals during incremental cycle ergometry. *Journal of Electromyography and Kinesiology, 11*(4), 299-305. doi: https://doi.org/10.1016/S1050-6411(00)00057-2

Peters, E. J. D., & Fuglevand, A. J. (1999). Cessation of human motor unit discharge during sustained maximal voluntary contraction. *Neuroscience Letters, 274*(1), 66-70. doi: https://doi.org/10.1016/S0304-3940(99)00666-7

Popov, N. S., Đozić, D. J., Stanković, M., Krajoski, G. M., & Stanišić, D. (2015). Development of a Closed-loop FES System Based on NARX Radial Based Network. In Á. Jobbágy (Ed.), *First European Biomedical Engineering Conference for Young Investigators: ENCY2015, Budapest, May 28 - 30, 2015* (pp. 70-74). Singapore: Springer Singapore.

Popović, D. B. (2014). Advances in functional electrical stimulation (FES). *Journal of Electromyography and Kinesiology, 24*(6), 795-802. doi: 10.1016/j.jelekin.2014.09.008

Popovic, M. R., Curt, A., Keller, T., & Dietz, V. (2001). Functional electrical stimulation for grasping and walking: indications and limitations. *Spinal Cord, 39*(8), 403-412. doi: 10.1038/sj.sc.3101191

Popovic, M. R., Masani, K., & Micera, S. (2012). Functional Electrical Stimulation Therapy: Recovery of Function Following Spinal Cord Injury and Stroke *Neurorehabilitation Technology* (pp. 105-121). London: Springer London.

Popovicc, L. Z., & Malesevic, N. M. (2009, 3-6 Sept. 2009). *Muscle fatigue of quadriceps in paraplegics: Comparison between single vs. multi-pad electrode surface stimulation.* Paper presented at the 2009 Annual International Conference of the IEEE Engineering in Medicine and Biology Society.

Previdi, F., Ferrarin, M., Savaresi, S. M., & Bittanti, S. (2005). Closed-loop control of FES supported standing up and sitting down using Virtual Reference Feedback Tuning. *Control Engineering Practice, 13*(9), 1173-1182. doi: http://dx.doi.org/10.1016/j.conengprac.2004.10.007

Qian, S., & Chen, D. (1999). Joint time-frequency analysis. *IEEE Signal Processing Magazine, 16*(2), 52-67.

Rainoldi, A., Melchiorri, G., & Caruso, I. (2004). A method for positioning electrodes during surface EMG recordings in lower limb muscles. *Journal of Neuroscience Methods, 134*(1), 37-43.

Rattay, F. (1999). The basic mechanism for the electrical stimulation of the nervous system. *Neuroscience, 89*(2), 335-346. doi: https://doi.org/10.1016/S0306-4522(98)00330-3

Re, L., Krans, F., Schultheiss, J., & Gerber, H. (1994, 29 June-1 July 1994). *Self-tuning PID controller for lower limb FES with nonlinear compensation.* Paper presented at the Procedings of 1994 American Control Conference, Baltimore, Maryland, USA.

Riener, R., Ferrarin, M., Pavan, E. E., & Frigo, C. A. (2000). Patient-driven control of FES-supported standing up and sitting down: experimental results. *IEEE Transactions on Rehabilitation Engineering, 8*(4), 523-529. doi: 10.1109/86.895956

Rongsawad, K., & Ratanapinunchai, J. (2018). Effects of Very High Stimulation Frequency and Wide-Pulse Duration on Stimulated Force and Fatigue of Quadriceps in Healthy Participants. *Annals of rehabilitation medicine, 42*(2), 250-259. doi: 10.5535/arm.2018.42.2.250

Rouhani, H., Rodriguez, K. E., Bergquist, A. J., Masani, K., & Popovic, M. R. (2017). Minimizing muscle fatigue through optimisation of electrical stimulation parameters. *J. Biomed. Eng. Informatics, 3*(1), 33-43.

Ruslee, R., Miller, J., & Gollee, H. (2019). Investigation of different stimulation patterns with doublet pulses to reduce muscle fatigue. *Journal of Rehabilitation and Assistive Technologies Engineering, 6*, 2055668319825808. doi: 10.1177/2055668319825808

Ryan, E. D., Beck, T. W., Herda, T. J., Hartman, M. J., Stout, J. R., Housh, T. J., & Cramer, J. T. (2008a). Mechanomyographic amplitude and mean power frequency responses during isometric ramp vs. step muscle actions. *Journal of Neuroscience Methods, 168*(2), 293-305. doi: https://doi.org/10.1016/j.jneumeth.2007.10.010

Ryan, E. D., Cramer, J. T., Egan, A. D., Hartman, M. J., & Herda, T. J. (2008b). Time and frequency domain responses of the mechanomyogram and electromyogram during isometric ramp contractions: A comparison of the short-time Fourier and continuous wavelet transforms. *Journal of Electromyography and Kinesiology, 18*(1), 54-67. doi: https://doi.org/10.1016/j.jelekin.2006.09.003

Sarlabous, L., Torres, A., Fiz, J. A., Morera, J., & Jané, R. (2013). Index for estimation of muscle force from mechanomyography based on the Lempel–Ziv algorithm. *Journal of Electromyography and Kinesiology, 23*(3), 548-557. doi: https://doi.org/10.1016/j.jelekin.2012.12.007

Shang-Ming, L., Shi-Hau, F., Jeih-weih, H., & Lin-Shan, L. (2001, 9-13 Dec. 2001). *Improved MFCC feature extraction by PCA-optimised filter-bank for speech recognition.* Paper presented at the IEEE Workshop on Automatic Speech Recognition and Understanding, 2001. ASRU '01., Madonna di Campiglio, Italy.

Shimada, Y., Sato, K., Matsunaga, T., Tsutsumi, Y., Misawa, A., Ando, S., . . . Hatakeyama, K. (2001). Closed-loop control using a stretch sensor for restoration of standing with functional electrical stimulation in complete paraplegia. *The Tohoku Journal of Experimental Medicine, 193*(3), 221-227.

Silva, J., Heim, W., & Chau, T. (2004). *MMG-based classification of muscle activity for prosthesis control.* Paper presented at the The 26th Annual International Conference of the IEEE Engineering in Medicine and Biology Society, San Francisco, CA, USA

Silva, J., Heim, W., & Chau, T. (2005). A Self-Contained, Mechanomyography-Driven Externally Powered Prosthesis. *Archives of Physical Medicine and Rehabilitation, 86*(10), 2066-2070. doi: https://doi.org/10.1016/j.apmr.2005.03.034

Simonsen, D., Spaich, E. G., Hansen, J., & Andersen, O. K. (2016). Design and Test of a Closed-Loop FES System for Supporting Function of the Hemiparetic Hand Based on Automatic Detection using the Microsoft Kinect sensor. *IEEE Transactions on Neural Systems and Rehabilitation Engineering, PP*(99), 1-1. doi: 10.1109/TNSRE.2016.2622160

Sinkjaer, T., Haugland, M., Inmann, A., Hansen, M., & Nielsen, K. D. (2003). Biopotentials as command and feedback signals in functional electrical stimulation systems. *Medical Engineering & Physics, 25*(1), 29-40. doi: https://doi.org/10.1016/S1350-4533(02)00178-9

Søgaard, K., Orizio, C., & Sjøgaard, G. (2006). Surface mechanomyogram amplitude is not attenuated by intramuscular pressure. *European Journal of Applied Physiology, 96*(2), 178-184. doi: 10.1007/s00421-004-1211-5

Spendiff, O., Longford, N. T., & Winter, E. M. (2002). Effects of fatigue on the torque-velocity relation in muscle. *British Journal of Sports Medicine, 36*(6), 431. doi: 10.1136/bjsm.36.6.431

Subasi, A. (2013). Classification of EMG signals using PSO optimised SVM for diagnosis of neuromuscular disorders. *Computers in Biology and Medicine, 43*(5), 576-586. doi: https://doi.org/10.1016/j.compbiomed.2013.01.020

Szecsi, J., Straube, A., & Fornusek, C. (2014). A biomechanical cause of low power production during FES cycling of subjects with SCI. *Journal of NeuroEngineering and Rehabilitation, 11*(1), 123. doi: 10.1186/1743-0003-11-123

Szu-Chen, J., Maier-Hein, L., Schultz, T., & Waibel, A. (2006, 14-19 May 2006). *Articulatory Feature Classification using Surface Electromyography.* Paper presented at the 2006 IEEE International Conference on Acoustics Speech and Signal Processing Proceedings, Toulouse, France.

Tan, C. O., Battaglino, R. A., & Morse, L. R. (2013). Spinal Cord Injury and Osteoporosis: Causes, Mechanisms, and Rehabilitation Strategies. *International Journal of Physical Medicine & Rehabilitation, 1*, 127.

Tanaka, M., Okuyama, T., & Saito, K. (2011). *Study on evaluation of muscle conditions using a mechanomyogram sensor.* Paper presented at the Systems, Man, and Cybernetics (SMC), 2011 IEEE International Conference on, Alaska, USA.

Tarata, M. T. (2003). Mechanomyography versus Electromyography, in monitoring the muscular fatigue. *BioMedical Engineering OnLine, 2*, 3-3. doi: 10.1186/1475-925X-2-3

Tarata, M. T. (2011). Noninvasive monitoring of neuramuscular fatigue: Techniques and results. *Univ. Pietisti. Sci. Bull.: Electron. Comput. Sci, 11*, 201-243.

Taylor, J. A., Picard, G., & Widrick, J. J. (2011). Aerobic Capacity With Hybrid FES Rowing in Spinal Cord Injury: Comparison With Arms-Only Exercise and Preliminary Findings With Regular Training. *PM&R, 3*(9), 817-824. doi: 10.1016/j.pmrj.2011.03.020

Thrasher, A., Graham, G. M., & Popovic, M. R. (2005). Reducing Muscle Fatigue Due to Functional Electrical Stimulation Using Random Modulation of Stimulation Parameters. *Artificial Organs, 29*(6), 453-458. doi: 10.1111/j.1525-1594.2005.29076.x

Vargas Luna José, L., Krenn, M., Cortés Jorge, A., & Mayr, W. (2013). Comparison of Current and Voltage Control Techniques for Neuromuscular Electrical Stimulation in the Anterior Thigh. *Biomedical Engineering / Biomedizinische Technik, 58*(Suppl. 1). doi: 10.1515/bmt-2013-4021

Veltink, P. H., & Donaldson, N. (1998). A perspective on the control of FES-supported standing. *IEEE Transactions on Rehabilitation Engineering, 6*(2), 109-112.

Veltink, P. H., Sinkjaer, T., Baten, C. T. M., Bergveld, P., van der Spek, J., & Haugland, M. (1998, 1-1 Nov. 1998). *Artificial and natural sensors in FES-assisted human movement control.* Paper presented at the Proceedings of the 20th Annual International Conference of the IEEE Engineering in Medicine and Biology Society. Vol.20 Biomedical Engineering Towards the Year 2000 and Beyond (Cat. No.98CH36286).

Vromans, M., & Faghri, P. D. (2018). Functional electrical stimulation-induced muscular fatigue: Effect of fiber composition and stimulation frequency on rate of fatigue development. *Journal of Electromyography and Kinesiology, 38*(Supplement C), 67-72. doi: https://doi.org/10.1016/j.jelekin.2017.11.006

Wahyuni, E. S. (2017, 1-2 Nov. 2017). *Arabic speech recognition using MFCC feature extraction and ANN classification.* Paper presented at the 2017 2nd International conferences on Information Technology, Information Systems and Electrical Engineering (ICITISEE), Yogyakarta, Indonesia.

Wei, H., Cheong-Fat, C., Chiu-Sing, C., & Kong-Pang, P. (2006, 21-24 May 2006). *An efficient MFCC extraction method in speech recognition.* Paper presented at the 2006 IEEE International Symposium on Circuits and Systems, Island of Kos, Greece.

Weir, J. P., McDonough, A. L., & Hill, V. J. (1996). The effects of joint angle on electromyographic indices of fatigue. *European Journal of Applied Physiology and Occupational Physiology, 73*(3), 387-392. doi: 10.1007/bf02425504

Weld, K. J., & Dmochowski, R. R. (2000). Association of level of injury and bladder behavior in patients with post-traumatic spinal cord injury. *Urology, 55*(4), 490-494. doi: https://doi.org/10.1016/S0090-4295(99)00553-1

Wigmore, D. M., Befroy, D. E., Lanza, I. R., & Kent-Braun, J. A. (2008). Contraction frequency modulates muscle fatigue and the rate of myoglobin desaturation during incremental contractions in humans. *Applied Physiology, Nutrition, and Metabolism, 33*(5), 915-921. doi: 10.1139/h08-085

Wilson, S., & Vaidyanathan, R. (2017, 17-20 July 2017). *Upper-limb prosthetic control using wearable multichannel mechanomyography.* Paper presented at the 2017 International Conference on Rehabilitation Robotics (ICORR).

Wood, D. E., & Dunkerley, A. L. (1999, 1999). *Controlling FES-assisted paraplegic standing-a case study.* Paper presented at the Proceedings of the First Joint BMES/EMBS Conference. 1999 IEEE Engineering in Medicine and Biology 21st Annual Conference and the 1999 Annual Fall Meeting of the Biomedical Engineering Society, Atlanta, GA, USA.

Woods, B., Subramanian, M., Shafti, A., & Faisal, A. A. (2018, 26-29 Aug. 2018). *Mechanomyography Based Closed-Loop Functional Electrical Stimulation Cycling System.* Paper presented at the 2018 7th IEEE International Conference on Biomedical Robotics and Biomechatronics (Biorob).

Woodward, R. B., Stokes, M. J., Shefelbine, S. J., & Vaidyanathan, R. (2019). Segmenting Mechanomyography Measures of Muscle Activity Phases Using Inertial Data. *Scientific Reports, 9*(1), 5569. doi: 10.1038/s41598-019-41860-4

Wu, H., Wang, D., Huang, Q., & Gao, L. (2018). Real-time continuous recognition of knee motion using multi-channel mechanomyography signals detected on clothes. *Journal of Electromyography and Kinesiology, 38*, 94-102. doi: https://doi.org/10.1016/j.jelekin.2017.10.010

Xiaogang, H., William, Z. R., & Nina, L. S. (2014). Motor unit firing rate patterns during voluntary muscle force generation: a simulation study. *Journal of Neural Engineering, 11*(2), 026015.

Xie, H.-B., Zheng, Y.-P., & Guo, J.-Y. (2009). Classification of the mechanomyogram signal using a wavelet packet transform and singular value decomposition for multifunction prosthesis control. *Physiological Measurement, 30*(5), 441-457. doi: 10.1088/0967-3334/30/5/002

Xu, Q.S. and Liang, Y.Z., 2001. Monte Carlo cross validation. *Chemometrics and Intelligent Laboratory Systems*, 56(1), pp.1-11.

Yamamoto, T., & Takano, H. (1994, 3-6 Nov 1994). *Application of muscle sound to assess muscle tonus of the electrically stimulated muscle for FES.* Paper presented at the Proceedings of 16th Annual International Conference of the IEEE Engineering in Medicine and Biology Society, Baltimore, MD, USA.

Yochum, M., Binczak, S., Bakir, T., Jacquir, S., & Lepers, R. (2010, 31 Aug.-4 Sept. 2010). *A mixed FES/EMG system for real-time analysis of muscular fatigue.* Paper presented at the 2010 Annual International Conference of the IEEE Engineering in Medicine and Biology, Buenis Aires, Argentina

Yoshitake, Y., & Moritani, T. (1999). The muscle sound properties of different muscle fiber types during voluntary and electrically induced contractions. *Journal of Electromyography and Kinesiology, 9*(3), 209-217. doi: https://doi.org/10.1016/S1050-6411(98)00035-2

Yoshitake, Y., Ue, H., Miyazaki, M., & Moritani, T. (2001). Assessment of lower-back muscle fatigue using electromyography, mechanomyography, and near-infrared spectroscopy. *European Journal of Applied Physiology, 84*(3), 174-179

Young, S., Evermann, G., Gales, M., Hain, T., Kershaw, D., Liu, X., . . . Povey, D. (2002). The HTK book. *Cambridge University Engineering Department, 3*, 175.

Yu, N.-Y., Chen, J.-J. J., & Ju, M. S. (2001). Closed-loop control of quadriceps/hamstring activation for FES-induced standing-up movement of paraplegics. *Journal of Musculoskeletal Research, 05*(03), 173-184. doi: 10.1142/S021895770100057X

Yusoff, N. M., & Hamzaid, N. A. (2014). Validation of In-built Muscle Activation Feedback Sensor for a Closed-loop Functional Electrical Stimulator Development. *Procedia Computer Science, 42*, 78-84. doi: http://dx.doi.org/10.1016/j.procs.2014.11.036

Zhang, Q., Hayashibe, M., & Azevedo-Coste, C. (2013). Evoked Electromyography-Based Closed-Loop Torque Control in Functional Electrical Stimulation. *IEEE Transactions on Biomedical Engineering, 60*(8), 2299-2307. doi: 10.1109/TBME.2013.2253777